Environmental Sustainability and Cost Evaluation for Stereolithography Additive Manufacturing Process

BY

YIRAN YANG

B.S., Beijing Institute of Technology, 2013

M.S., Purdue University, 2015

THESIS

Submitted as partial fulfillment of the requirements for the degree of Doctor of Philosophy in Industrial Engineering and Operations Research in the Graduate College of the University of Illinois at Chicago, 2019

Defense Committee:

Dr. Lin Li, Chair and Advisor

Dr. David He

Dr. Michael J. Scott

Dr. Yayue Pan

Dr. Didem Ozevin, Civil and Materials Engineering

DEDICATION

To my loving parents, Mr. Feng Yang and Ms. Yazhe Cao.

ACKNOWLEDGEMENTS

First, I would like to thank my parents, Mr. Feng Yang and Ms. Yazhe Cao for their unconditional love and unwavering support. They trust in higher education, and they trust in me. They motivated me to become the best of myself, and they stood by me during this entire journey. Additionally, I would like to express my sincere appreciation to my extended family especially my grandparents, aunts, uncles, and cousins.

Furthermore, I would like to thank my advisor Dr. Lin Li, Associate Professor in the Department of Mechanical and Industrial Engineering at the University of Illinois at Chicago, for his guidance and advice during my Ph.D. study. Additionally, I would like to thank my Ph.D. committee members, Dr. David He, Dr. Michael Scott, Dr. Yayue Pan and Dr. Didem Ozevin, for their valuable comments and suggestions on my Ph.D. dissertation as well as their help during my job searching.

Meanwhile, I would like to extend my sincere appreciation to my current and previous colleagues, Dr. Fadwa Dababneh, Dr. Zeyi Sun, Dr. Yong Wang, Dr. Yukan Hou, Dr. Weiwei Cui, Ms. Jing Zhao, Ms. Muyue Han, Mr. Lingxiang Yun, Mr. Rahul Shah, Mr. Yuntian Ge, and Ms. Azadeh Haghighi. It has been my great honor to be a member of the Sustainable Manufacturing Systems Research Laboratory (SMSRL).

Last but not the least, I would like to acknowledge the financial support from the U.S. National Science Foundation (CBET-1604825) and U.S. Department of Energy (DE-EE0007722).

Yiran (Emma) Yang

CONTRIBUTION OF AUTHORS

Chapter 1 is an overall introduction of the dissertation including general background knowledge as well as literature review in order to highlight the significance and academic contributions of this research.

Chapter 2 contains content shown in a published journal paper ("Yang, Y., Li, L., Pan, Y., and Sun, Z., 2017. Energy Consumption Modeling of Stereolithography-based Additive Manufacturing Toward Environmental Sustainability. *Journal of Industrial Ecology* 21(S1) S168-S178"). The dissertation author Yiran Yang was the main driver of this published journal paper. Dr. Lin Li contributed by guiding the research direction and quality. Dr. Yayue Pan offered comments in the experiment and provided the stereolithography additive manufacturing machine for experiment purposes. Dr. Zeyi Sun contributed to the manuscript revision process. The version of scholarly record of this article is published in Journal of Industrial Ecology (2017), available online at https://onlinelibrary.wiley.com/doi/full/10.1111/jiec.12589.

Chapter 3 represents a published journal paper ("Yang, Y., and Li., L., 2018. Total Volatile Organic Compound Emission Evaluation and Control for Stereolithography Additive Manufacturing. *Journal of Cleaner Production* 170(1): 1268-1278") and a published conference paper ("Yang, Y., and Li, L., 2017. Evaluation of Environmental Sustainability for Additive Manufacturing Batch Production. ASME 2017 12th International Manufacturing Science and Engineering Conference. P. V002T01A038. DOI: 10.1115/MSEC2017-2957"). For the journal publication, the dissertation author Yiran Yang was the main contributor. Dr. Lin Li guided the research direction and offered valuable comments and suggestions in the revision process. The version of scholarly record of the journal article is published in Journal of Cleaner Production

(2018), available at https://www.sciencedirect.com/science/article/pii/S0959652617321947. For the conference paper, the dissertation author Yiran Yang was the main contributor. Dr. Lin Li revised the manuscript and provided comments. The version of scholarly record of this article is published in ASME (The American Society of Mechanical Engineers) proceedings 2017, available at http://proceedings.asmedigitalcollection.asme.org/proceeding.aspx?articleid=2646236.

Chapter 4 includes content from two published journal papers (Publication A "Yang, Y., and Li, L., 2018. Cost Modeling and Analysis for Mask Image Projection Stereolithography Additive Manufacturing: Simultaneous Production with Mixed Geometries. *International Journal of Production Economics* 206: 146-158" and Publication B "Li, L., Haghighi, A., and Yang, Y., 2018. Theoretical Modeling and Prediction of Surface Roughness for Hybrid Additive-Subtractive Manufacturing Processes. *IISE Transactions* 1-40"). The version of scholarly record of Publication A is published in International Journal of Production Economics (2018), available online at https://www.sciencedirect.com/science/article/pii/S0925527318303931. The dissertation author Yiran Yang was the main driver of the Publication A. Dr. Lin Li offered insightful comments and advice to improve the paper quality and offered suggestions in the manuscript revision process. The version of scholarly record of Publication B is published in IISE Transactions (2019), available online at https://www.tandfonline.com/doi/abs/10.1080/24725854.2018.1458268. Dr. Lin Li was the main driver of this published paper. Ms. Azadeh Haghighi and the dissertation author Yiran Yang jointly contributed to the article in terms of modeling and experiments.

Chapter 5 presents the conclusions and discussions regarding the future work for the presented dissertation. More specifically, the academic contributions and broader impacts of this research are summarized; and the future research directions are also discussed.

TABLE OF CONTENTS

LIST OF FIGURES

LIST OF TABLES

SUMMARY

Additive manufacturing has been rapidly evolving since its emergence in the 1980s, and it has obtained considerable public attention due to its unique manufacturing capabilities ensured by the layer-by-layer production method. Comparing to traditional manufacturing processes, additive manufacturing has great potentials for shorter product development cycle, easier process control, and enhanced manufacturing complexity with higher material efficiency and less material wastes. As a result, different additive manufacturing technologies have been developed and adopted in various industries such as aerospace, automotive, electronics, healthcare, etc. Currently, the growing public interest in developing additive manufacturing into a mainstream manufacturing technology has led to the proliferation of academic achievements. In the meantime, increasing concerns have been presented regarding the potential environmental and economic sustainability of different additive manufacturing processes.

To date, the majority of current literature on environmental sustainability of additive manufacturing follows empirical approaches and lacks theoretical estimation and prediction capabilities. Hence, there is an urgent need for analytical modeling on the environmental performance of additive manufacturing process in terms of energy consumption and process emission. However, reducing the adverse environmental impacts from additive manufacturing processes usually implies increasing the production cost as well as life cycle cost. Additionally, in current literature, the cost performance of additive manufacturing especially for more complex production layouts has not yet been well studied. A joint study considering both environmental sustainability and cost evaluation for additive manufacturing will benefit the area and help further develop sustainable additive manufacturing by estimating and predicting the environmental and economic performance of additive manufacturing.

To advance the state-of-the-art in the environmental sustainability and cost analysis of additive manufacturing, this dissertation is conducted to promote sustainable additive manufacturing and enhance the life cycle performance of stereolithography additive manufacturing. This dissertation is mainly focused on the stereolithography production process and will be extended to a comprehensive life cycle assessment to evaluate the potential environmental and economic impacts from a life cycle perspective. The results of this dissertation can enable the theoretical estimation and prediction on the sustainability performance of stereolithography additive manufacturing in terms of energy consumption, process emission and production cost. More specifically, the analytical models established in this research is capable of quantifying, predicting, and reducing the electricity usages, volatile organic compound emissions as well as production cost. The results of this research indicate the potentials for reducing more than 50% of energy consumption without sacrificing the print quality, reducing the average total volatile organic compound concentration levels by more than 70%, and reducing the cost by around 25% while maintaining the production throughput and printed surface roughness. The outcomes of this research can be incorporated in the design and redesign stages of additive manufacturing, and provide useful insights aiming to facilitate sustainable designing and planning in additive manufacturing and promote long-term development of sustainable additive manufacturing.

LIST OF ABBREVIATIONS

AM	Additive Manufacturing
GHG	Greenhouse Gas
SLA	Stereolithography
VOC	Volatile Organic Compound
ABS	Acrylonitrile Butadiene Styrene
PLA	Polylactic Acid
TVOC	Total Volatile Organic Compound
LCA	Life Cycle Assessment
LCI	Life Cycle Inventory
IM	Injection Molding
FDM	Fused Deposition Modeling
EBM	Electron Beam Melting
DOE	Design of Experiment
PM	Particulate Matter
UV	Ultraviolet
SEC	Specific Energy Consumption
PID	Photoionization Detector

1. INTRODUCTION

1.1 General Introduction

1.1.1 Additive Manufacturing

Additive manufacturing (AM), also referred to as three-dimensional (3D) printing, is defined as “the process of joining materials to make objects from 3D model data usually layer upon layer, as opposed to subtractive manufacturing technologies” (ASTM, 2012). According to different types of raw materials and production technologies, AM processes can be classified into seven different categories (Newman, 2012) as shown in Table 1 , i.e., Material Extrusion, Binder Jetting, Directed Energy Deposition, Vat Photopolymerization, Powder Bed Fusion, Material Jetting and Sheet Lamination.

Table 1. The different categories for additive manufacturing technologies

Category	AM Process Description
Vat Photopolymerization	It uses a vat of photosensitive liquid polymer to fabricate parts layer by layer, e.g., Stereolithography.
Material Jetting	It builds the part by jetting the liquid material onto a build platform, e.g., PolyJet.
Binder Jetting	It uses two materials: a powder-based material and a liquid binder.
Material Extrusion	It extrudes the material through a nozzle and deposits the heated material layer by layer, e.g., Fused Deposition Modeling.
Powder Bed Fusion	It uses “either a laser or electron beam to melt and fuse material powder together” (Galante et al., 2019), e.g., Direct Metal Laser Sintering.
Sheet Lamination	It uses sheets or ribbons of metal, which are bound together using ultrasonic welding, e.g., Laminated Object Manufacturing.
Direct Energy Deposition	It is consisted of “a nozzle mounted on a multi-axis arm, which deposits melted material onto the specified surface” (Srinivas and Babu, 2017).

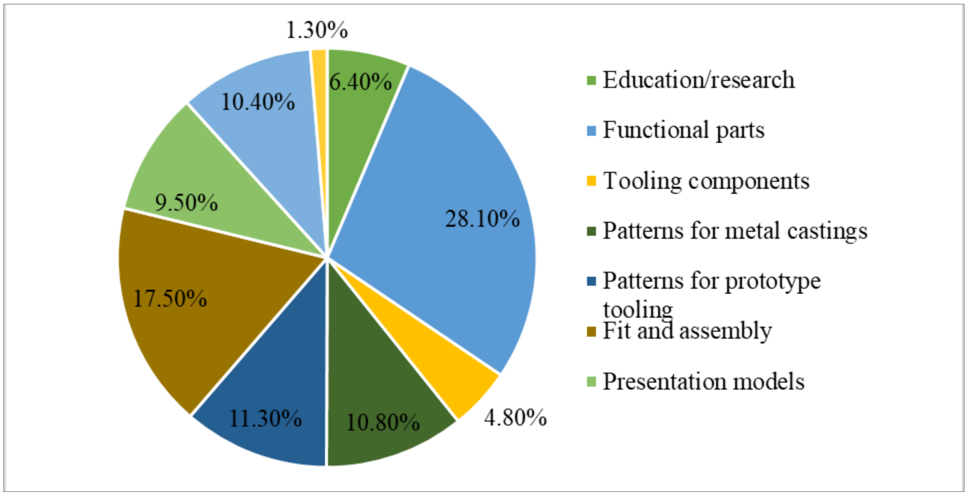

Figure 1. The additive manufacturing implementation by purposes, adapted from (Wohlers Associates, 2015)

As shown in Table 1, these AM processes adopt different types of raw materials, e.g., nylon, Acrylonitrile Butadiene Styrene (ABS), Polylactic Acid (PLA), polymers, stainless steel, titanium, ceramics, gypsums, graded material, etc. In addition, these AM technologies can process different forms of raw materials including solid, liquid, and powder. Because of the increasing diversities in AM technologies and raw materials, AM has obtained unprecedented popularity and has been developed rapidly since its first emergence in the 1980s.

To date, AM has evolved from its initial use, i.e., rapid prototyping, to rapid tooling, rapid manufacturing, and even larger scale manufacturing. The current AM technologies have been implemented for different purposes as illustrated in Figure 1. AM fabricated products are often adopted in industries such as aerospace (Lyons, 2012), automobile (Marchesi et al., 2015), healthcare (Giannatsis and Dedoussis, 2009), food (Lipton et al., 2015), etc. The main reasons for such wide range of different applications and implementations are the unique characteristics of AM technologies ensured by the layer-wise production method. The distinguished advantages of using AM technologies versus traditional manufacturing processes are summarized as follows.

First, AM is capable of fabricating parts with more complex geometries, which can be costly, time consuming or even not feasible using traditional manufacturing processes such as subtractive manufacturing techniques. Second, because of the reduction or elimination of tooling, lubricants and cutting fluids, AM has potentials for shorter product development cycle and easier process control. Finally, compared to traditional manufacturing technologies, AM is capable of significantly improving the material usage efficiency and reducing the life cycle environmental impacts and carbon footprints (Huang et al., 2015).

Owing to the great advantages of AM and the enhanced manufacturing capabilities offered by AM, numerous efforts have been dedicated to developing AM as one of the mainstream manufacturing technologies. In other words, AM is expected to take over a certain portion of the manufacturing quota in the near future, especially for industries with small to medium sized production volumes. Due to the growing applications and extinguished characteristics of AM processes, the global AM market has been rapidly growing. It has been estimated that the economic impact of AM will be up to $550 billion per year in 2025 (Manyika et al., 2013).

Within the global AM market, the U.S. is currently a major user and primary producer of different AM systems. As shown in Figure 2, the U.S. accounted for around 38% of the global AM market in 2012 (Wohlers Associates, 2012). The U.S. AM market is promising and has great potentials for increasing applications. For example, according to a report published by the U.S. Postal Service (USPS), an incremental $646 million dollars in commercial package revenue can be generated by turning the current postal processing stations into AM hubs (Columbus, 2015; U.S. Postal Service, 2014). In addition, more countries (including the U.S.) have realized the importance of AM for military applications. For example, a U.S. military Fab Lab was established in Afghanistan which has 3D printers as well as other industrial machines (Peels, 2017). In addition, a great number of companies have developed and/or expanded their service to AM such as Autodesk, Amazon, Stratasys, 3D Systems, Intel, GE, Home Depot, Makerbot, Formlabs, Carbon, 3D Hubs, Prusa3D, BigRep, Local Motors, etc.

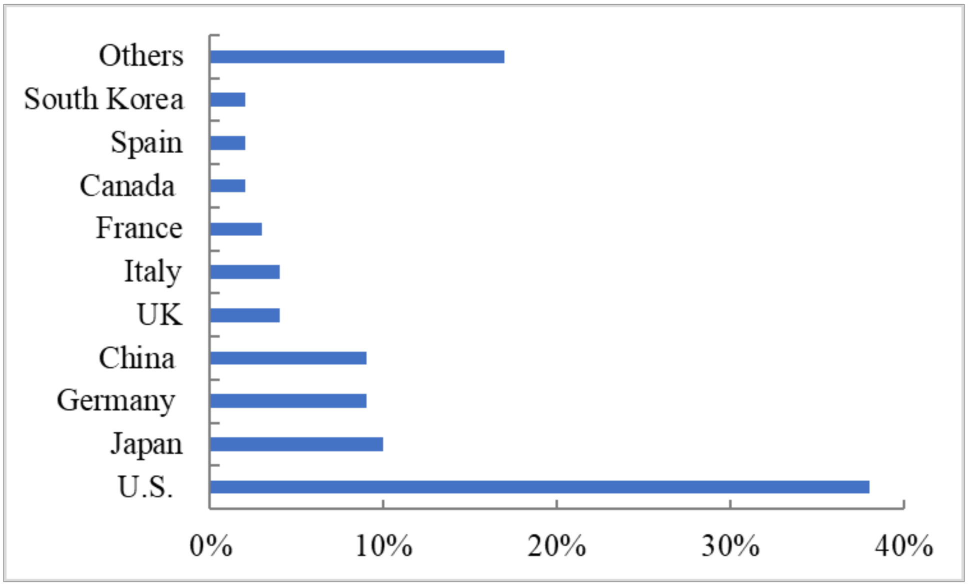

Figure 2. The global additive manufacturing market share, adapted from (Wohlers Associates, 2012)

While the AM market is growing rapidly and continuously, some limitations still exist and are hindering the further implementations of AM in different industries. For example, the accuracy of current AM technologies is generally lower than traditional manufacturing processes such as computer numerical control process (Campbell et al., 2012). As a result, adopting AM usually implies producing parts with unsatisfactory quality (Dai and Gu, 2015) and longer production time (Ponche et al., 2014). Other disadvantages of AM include limited types of raw materials, restricted print size, additional need for post-processing or surface finishing activities, etc. In addition, increasing concerns regarding the environmental and economic sustainability of AM have appeared in both industrial and academic fields. According to a report published in 2014 (Lyndsey, 2014), negative consequences of different AM processes and materials include intense electricity use, unhealthy air emissions, reliance on plastics, cyber security risks, etc.

1.1.2 Environmental Concerns on Additive Manufacturing

As the global AM market is continuously growing, some serious concerns are arising focusing on the environmental consequences that can be caused by different AM processes and materials, including energy consumption, electricity related Greenhouse Gas (GHG) emissions, AM process emissions, and material waste. More specifically, some types of AM processes utilize high energy intensive techniques like laser or heating system, which can lead to high demand for power level as well as electricity consumption. As a result, GHG emissions are caused by the electricity generation process and can seriously harm the environment by causing global warming and climate change. In addition, due to the use of certain types of raw materials, the AM production activities can cause process emissions such as Particulate Matter (PM) emissions or Volatile Organic Compound (VOC) emissions.

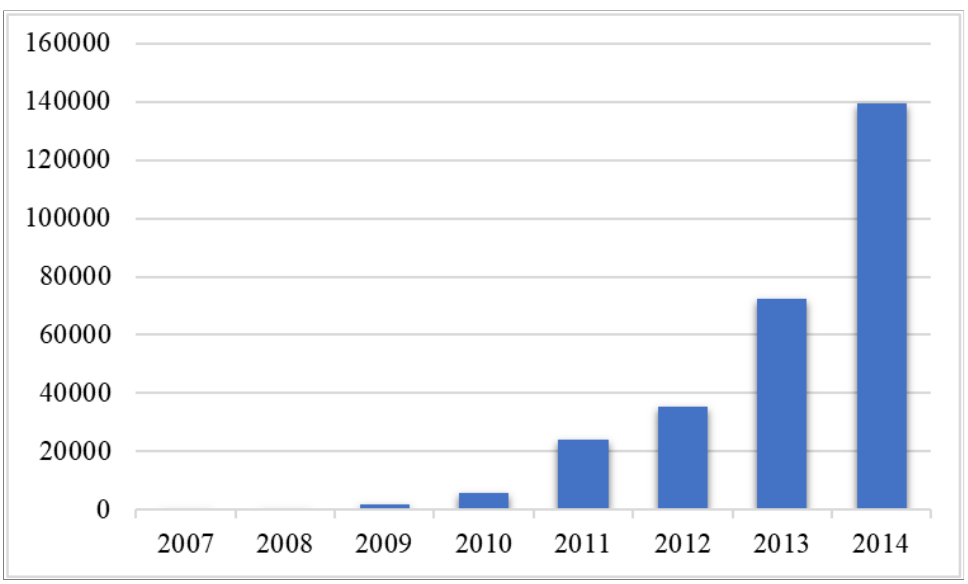

Figure 3. The global desktop AM Market, adapted from (Wohlers Associates, 2015)

The AM process emissions need to be carefully evaluated and controlled, as most of these AM processes and/or machines are currently used in indoor environments, especially desktop 3D printers. According to the Wohler's Report, a steadily increasing trend was observed in the desktop 3D printing market, and more than 140,000 desktop 3D printers were sold worldwide in 2014 (Wohlers Associates, 2015) as shown in Figure 3. Most desktop 3D printers are used in indoor environments such as schools (for education purposes) and hospitals; where children and patients are likely to be exposed to adverse health effects of 3D printers. Also, most current AM processes do not have an end-of-life management system for further recycling, reusing, or remanufacturing. Most material wastes are improperly disposed or locally processed, leading to undesired environmental consequences. Therefore, to provide insights on reducing hazardous health and environmental effects from AM processes and materials, the environmental impacts need to be thoroughly evaluated and controlled considering energy consumption, GHG emissions, process emissions, etc.

1.1.3 Energy Consumption and Greenhouse Gas Emissions

The energy consumption and associated GHG emissions are of great importance for the development of sustainable manufacturing as well as sustainable society. It has been estimated the total U.S. GHG emissions in 2015 were almost 7,000 million metric tons of carbon dioxide (National Energy Technology Laboratory, 2019; U.S. Environmental Protection Agency, 2016a). As shown in Figure 4, the electricity sector had the biggest share (29%) out of the total GHG emissions in 2015 in the U.S. Therefore, to reduce the GHG emissions and to relieve the accompanying environmental consequences, it is significantly critical to investigate and reduce the electricity use. More specifically in the manufacturing sector, reducing the machine related electricity consumption can be substantial because it accounted for 49% of the total electricity consumption in the U.S. manufacturing sector in 2013, as also illustrated in Figure 5. The AM process/machine related electricity consumption and electricity related GHG emissions have not yet been well studied.

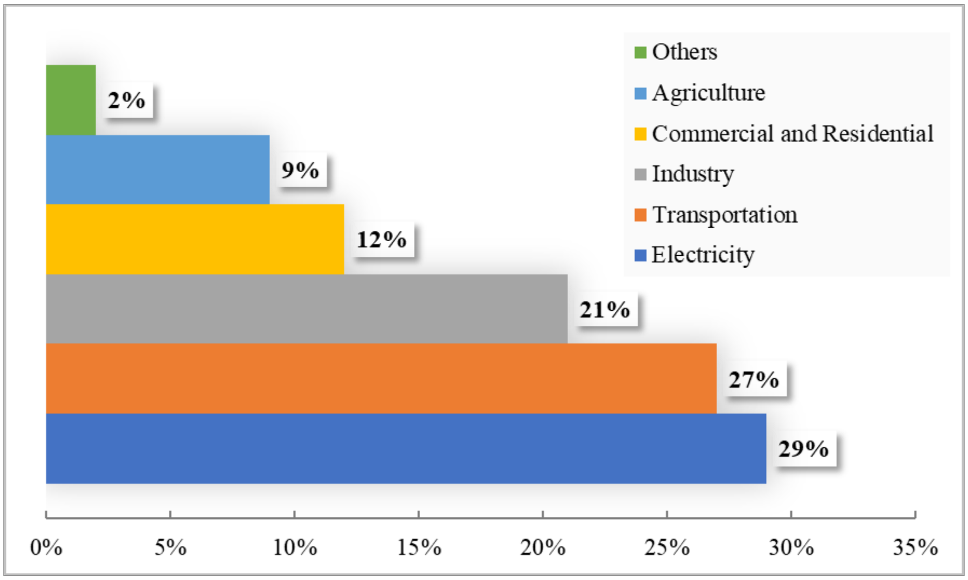

Figure 4. Total U.S. GHG emissions by economic sector in 2015, adapted from (U.S. Environmental Protection Agency, 2016a)

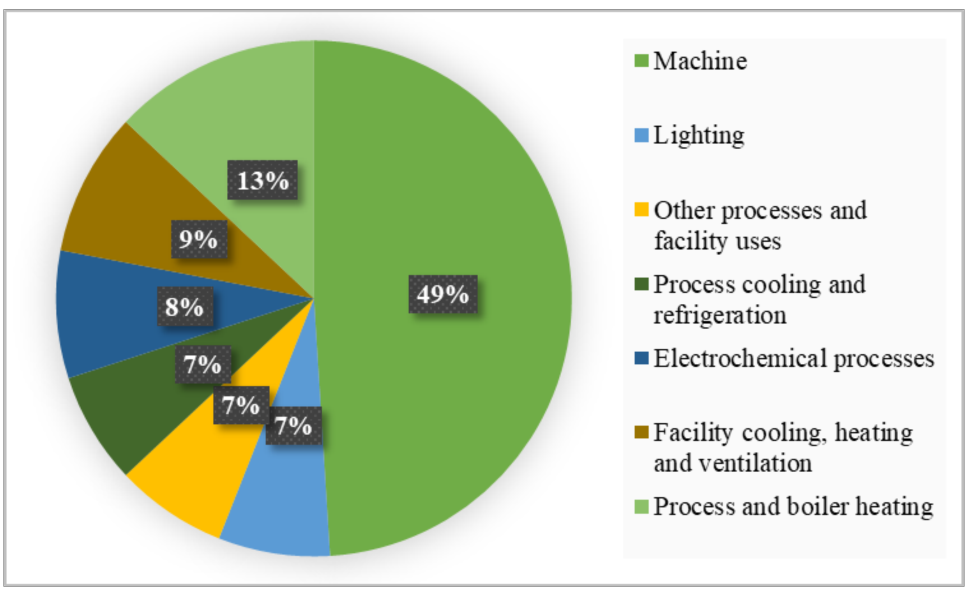

Figure 5. U.S. manufacturing electricity consumption, adapted from (U.S. Energy Information Administration, 2010)

1.1.4 Volatile Organic Compound Emissions in Additive Manufacturing

In addition to the electricity consumption and associated GHG emissions, the different types of hazardous process emissions from the various AM technologies and materials also need to be studied and reduced. As one of the most common AM technologies for indoor desktop 3D printers, the Stereolithography (SLA) process has two possible sources of gaseous emissions: one is the raw material volatilization process, where the photosensitive liquid resin volatilizes organic compounds to air even when the SLA machine is not in operation; and the other source is AM-caused emissions, such as the hazard compounds released from the solidification of liquid resin in the curing process. It has been reported by some researchers that a wide variety of VOCs are emitted during the AM processes involved with ABS and/or PLA (Kuo et al., 2016), which are two of the main SLA raw materials.

As the most common toxic component of emitted gases from AM processes, VOCs usually include benzene, ethylbenzene, toluene, etc. The long-term exposure to VOCs can cause eye and throat irritation and damage to liver and central nervous system. In addition, the VOC exposure can also lead to carcinogenic effects (de Gennaro et al., 2013) and increase relative rates of leukemia and lymphoma (Goodman et al., 2012). It was reported that in the city of New York and Los Angeles, around 957 and 486 cancer cases per million populations were involved with carcinogenic VOCs in 2006, respectively (Sax et al., 2006). In addition to the adverse impacts on human health, VOCs can also be emitted to the atmosphere and contaminate the air due to their low boiling points. Also, it has been identified that VOCs are the key reasons for the ozone formation (Cardelino and Chameides, 1995), photochemical smog formation (Guo, 2012) and can lead to serious air pollution and environmental burdens. In summary, due to the potential hazardous human health risks and adverse environmental effects, it is critical to evaluate the VOC emissions from SLA AM process and assess the potential effects on human health and environment.

1.1.5 Additive Manufacturing Cost

In current literature, the cost performance of AM cost has not been well studied. As a critical part of the sustainability, production cost refers to all the cost components required during the process of fabricating a part. As discussed by Son (1991), the production costs are mainly categorized into two groups, i.e., well-structured costs and ill-structure costs. More specifically in AM, well-structured costs include material, machine, energy consumption, and labor costs; whereas ill-structured costs of AM include inventory, transportation, build failure, and machine setup costs. The cost components can also be categorized into AM process costs and life cycle level costs, based on their different scopes and considerations. Both AM process and life cycle level costs are necessary to evaluate the cost performance of AM.

The cost analysis especially for newly developed manufacturing technologies like AM is critical for the evaluation of implementation feasibility. Compared to conventional manufacturing processes, AM has less need for inventory, hence leading to the decreased inventory costs. Inventory cost savings alone can contribute to significant cost reductions. According to the latest report from U.S. Department of Commerce, it was estimated the manufacturers' and trade inventories for the month of July 2017 was $1,873.0 billion dollars (U.S. Department of Commerce, 2017).

1.1.6 Additive Manufacturing Batch Production

To reduce the AM production cost per part, small to medium sized batch production is often adopted in AM processes (Weller et al., 2015), where multiple parts are fabricated simultaneously at one batch. For example, the direct fabrication of functional end use parts has been the main trend for AM processes (Guo and Leu, 2013). For such small to mid-scale productions, AM has shown to have the capability of reducing the manufacturing cost (Buswell et al., 2007). The reason that AM is currently not suitable for large scale mass production is that current AM systems do not have sufficient throughput and capabilities, and therefore need to be further improved (Baumers et al., 2016a). The inadequate production throughput is caused by low productivity, as AM is still in its early developmental stage (Huang et al., 2013).

To enhance the AM production throughput, medium sized batch production has obtained considerable research interest, where multiple parts are fabricated in groups or batches. As one of the most popular AM processes, the projection-based SLA process is suitable for adopting the batch production method, because the production time for projection-based SLA process does not necessarily change due to the increasing production scale. In addition to improving AM system throughput, batch production is also be suitable for fabricating low-demand customized parts. In current literature, the feasibility of batch production has not yet been thoroughly evaluated considering its cost analysis and environmental performance. Subsequently, to further facilitate the adoption of batch production in AM, a comprehensive evaluation is necessary and critical.

1.1.7 Life Cycle Assessment

As a popular tool for assessing the environmental sustainability and cost, life cycle assessment (LCA) has been the most widely used methodology over the past four decades. Instead of process assessment, LCA is based on the standpoint of the entire life cycle. The principles and framework for performing LCA (De Benedetto and Klemeš, 2009) include: "definition of the goal and scope of the LCA, life cycle inventory (LCI) analysis, life cycle impact assessment, and life cycle interpretation" (International Organization for Standardization, 2006), which are also illustrated in Figure 6. The LCI consists of material and energy consumption as well as emissions of all unit processes involved in product life cycle, and it provides the data foundation for the LCA study, and usually is the most resource demanding step. As a result, commercial database with unit process LCI as the datasets have been established to facilitate LCI analysis, e.g., National Renewable Energy Laboratory (NREL), U.S. General Services Administration (GSA), Athena Sustainable Materials Institute, etc. However, current commercial LCI databases only cover a limited number of manufacturing processes while largely neglecting different types of AM processes.

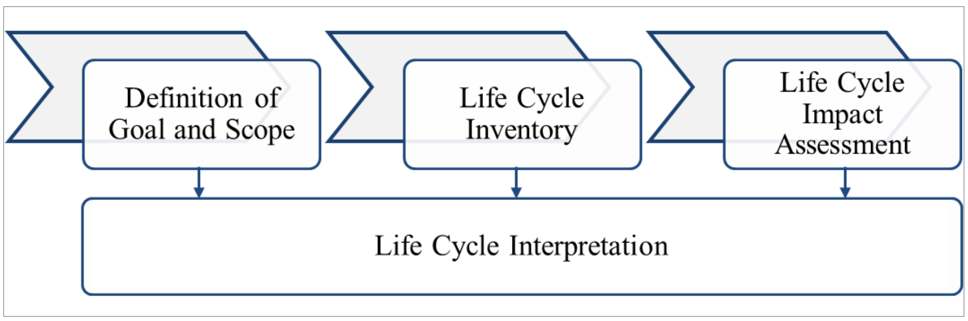

Figure 6. The life cycle assessment procedure, adapted from (International Organization for Standardization, 2006)

Currently, several attempts have been made to analyze the true environmental impacts of AM processes using LCA methodology, i.e., quality material and energy consumption as well as air emissions of several AM processes, but these studies are limited by the quality and availability of the inventory data of feedstock materials and AM processes. In addition, these studies tend to focus on specific case studies and therefore are highly unlikely to draw any general conclusions. As a result, most of these studies follow the traditional LCA/LCI approach. That is, the AM process considered is treated as a black box with the mechanisms and fundamentals connecting process parameters (including the selection of feedstock materials) and the output inventory largely missing. This makes it extremely challenging to apply the LCA/LCI results to support the AM process and machine improvement. Moreover, the chemical composition of AM feedstock materials and process emissions as well as the connections between the two remain unknown. This greatly hinders any rigorous assessment of environmental impact and occupational health risks.

1.2 Literature Review

In this section, an overview of current literature on the environmental sustainability and cost evaluation from both the AM process and life cycle level is illustrated. More specifically, a comprehensive literature review on AM process energy consumption is presented in Section 1.2.1, current studies on AM emissions are reviewed and discussed in Section 1.2.2, the batch production method and its performance considering the environmental sustainability and cost are discussed and reviewed in Section 1.2.3, the existing research on cost analysis and evaluation for AM process is examined in Section 1.2.4, and the academic achievements and limitations on LCA for AM are reviewed in Section 1.2.5.

To date, numerous academic achievements and research efforts have been conducted for different aspects of AM. The majority of current literature on AM is focused on the enhancement and improvement of the process technologies, including laser technique (Aboutaleb et al., 2017; Chang and Tu, 2012; Jeng and Lin, 2001; Sreenivasan et al., 2010), curing method (Brady et al., 1996; Eschl et al., 1999; Lopes et al., 2014; Xie and Li, 2012; Zhou et al., 2011), material properties (Nikzad et al., 2011; Tymrak et al., 2014; Wang, 2012; Weng et al., 2016; Yang et al., 2019; Ziemian et al., 2012), process planning (Ding et al., 2017; Lynn-Charney and Rosen, 2000; Newman et al., 2015; Ruan et al., 2005), computational algorithms (Lavery et al., 2014; Martukanitz et al., 2014), etc. Recently, due to the growing public concerns in climate change, the environmental sustainability-related performance of AM processes has obtained great attention such as energy, ecological and economic sustainability (Burkhart and Aurich, 2015). Among the different fields, energy consumption is considered as one of the main unsolved issues in AM processes (Drizo and Pegna 2006; Short et al. 2015).

1.2.1 Literature Review on Additive Manufacturing Process Energy Consumption

Several academic studies have been committed to the measurement of energy consumption of different AM processes. For example, the electricity consumed by the SLA process was investigated by Sreenivasan and Bourell (2009); the energy consumption for Binder Jetting (BJ) AM process was investigated by Xu et al. (2015); and the energy flow of BJ AM process was monitored by Meteyer et al. (2014). In addition, some studies have been conducted to compare the energy consumption of AM processes and traditional manufacturing processes. For instance, a comparative assessment of the electricity consumption of two Laser Sintering (LS) AM machines is presented in (Baumers et al., 2011). In this work, the authors argue that LS process energy consumption is mainly dominated by time-dependent terms. In addition, case studies for SLA, Selective Laser Sintering (SLS), and Fused Deposition Modeling (FDM) AM processes were conducted by Luo et al. (1999). For each type of AM processes, the energy consumption differed with varying combinations of material types, equipment and disposal scenarios. Furthermore, the energy consumption for building nylon parts using SLS and Injection Molding (IM) processes are compared by Telenko and Conner Seepersad (2012). It is concluded that the SLS process consumes significantly more energy than the IM process; however, this can be offset by the energy contributed by the production of the injection mold from a life cycle viewpoint. Additionally, the energy consumption and environmental impacts of FDM, PolyJet, and traditional computer numerical control processes were compared by Faludi et al. (2015). The authors conclude that electricity consumption has a significant impact on the sustainability related performance of both AM process and traditional computer numerical control process.

In addition to comparative or experimental energy consumption studies, a few energy consumption modeling studies aiming to uncover the relationships between different process parameters and energy consumption have been performed. For example, Mognol et al. (2006) investigated the influence of several parameters (i.e., layer thickness, support design, part orientation and production time) on the energy consumption of three AM systems: Thermojet, FDM, and Direct Metal Laser Sintering (DMLS). Kellens et al. (2014) presented parametric process models to estimate the environmental footprint of the SLS AM process. More recently, Baumers et al. (2016b) studied the relationships between geometry shape complexity and process energy consumption in the Electron Beam Melting (EBM) process. It has been concluded that the EBM process does not show a strong association between geometry shape complexity and energy consumption on a per-layer basis. Nonetheless, the current literature on energy modeling for AM processes is limited. Several popular AM processes (e.g., SLA) have not been well studied for their energy consumption as a part of the environmental sustainability performance. More specifically for the SLA AM process, various process parameters are capable of affecting the energy consumption, but they have not yet been investigated. Additionally, mathematical models for quantifying the energy consumption of AM processes are still lacked in the current literature.

This dissertation is focused on the projection-based SLA AM process, which is one of the most popular AM processes that can build parts by curing the liquid photopolymer resin layer by layer using an ultraviolet (UV) light source. The energy consumption model is established by quantifying the energy contributions of each subsystem of the SLA AM machine. Design of Experiments (DOE) methodology is used to guide the physical measurements to quantify the effects of various parameters on the overall energy consumption, explore the interactions between/among different parameters, optimize the combination of parameters to reduce the overall energy consumption, and validate the proposed energy consumption model. The potential GHG emission reduction due to the reduction of electricity consumption is also estimated.

1.2.2 Literature Review on Volatile Organic Compound Emissions

Emission evaluation is also very critical for AM processes because most 3D printers sold are used in indoor environments that lack necessary ventilation or filtration. As one of the most common AM technologies for indoor desktop 3D printers, SLA has two possible sources of gaseous emissions. One is the raw material volatilization process, where the photosensitive liquid resin volatilizes organic compounds to air; and the other is AM-caused emissions, such as the hazard compounds released from the solidification of liquid resin in the curing process. It has been pointed out by some researchers that a wide variety of VOCs are emitted during processes involving ABS and/or PLA (Kuo et al., 2016), which are two of the main SLA raw materials.

When evaluating the indoor environment air quality, the total volatile organic compound (TVOC) measure is often used (Zhang and Zhang, 2007) and treat all types of VOCs as one target gas in the measurement. To help regulate TVOC emission standards, several agencies and companies provide recommended indoor TVOC concentration levels. For example, GREENGUARD Environmental Institute published an emission criterion for indoor environment in 2009 including TVOCs and other common indoor air pollutants (GREENGUARD Certification, 2013). The latest LEED-NC guidance specifies that the maximum allowed TVOC concentration inside a building is 500μg/m^3 (Environmental, 2009).

Due to the lack of TVOC emission standards, some studies have been conducted to characterize and analyze the emissions from AM processes. Afshar-Mohajer et al. (2015) investigated the PM and TVOC emissions from the BJ AM process, and observed that raw materials emitted VOCs even when the AM machine was not in operation. They used Isobutylene as the target gas in the

TVOC measurement. Another emission study concerning ultrafine particles and VOCs was conducted for five commercial filament extrusion 3D printers with nine different filaments (Azimi et al., 2016). They identified different types of VOCs emitted from various filaments with diverse emission ranges. Nevertheless, an emission control approach was not proposed in literature. Kim et al. (2015) analyzed nanoparticles and gaseous emissions from FDM 3D printers. They found that both nanoparticles and VOC concentrations increased during AM production stages, where the concentrations differed based on the cartridge type and the 3D printer manufacturer. However, the mathematical relationship between the emissions and AM process characteristics was not explored. In all, current literature on VOC or TVOC emissions from AM activities only covers limited types of AM processes and lacks well-documented emission data. Furthermore, an analytic model that can describe the emission process has not been established. Without such an analytical approach, the emission level from AM processes cannot be estimated or accurately predicted.

In this dissertation, an emission evaluation methodology is proposed to theoretically estimate the TVOC emission for indoor environment equipped with SLA machines. To achieve this goal, an analytic model that describes the TVOC emission from both the raw material volatilization process and AM production activities is established and validated through experiments. Using this model, the TVOC concentration for an indoor space can be estimated with/without a 3D printer in operation. Furthermore, current commercial emission control technology is tested and compared to two new approaches proposed in this research. Proper emission control strategies provide promising opportunities to improve the environmental sustainability for AM and lower the associated health risks by significantly reducing the TVOC emission towards cleaner production. The results of this research will help provide understanding on the emissions of AM processes, evaluate the emission level, and establish emission guidelines for AM processes.

1.2.3 Literature Review on the Environmental Sustainability Evaluation for Batch Production

Several studies focusing on the economic impact and feasibility of AM batch production are found in literature. One study was conducted by Hopkinson and Dickens (2003), in which traditional manufacturing methods (IM) are compared to AM processes (SLA, FDM, and LS) to demonstrate that AM can be cost effective for small volume batch production. Additionally, Lindemann et al., (2012) conducted studies on how machine utilization affects AM batch production cost. They concluded that some types of AM processes are cost effective when considering AM batch production if a high degree of machine utilization can be reached. Another comparison between a traditional fabrication method (high-pressure die-casting) and a AM (direct laser sintering) was studied by Atzeni and Salmi (2012) for metal parts, and provided evidence that AM can be more economically competitive for small to medium volume batch production. In summary, most of the current literature regarding AM batch production focuses on cost estimation and comparison between AM and traditional manufacturing processes. To comprehensively evaluate the AM batch production method, other important aspects also need to be assessed.

Environmental sustainability plays a critical role in AM technology development and faces substantial challenges (Ford and Despeisse, 2015). However, in the current literature, only few papers have studied the environmental sustainability for AM batch production. Although it has been proven by Baumers et al. (2011) in that higher batch size leads to lower specific energy consumption (energy consumption per mass unit of part built) for some types of AM platforms, more experimental and theoretical results are needed to identify the quantitative relationship between batch size and specific energy consumption (SEC). Furthermore, almost no papers have studied the emission and material waste for AM batch production. Without thorough investigation of these three aspects (SEC, emission, and material waste) that drive environmental sustainability, the feasibility of AM batch production cannot be fully assessed.

To fill in the research gap, an evaluation on the environmental sustainability of AM batch production is conducted in this research by experimentally identifying the relationships between different batch production sizes and three key environmental performance metrics (i.e., energy consumption, emission, and material waste). Experiments are designed to characterize the three chosen environmental aspects with different batch sizes, followed by experimental results and discussions. The outcomes of this evaluation can be used to aid the evaluation of AM batch production method from an environmental sustainability perspective, enhance the understanding of AM batch production performance from different environmental aspects, and facilitate the development and improvement of feasible AM batch production methods.

1.2.4 Literature Review on Additive Manufacturing Cost Analysis

In addition to the environmental sustainability, cost analysis is also critical for the development of sustainable additive manufacturing. To date, a large number of research efforts have been dedicated to the cost analysis for AM (Thomas and Gilbert, 2014). According to the different scope, two types of cost studies are summarized from literature, i.e., AM process cost analysis and life cycle cost analysis. In this section, only AM process cost analysis literature is reviewed. The life cycle cost analysis will be discussed in Section 1.2.5.

Most existing studies on AM process cost analysis focus on linking the process parameters with different cost components. As early as 1998, Alexander et al. established models for build orientation and production cost for FDM and SLA processes, and provided some initial understanding on optimal build orientation and production cost minimization (Alexander et al., 1998). The activity-based cost modeling shown in this study works well for individual part production, however, it is not valid for fabricating multiple parts simultaneously. The proposed cost model was later extended by Rickenbacher et al. (2013), where the authors developed a process-based cost model for Selective Laser Melting (SLM) process. The proposed cost model can obtain the cost for each single part in a mixed build job with multiple parts of different geometries, complexities, and quantities.

In literature, several studies comparing the cost between AM and traditional manufacturing processes have been conducted. For example, Hopkinson and Dickens (2003) compared the unit cost per part from conventional IM and several AM processes (i.e., SLA, FDM, and LS) in. The cost components considered included machine, labor, and material costs. The comparison shows that for some geometries, rapid manufacturing can be more competitive for high production volumes. The cost estimation results obtained by the cost model developed by Hopkinson and Dickens (2003) were then compared with the cost model established in (Ruffo et al., 2006) for LS process. The comparison shows that the newly developed model by Ruffo et al. (2006) has a more accurate cost estimation especially for low production volumes. In addition, the proposed cost model incorporated the indirect cost components, where such consideration emphasized the significance of machine investment and maintenance for modern manufacturing technologies. Ruffo and Hague (2007) later further modified their previous cost model in and proposed several different mathematical methods for the calculation of unit cost for simultaneous productions of mixed parts. The authors assigned the unit cost using different methodologies: (1) parts volume, (2) the cost of building a single part, or (3) the cost of building a part in high-volume production. According to the case study results, the third method proved to be an equitable method for cost assignment.

In another example of cost comparison studies, Atzeni et al. (2010) compared two different technologies (i.e., IM and rapid manufacturing (RM)) to fabricate plastic parts from geometrical capabilities and economic aspects. According to the analysis, RM shows great potential to be economically competitive for medium volume production of plastic parts in Europe. The authors then performed an economic comparison (Atzeni and Salmi, 2012) between two different manufacturing technologies (i.e., die casting and DMLS) for fabricating end-usable metal parts. The results show that AM is promising for small to medium production volumes. In addition, the analysis also indicates that AM design and redesign can significantly reduce the AM costs.

More recently, researchers have started to consider the cost analysis for metal AM. Piili et al. (2015) performed an economic analysis for laser additive manufacturing (LAM) process, and the authors concluded that LAM was depended heavily on the machine investment. It was also pointed out that simultaneously building as many parts as possible could reduce the cost by 81% to 92% compared to building parts separately. In addition, Baumers et al. (2016a) established a production cost model for EBM and DMLS processes and identified machine productivity as the main cost driver. The authors suggested that further AM technology improvement would enable significant productivity enhancement as well as production cost savings. The authors then performed an inter-process cost comparison in (Baumers et al., 2017) between conventional manufacturing and AM using DMLS process, and considered several new aspects into the cost model (i.e., optimized capacity utilization, ancillary process, build failure, and design adaptation). The results show that the unit part cost in mixed productions with full capacity is lower than productions with single type geometry. In addition, Huang et al. (2017) established a process-based cost model for EBM process, and minimized cost through topology design. The results show that it is more cost effective when adopting larger layer thickness, faster laser speed, and smaller laser velocity. Fera et al. (2017) developed a more general cost model for AM technologies, where these AM processes are integrated in an existing shop floor. Such consideration will help further optimizing and scheduling AM activities. Also, cost evaluation guidelines are proposed in literature (Zanardini et al., 2015) for assessing AM applications considering benefits and costs.

1.2.5 Literature Review on Life Cycle Assessment for Additive Manufacturing

Life cycle assessment (LCA), as a more systematic cradle-to-grave approach to evaluate additive manufactured parts along the different stages of their life cycle, is a prevalent tool to quantify and evaluate the environmental sustainability of AM process. AM, due to its unique characteristics, provides new production scheme possibilities. Conventional manufacturing industries usually adopt centralized manufacturing systems; whereas AM, due to its unique characteristics and its aim towards small to medium sized customized production, provides more possibility for distributed manufacturing system.

To date, most studies on life cycle environmental sustainability analysis are comparative (Kafara et al., 2017; Faludi et al., 2015; Yang et al., 2017), where environmental performance when fabricating the same part for AM and conventional manufacturing processes are compared. For example, Cerdas et al. (2017) performed a comparative LCA in for additive manufactured parts in two different scenarios, the conventional centralized manufacturing system and the new distributed manufacturing system provided by AM. According to the analysis, the authors concluded that throughout the whole life cycle, the optimization potential is concentrated in the AM process energy consumption, which is highly linked to the printing material employed. Kreiger and Pearce (2013a) conducted an LCA for plastic parts fabricated by open-source 3D printers under a distributed manufacturing system. Compared with the environmental impact caused by conventional manufacturing, distributed manufacturing consumes less energy, and causes less emissions when using PLA and ABS with solar photovoltaic power. The authors further extended their analysis and studied how process parameters like fill density affect the life cycle environmental impact (Kreiger and Pearce, 2013b). The analysis results show that cumulative energy demand of fabricating polymer parts can be reduced by 41%-64% and emissions can be reduced using a distributed manufacturing system when the fill density is less than 25%.

Peng et al. (2017) studied three different manufacturing methods for impellers (i.e., plunge manufacturing, laser cladding forming, and additive remanufacturing), and compared the life cycle environmental impacts between them. The results show that additive remanufacturing is the most environmental favorable option, followed by AM and conventional manufacturing, when considering multiple environmental aspects such as global warming potential (GWP), resource depletion potential (RDP), water eutrophication potential (EP), and acidification potential. On the other hand, using only AM can lead to twice of the environmental burdens than conventional manufacturing. Walachowicz et al. (2017) compared the environmental impacts of conventional manufacturing methods with laser beam melting (LBM) AM process. More specially, the LCA study was conducted for the process of repairing a burner, which is often used in industrial gas turbines. The results show that AM can reduce material footprint, primary energy consumption, and carbon footprint.

In addition, some researchers proposed frameworks for assessing and evaluating the environmental sustainability for AM (Burkhart and Aurich, 2015). For example, Bours et al. (2017) developed a framework that considers environmental impacts as well human hazards, and identified suitable methodologies to evaluate these concerns. The authors then adopt the methodologies for material selection. Two types of materials are compared: Autodesk standard clear prototyping resin and bio-polylactic acid.

So far, only a few research efforts are dedicated to quantifying and evaluating the life cycle level or supply chain level costs for AM. (Lindemann et al. (2012) performed a life cycle cost analysis for additive manufactured metal parts, in order to identify and study the cost drivers which have the most significant impact on unit costs. The authors further extended their research and studied the effect from AM building rate on the life cycle cost (Lindemann et al., 2013). A life cycle economic analysis was conducted by Wittbrodt et al. (2013) for open-source 3D printers, which shows promising results considering the case where the self-replicating 3D printers are used in households. A stochastic cost model to quantify the supply-chain level costs of biomedical implants using AM technologies was proposed in (Emelogu et al., 2016), and solved using a customized Sample Average Algorithm (SAA). In addition, some real-life case studies are performed, and the results show that the key factors for the economic feasibility of AM adoption include the unit production costs and product lead time and demands (Emelogu et al., 2016).

Although several attempts have been made to analyze the environmental sustainability and cost using LCA methodology, these studies (1) do not simultaneously consider both environmental sustainability and cost; (2) are limited by the quality and availability of the life cycle inventory data; and (3) tend to focus on specific cases so it is unlikely to draw any general conclusions. Therefore, current literature on LCA for evaluating the environmental sustainability and cost analysis for AM process is far from complete, and there is a critical knowledge gap in comprehensively considering both environmental and economic performance of AM process.

1.3 Motivations

As a newly developed manufacturing technique, the vitality of implementing AM needs to be properly and comprehensively evaluated. Given the current concerns and challenges related to GHG emissions and limited energy resources, sustainable manufacturing should be incorporated to the long-term development of AM. Sustainable manufacturing is defined as "the creation of manufactured products through economically-sound processes that minimize negative environmental impacts while conserving energy and natural resources" (U.S. Environmental Protection Agency, 2016b), and it will benefit manufacturers, users, as well as society. According to the definition, the development of sustainable manufacturing is twofold: one is to ensure the manufacturing process is economically sound; and the other one is to minimize the harmful environmental impact. Developing sustainable AM will help further increase the AM operational efficiency by minimizing the cost and waste while reducing the negative environmental consequences.

In terms of the environmental sustainability, increasing concerns have been presented in multiple aspects including energy consumption, process emissions, material waste, etc. In general, minimizing the environmental impact has been touted as one of the main advantages of AM when compared to traditional manufacturing processes, because AM seems to have higher material efficiency and lower scrap rate. Also, AM makes regional and local production possible, where the shortened supply chain suggests lower energy consumption and less emissions from the transportation process. However, some types of AM technologies (especially the ones involving laser technologies) require high energy intensity; and some types are found to release hazardous emissions. Therefore, the environmental sustainability still needs to be comprehensively evaluated for AM processes from both the process and life cycle standpoints.

In addition to the environmental sustainability, cost evaluation is also critical for developing sustainable AM. In reality, reducing the adverse environmental impacts from AM usually leads to higher production costs. For example, to filter or absorb the harmful gaseous emissions from AM production activities, additional equipment or accessories need to be installed leading to higher machine and labor costs. Therefore, it is critical to jointly consider both environmental sustainability and cost for AM process. However, in current literature, most existing studies follow empirical approaches and lack theoretical estimation and prediction capability. Hence, there is an urgent need to analytical model the environmental sustainability and cost of AM.

Therefore, motived by (1) the increasing concerns (i.e., energy consumption, GHG emissions, VOC emissions, material waste, etc.) on the environmental sustainability of current AM processes; (2) the lack of combined cost analysis and environmental sustainability evaluation; and (3) the incomprehensive life cycle inventory databased for SLA AM, this research work is carried out aiming to study and evaluate the environmental sustainability and cost performance of projection-based SLA AM process.

More specifically, to advance the state-of-the-art of the research on energy consumption modeling of the SLA AM process, this dissertation is focused on theoretically modelling the energy consumption from each subsystem of SLA AM process, and using Design of Experiment (DOE) methodology to validate the model and further explore the effects of multiple process parameters and their interactions on the total energy consumption. Response Surface Methodology (RSM) is also used to obtain the optimal combination of process parameters in order to minimize the overall energy consumption. In addition, the associated GHG emission reduction is also estimated. Furthermore, to characterize and study the TVOC emissions from SLA AM processes, an analytical model is established and validated experimentally. To reduce the TVOC emissions as well as any possible health risks caused by the TVOC emissions, two effective emission control strategies are proposed and implemented in SLA AM process. Using the methodologies from energy consumption and TVOC emission modeling, AM batch production method is assessed. Finally, the cost analysis and life cycle assessment will be conducted. Furthermore, to estimate the cost of projection-based SLA AM process, a theoretical cost model is established that can tackle different production layouts including simple one-off production, non-mixed batch production, and mixed batch production. An optimization problem is formulated based on the cost model aiming to reduce the cost while maintaining production throughput and achieved surface quality by selecting appropriate values of process parameters (layer thickness and stratification angle). In addition, sensitivity analysis is performed to identify the key cost drivers in the current AM market.

1.4 Research Framework

Based on the above literature review and motivations, the research goal of this dissertation is to advance the state-of-the-art in the environmental and economic sustainability evaluation for SLA process by theoretically modeling multiple sustainability measures (i.e., energy consumption, VOC emission, and cost performance) and exploring opportunities for enhancing the environmental and economic sustainability through production layout selection as well as production process planning. The research framework is proposed as shown in Figure 7.

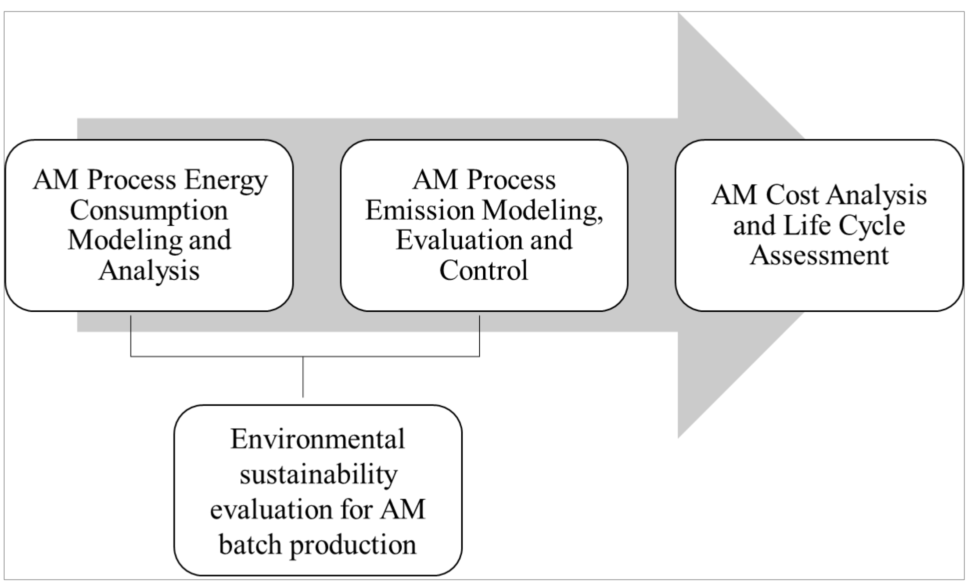

Figure 7. The proposed research framework

The rest of this dissertation is organized as follows. The energy consumption of SLA process is studied in Section 2, including the theoretical modeling, experimental validation and the investigation on the relationships between energy consumption and process parameters. Next, the VOC emission model is established and experimentally validated in Section 3. The cost modeling and optimization are performed in Section 4. Finally, the summary and future work of this dissertation are discussed in Section 5.

2. ENERGY CONSUMPTION MODELING AND ANALYSIS IN STEREOLITHOGRAPHY ADDITIVE MANUFACTURING

(Previously published as "Yang, Y., Li, L., Pan, Y., and Sun, Z., 2017. Energy Consumption Modeling of Stereolithography-based Additive Manufacturing Toward Environmental Sustainability. Journal of Industrial Ecology 21(S1) S168-S178.")

The energy consumption of SLA AM process is studied in this section. First, the SLA AM process mechanism is introduced in Section 2.1. Then, the theoretical model for energy consumption is established in Section 2.2. Next, experiment design is illustrated in Section 2.3. The model validation and factorial analysis are shown in Section 2.4. Finally, the conclusion of this part of the research is discussed in Section 2.5. Note that the majority of the content presented in this Chapter has been previously published in (Y. Yang et al., 2017).

2.1 Stereolithography Additive Manufacturing Process Introduction

As the most popular desktop 3D printer, the SLA AM process has been mostly used in indoor environments. It has a faster production speed comparing to other AM processes, contributed by its innovative image projection method by exposing 2D cross section images instead of scanning them with laser beam (Pan et al., 2012b). Besides, it has ability to produce a wide variety of shapes (Reeves, 2009) while ensuring good quality and reasonable costs. Generally, the SLA AM process provides more freedom for designers as some process parameters in the process can be configured and changed. Such process parameters include layer thickness, curing time, and other parameters in the building files. In addition, geometry related parameters can also be adjusted in the control software.

As presented in Figure 8, the SLA process is comprised of a computer, a material tank with transparent bottom, a building platform, a Z stage, a Digital Micro-Mirror Device (DMD), a UV light source, and a lens. All components are stationary during production process except the building platform which moves along the Z stage (in vertical direction), allowing the part to be built on the platform layer-by-layer. The material tank contains liquid resin, which is solidified by the UV light source based on the layer image projected by DMD.

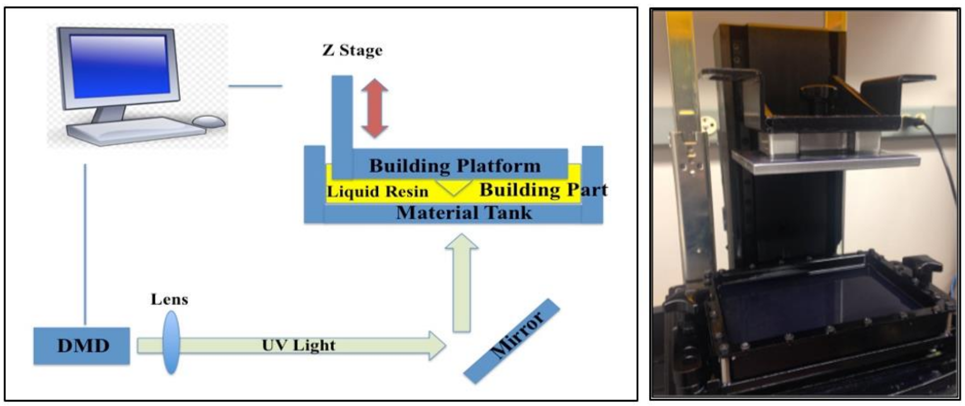

Figure 8. The Stereolithography process diagram and image

The production processes are summarized as follows. First, the 3D geometry built in CAD software is imported into the SLA machine control software and sliced into layers of 2D images with uniform layer thickness. Then, the control software generates the building files including all the process parameters that the machine requires to build the designed part, such as material type, layer thickness, layer image, curing time, etc. After the building files are sent to the SLA machine, the building platform moves down to the liquid resin and touches the bottom of material tank as the starting position before the actual building process, which is also called “home” position. To start the production, DMD projects the first layer image on the bottom of the building platform through the transparent material tank so that UV light can cure the certain exposure area. During UV curing process, the liquid resin transforms to a non-tacky solid (Bajpai et al., 2002). After the first layer is solidified, the building platform moves up along the Z stage by the distance of layer thickness, preparing the new building surface for the next layer. Afterwards, according to the building files, the DMD automatically projects the next layer image. These procedures are repeated until the part is finished. Then, the building platform moves up to its original position. The procedure is also illustrated in Figure 9.

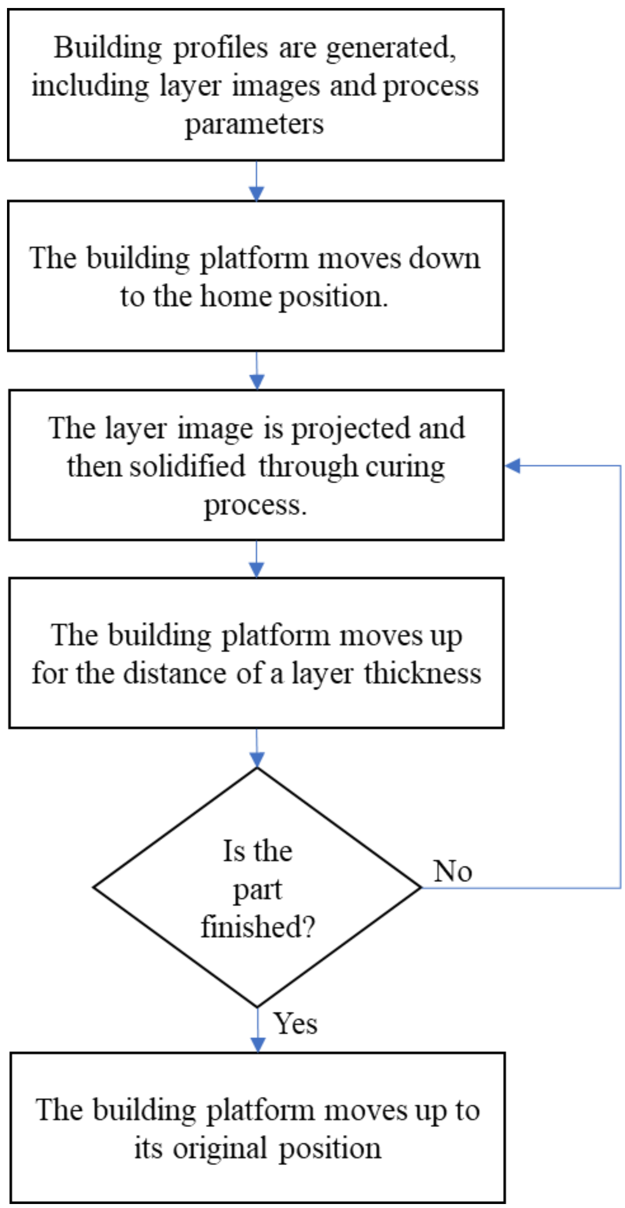

Figure 9. The Stereolithography process flowchart

2.2 Additive Manufacturing Process Energy Consumption Modeling

As illustrated in Figure 10, the SLA AM process contains multiple subsystems with their corresponding functionalities, i.e., layer image projection, UV curing, building platform movement, lighting, and fan cooling. Each subsystem contributes different portions of energy consumption. Thus, it is critical to mathematically model the energy consumption for the overall production process as well as for each subsystem.

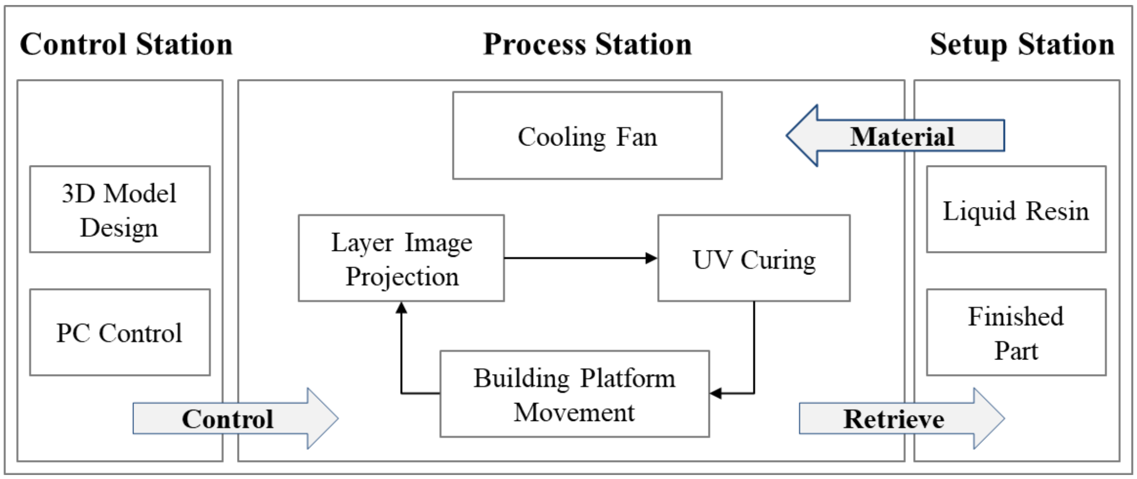

Figure 10. The Stereolithography subsystem illustrations

It should be noted that some subsystems with minor contribution regarding energy consumption are not included in the mathematical model, such as layer image projection and lighting. The energy consumption for each subsystem is modeled as follows.

<u>(1) Energy Consumption of UV Curing Process</u>

For a specific part geometry with a total height of h and layer thickness of d, the total number of layers K can be calculated through dividing h by d. For the ith layer, the UV curing energy consumption e_{curing} can be calculated as follows.

$$e_{curing} = \frac{P_{UV} \times t_i}{a} \tag{1}$$

In Equation (1), P_{UV} is UV light source power output; and a is a constant determined by the UV source characteristics, which can be obtained by Equation (2).

$$a = \eta_1 \times \eta_2 \times \eta_3 \tag{2}$$

In this equation, η_1, η_2, and η_3 are the UV lighting efficiency, the ratio of effective wavelength over the total wavelength, and the material absorptivity for a specific UV source, respectively. They can be obtained from machine documentation. In addition, t_i in Equation (1) is curing time for the ith layer, and it can be calculated by Equation (3).

$$t_i = \begin{cases} t_1 & i \in [1, i_b] \\ t_1 - s \times (i - i_b) & i \in [(i_b + 1), i_t] \\ t_2 & i \in [(i_t + 1), (h/d - 3)] \\ t_1 & i \in [(h/d - 2), (h/d)] \end{cases} \tag{3}$$

Equation (3) describes the relationships between curing time and the layer that is being processed. From the first layer to layer i_b, the curing time is t_1. In order to ensure that several layers at the beginning can be fully cured, t_1 is usually longer than solidification needs. Starting from the layer (i_b+1), curing time decreases from t_1 to t_2 with a linear rate s (seconds per layer) until layer i_t. Thus, the layers from (i_b+1) to i_t are defined as "transition layers" due to the transition of curing time from t_1 to t_2. After that, the curing time maintains at the value of t_2 for the layers from (i_t+1) to (h/d-3). These layers are defined as "stable layers" because they have uniform curing time. The curing time for the last three layers changes back to t_1 to ensure that the part is fully cured with good quality.

Therefore, the total energy consumption due to UV curing for all K layers is calculated as follows.

$$E_{curing} = \sum_{i=1}^{K} \frac{P_{UV} \times t_i}{a} \tag{4}$$

(2) Energy Consumption of Building Platform Movement

During the production process, the material tank maintains the same position all the time, while the building platform moves along vertical direction (Z stage). An electric stepper motor provides power for the vertical movement of the building platform, and its power output is represented by P_m . The energy consumption of this movement can be calculated by the following equation.

$$E_{platform} = \sum_{i=1}^{K} (P_m) \times t_i \tag{5}$$

(3) Energy Consumption of Cooling System

The energy consumption of cooling fan can be formulated as follows.

$$E_{cooling} = P_{cooling} \times t_{cooling} \tag{6}$$

In this equation, $P_{cooling}$ is the power output of cooling fan, and $t_{cooling}$ is the cooling time which is slightly longer than the production time.

Thus, the total energy consumption can be obtained by:

$$E_{total} = E_{curing} + E_{platform} + E_{cooling} \tag{7}$$

2.3 Experimentation

2.3.1 Experiment Design

The energy consumption mathematical model is established by modeling the energy consumption contributed from each subsystems of the SLA machine. Different parameters such as the number of the layers and curing time are integrated into the energy consumption of these subsystems. However, we do not know if the interactions between different parameters are significant or not. The interaction between different parameters means that the response of the energy consumption may be different when changing one parameter while keeping the other parameter at different levels. To study such interactions, multiple runs of experiments with different combinations of input parameters need to be implemented. The DOE methodology can provide the smallest number of runs in which the influences of a given number of input parameters on the response can be studied. It is more efficient than one-factor-at-a-time strategy (Montgomery, 2012). Therefore, in addition to the mathematical model of energy consumption, DOE is also used to design the experiment with different combinations of the input parameters so that the interactions between different parameters can be examined; the optimal parameter setting to minimize the energy consumption can be identified; and the mathematical model can be validated.

Table 2. Description of experimental control factors

Symbol	**Control Parameter**	**High Level (+1)**	**Low Level (-1)**	**Center Point**
A	Layer thickness d (mm)	0.05	0.025	0.0375
B	Curing time for stable layers t_2 (s)	6.5	4	5.25
C	Curing time transition rate s (s/layer)	2.7	1.125	1.9125
D	Orientation	90^o	0^o	45^o

* The detailed definitions of Factors *B* and *C* can be found in Equation (3).

The detailed configurations of the experiment designed by DOE are illustrated as follows. A two-level factorial design is adopted to establish the experiments including four controllable factors (or input parameters), i.e., layer thickness (d), curing time for stable layers (t_2), curing time transition rate (s), and orientation as shown in Table 2. Factors layer thickness, curing time for stable layers and curing time transition rate are process-related factors, while the orientation is a geometry-related factor. Two levels, i.e., low and high, for each factor are considered. Two replications are used. Moreover, four center points are added to the experiment design to "provide a measure of process stability and inherent variability and to check for curvature" (Serrano et al., 2016). A 2^4-factorial design combined with four center points results in total 36 experiment runs.

In the SLA AM machine control software, the default value for the layer thickness is 0.025mm, which is used as the low-level value in the experiment, where the higher level of this parameter is set as 0.05mm. The curing time for stable layers is originally 6.5s and it is used as the high-level value, where a low-level value of 4s is investigated in the experiments. The transition rate from longer curing time to shorter curing time is set as 1.123s per layer for low-level value and 2.7s for high-level value. The orientation is considered for low-level value of 0º and high-level value of 90º. These four input factors are coded as +1, -1 and 0 in Minitab, where +1 denotes the high level; -1 denotes the lower level; and 0 denotes the center point. Coded variables are used to ensure that factors with different numerical value scales can be compared to determine the significance of the factors' impact on the response, in this case, the overall energy consumption.

2.3.2 Experiment Apparatus

The SLA AM machine used for experimentation is Perfactory Micro EDU 3D printer. It is the smallest desktop 3D printer in size with the highest resolution of 150μm for XY axis and 50 to 100μm for Z axis (EnvisionTEC, 2015). Equipped with state-of-the-art direct light projection technology from Texas Instruments, it can achieve a precise layer image projection by DMD. The LED UV light source is used for curing process, solidifying the liquid resin to solid form. With all mentioned advanced machine specifications, this 3D printer can achieve a fast building speed up to 20mm/hour for full building capacity (100*75*100mm). In addition, seven types of materials can be built through this AM machine, including "LS600 M (used in the experiments), HTM140

M, ABS Tough M, E-Denstone M Ivory, E-Denstone M Tough, ABS Flex M, and Superflex M" (EnvisionTEC, 2015). The measurement equipment is the single clamp-on power meter CW10 by Yokogawa, with a maximum AC/DC current of 600A and a maximum AC/DC voltage of 1000V. It can also measure power factor, frequency, resistance, etc. The measured data was recorded every five seconds.

Due to the exist power factor, the current and voltage data obtained from the power meter aforementioned cannot be directly used to calculate the electricity consumption. Since the Perfactory Micro EDU 3D printer adopts single-phase power supply, its power factor can be measured by the wattmeter-ammeter-voltmeter method (Prasanna Kumar et al., 1995), and thus the real power consumption $P_{real\ power}$ can be calculated by the following equation.

$$\begin{aligned} P_{real\ power} &= power\ factor \times S_{apparent\ power} \\ &= power\ factor \times (U_{measured} \times I_{measured}) \end{aligned} \tag{8}$$

In this equation, $S_{apparent\ power}$ stands for the apparent power calculated using the measured voltage $U_{measured}$ and the measured current $I_{measured}$. Test runs are conducted to obtain the power factor of the system, which turns out to be 0.85.

2.4 Model Validation and Factorial Analysis

In this section, the experimental results when the SLA machine is working under default conditions are first presented, then the factorial analysis results are illustrated, and finally the part surface quality (surface roughness) when changing different process parameters is compared.

2.4.1 Base Case Results Using Default Condition

Under the default working conditions (i.e., A is 0.025mm, B is 6s, C is 1.125s/layer, and D is 0º), the measured energy consumption is 278,707.35J for building a threaded bolt with height of

1cm. The absolute percentage error compared to the calculated result using the proposed mathematical model (264,531.672J) is around 5.36%. The difference may come from using of rated power of each subsystem provided by the machine nameplate documentation rather than the actual power in the mathematical model. The actual power output from each subsystem cannot be obtained, due to the limitations of measuring equipment and the complexity of subsystems. Therefore, the power rating acquired from machine documentation is used as an approximate calculation, hence leading to the error.

Table 3. The energy consumption results comparison with literature

Case No.	AM Process	Material	Capacity Utilization (%)	Layer Thickness (mm)	SEC (kWh/kg)	Reference
1	SLS	PA2200	3.41%	0.12	39.20	(Kellens et al., 2014)
2		PA2200	3.02%	0.15	40.30	
3		PA3200	2.50%	0.15	36.00	
4	SLS	Polymer	/	0.15	40.1	(Luo et al., 1999)
5	SLA	Epoxy resin	/	0.15	32.47	
6	FDM	ABS	/	0.4	115.20	
7	SLA	LS600M	0.05%	0.025	175.95	Measured results

The measurement results based on the default condition are compared with results from existing literature as listed in Table 3. Kellens et al. (2014) investigated the SLS process through experiments using three types of materials with different layer thicknesses. Luo et al. (1999) compared three AM processes: SLS, SLA, and FDM, and they found that FDM has the largest energy consumption. The energy consumption from our results using the default configuration (Case No. 7) is relatively higher than the results reported in literature.

The main reasons for causing the different energy consumption results (as shown in Table 3) are considered as follows. First, different types of AM processes adopt diverse manufacturing technologies and produce dissimilar types of material, thus they might possess different energy consumption characteristics. Second, the capacity utilization (the ratio of printed part volume and the maximum building volume provided by the AM machine) also influences the specific energy consumption. According to Baumers et al. (2011b), a lower capacity utilization possibly leads to larger SEC for some types of AM processes. Compared to a 2.50%-3.41% capacity utilization ratio from Kellens et al. (2014), the lower capacity utilization ratio in this research is another probable reason why the SEC is high. Third, the layer thickness in this research is much smaller than the others, leading to better product quality as well as higher energy consumption.

2.4.2 Factorial Analysis Results

The factorial analysis results are shown in Table 4 with a significance level of 0.05. According to the factorial analysis results shown in Table 4, Factors *A, B, D*, and interactions *A*B, A*D, B*D, C*D, A*B*C, A*B*D, B*C*D* are of great, and Factor *C* as well as interactions *A*C, B*C, A*C*D, A*B*C*D* lack significance. As illustrated in the table, Factors *A*, *B* and *D* have a substantial effect on the response due to their direct influence on production time, which is also the reason for the high significance of interactions between these three factors. Although Factor *C* also affects the production time, it only lasts for a very short period (usually 25 layers). Therefore, the effects from Factor *C* are negligible. From the observations from the SLA production process, the duration of Factor *C* changes with Factor *D*, where *C* lasts longer when the part is built horizontally and shorter when the part is built vertically. Therefore, the interaction between Factors *C* and *D* is important.

Table 4. The factorial analysis results

Factor	Sum of Squares	P-Value
A	2.12e11	0.000
B	5.83e9	0.000
C	2.20e6	0.556
D	6.27e9	0.000
*A*B*	1.41e8	0.000
*A*C*	9.89e5	0.692
*A*D*	3.29e8	0.000
*B*C*	1.37e7	0.150
*B*D*	7.95e7	0.002
*C*D*	6.78e7	0.004
*A*B*C*	4.38e7	0.015
*A*B*D*	2.27e8	0.000
*A*C*D*	3.82e5	0.805
*B*C*D*	5.80e7	0.006
*A*B*C*D*	1.38e7	0.640

Given the statistical analysis result, the Pareto chart of the standardized effects is shown in Figure 11, and the normal plots of the standardized effects are shown in Figure 12. It can be observed from the figure that Factor *A* has a negative impact on the output *E* (total energy consumption), while Factors *B* and *D* have a positive impact on the output *E*. The interaction terms of *A*D*, *A*B*D*, *B*D*, *C*D*, *B*C*D*, *A*B*C*, and *B*C* have relatively minor influence on the output *E*, where Factor *C* and interaction *A*C* have basically ignorable effects. In addition, the normality assumption of the statistical model is validated by the normality plot, where the significance of factors and interactions are also presented.

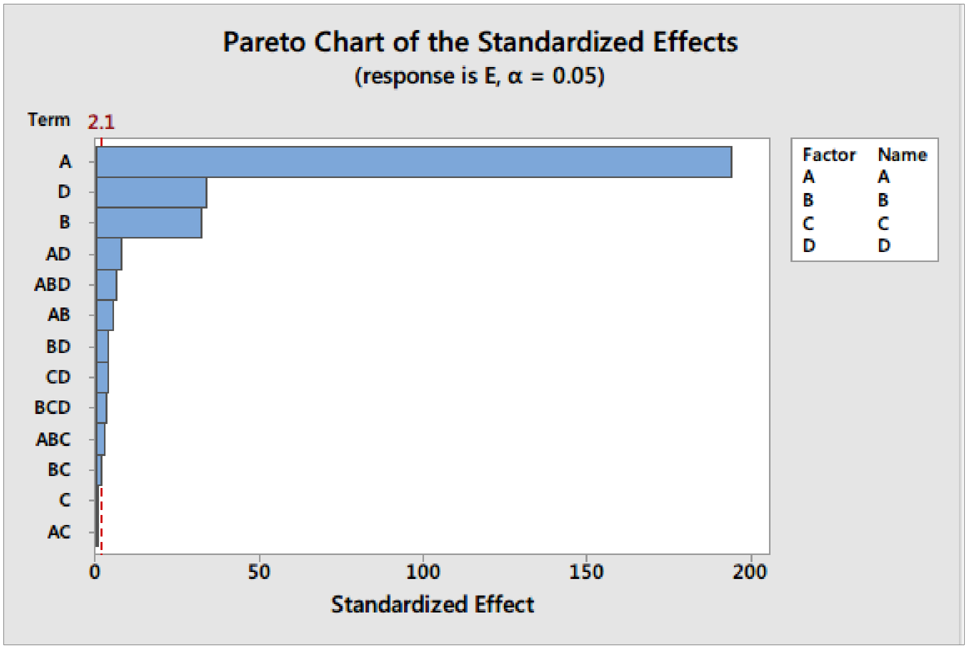

Figure 11. Pareto chart of the standard effects

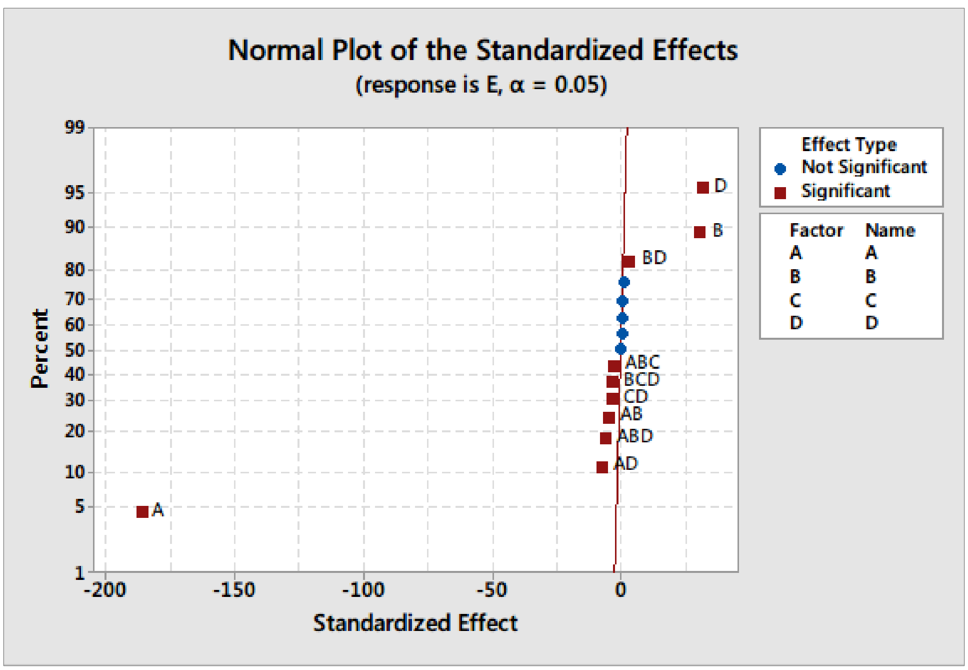

Figure 12. Normality plot of the standard effects

The model adequacy is checked as shown in Figure 13. The normality and histogram plots are shown to confirm the assumption of normality. The residual versus observation order plot is used to illustrate that the residuals are independently distributed. In addition, the residual versus fitted value plot is adopted to check the constant variance assumption. After the model adequacy checking, to improve the accuracy of obtained statistical analysis results, the statistical model is refined by removing all insignificant terms from the initial statistical model. It should be noted that although Factor C is not significant, some interactions that include Factor C are significant, which are therefore kept in the refined statistical model.

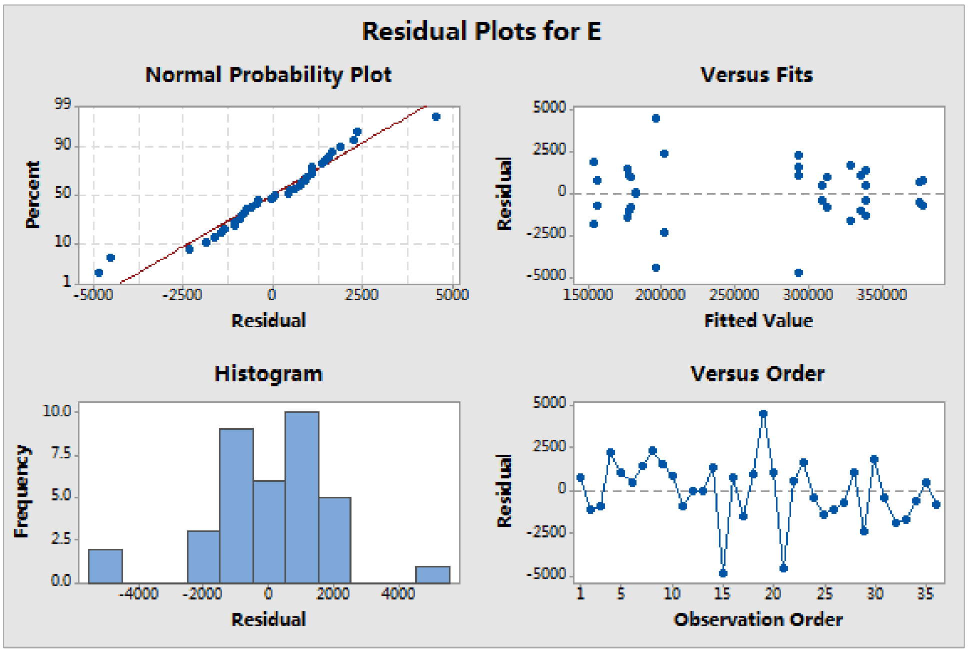

Figure 13. Model adequacy checking for statistical model

The corresponding refined statistical model can be written as follows. The regression model adequacy check is shown in Figure 14. In this equation, *CtPt* is the center point.

$$\begin{aligned} E &= 259{,}101 - 81{,}321A + 13{,}492B + 13{,}993D - 2096A\times B \\ &-3207A\times D + 1576B\times D - 1456C\times D - 1170A\times B\times C \\ &-2662A\times B\times D - 1346B\times C\times D + 34{,}970CtPt \end{aligned} \tag{9}$$

Based on the factorial analysis, the optimal levels of the input factors that can lead to minimized energy consumption are identified using RSM as shown in Figure 15. A higher level of Factor *A*, and lower level of Factors *B* and *D* would lead to the minimum energy consumption for this SLA AM process. In addition, Figure 16 illustrates the surface plots regarding the Factors *A*, *B*, and *D* and the total energy consumption of the process. The measured energy consumption using the optimal combination of control parameters is 127,707.35J. About 54.16% reduction in energy consumption can be achieved compared to default working condition where the measured energy consumption is 278,707.35J.

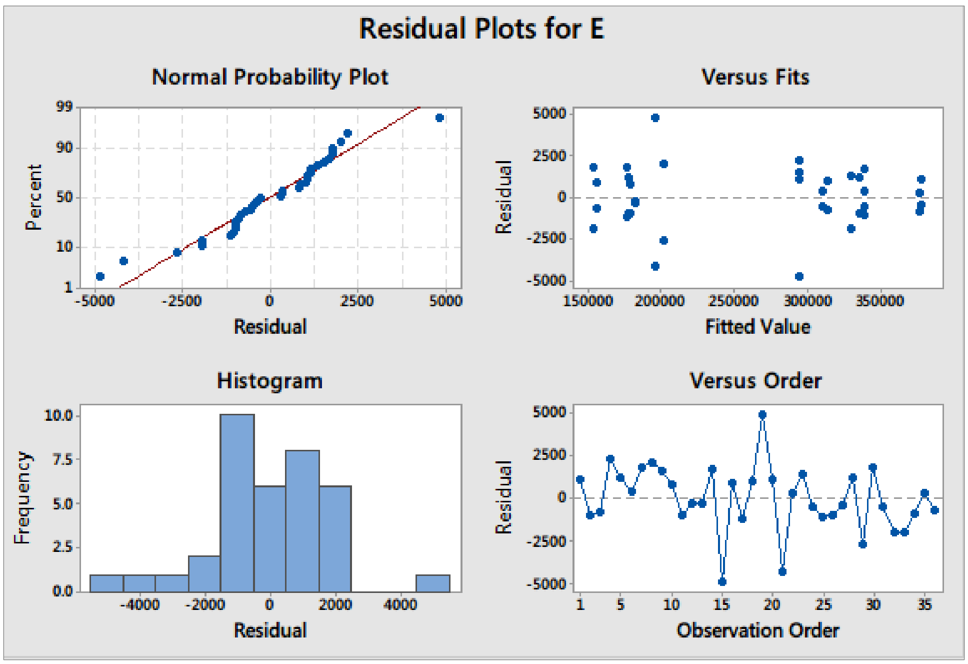

Figure 14. Model adequacy checking for refined statistical model

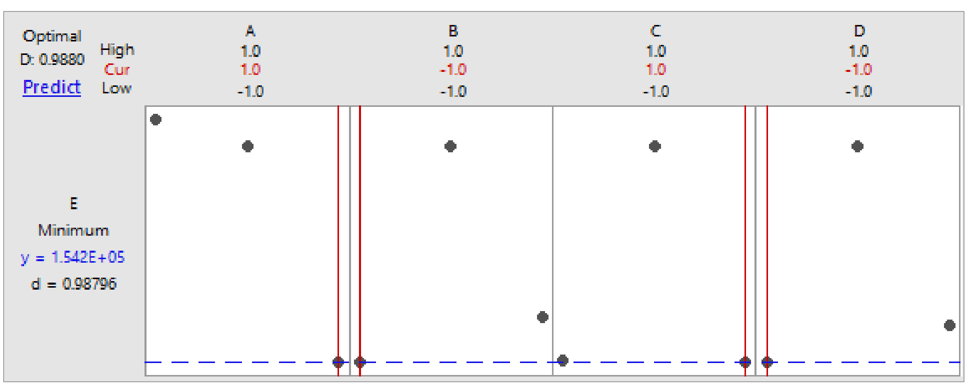

Figure 15. Response surface optimization results

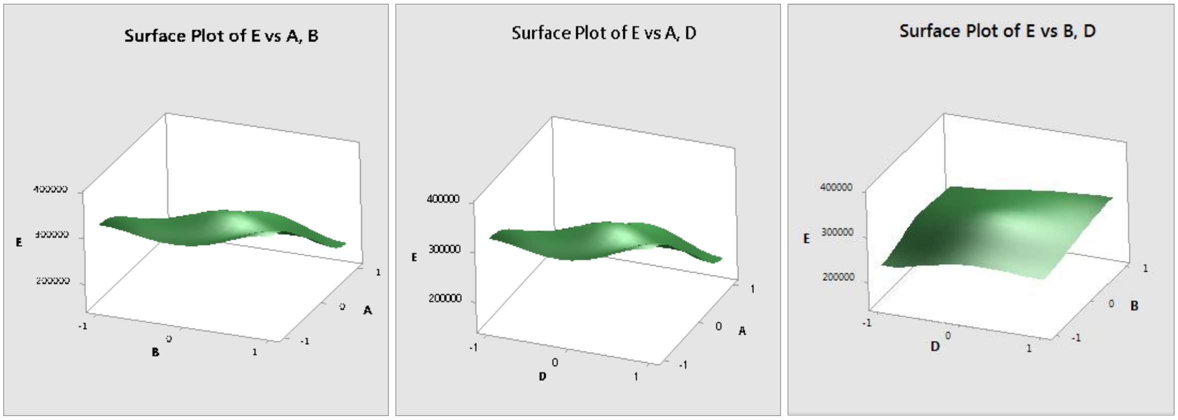

Figure 16. Surface plots of Factor A, B, and D

The optimal parameters obtained can also reduce GHG emissions due to the reduction of electricity consumption of the process. According to U.S. Energy Information Administration, one kWh electricity generation may incur 1.52 pound Carbon Dioxide (CO_2) emission (EPA, 2010). For a regular factory equipped with the SLA machines, in order to produce 3000 parts per month, the CO_2 emission can be reduced from 414.96 pounds per month (under default condition) to 191.52 pounds per month (with optimal factors).

2.4.3 Part Surface Quality Comparison

The reduction of energy consumption through adopting the optimal combination of process parameters leads to possible reduction of part quality. Therefore, the part quality is investigated and compared under different process parameter combinations. A Micro-Vu vision system is utilized to obtain the surface images, and a 3D optical profiler is used for surface roughness measurement.

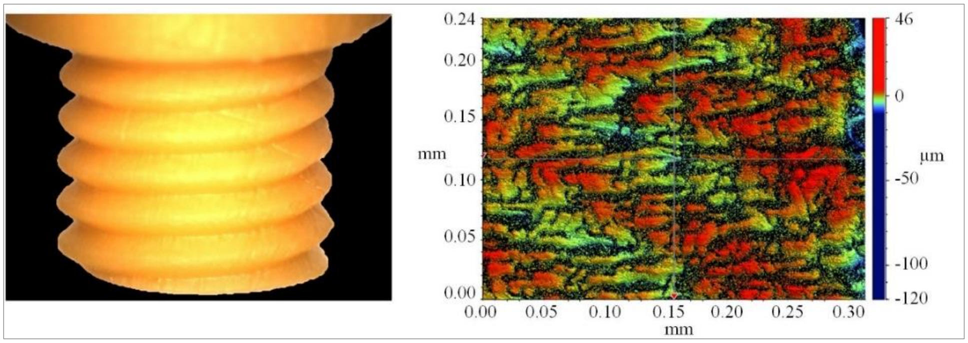

Figure 17. Part surface quality (default condition)

Figure 17 shows the surface quality of the part that is fabricated under default conditions, which indicates good quality for the screw thread. For the part shown in Figure 18, the layer thickness is changed to 0.05mm with all the other parameters set to the default conditions. In Figure 19, the curing time for stable layers is set to a lower level. The optimized condition is presented in Figure 20, where the layer thickness is 0.05mm; curing time for stable layers is 4s; curing time transition rate is 1.125s/layer; and the orientation is 0º. R_a, the arithmetic mean surface roughness, is measured to indicate different levels of surface roughness of the thread on the parts. All the results of R_a are within the order of 10 μm magnitude (from 2.599 μm to 4.946 μm). Therefore, we can conclude that the reduction of energy consumption can be achieved without significantly sacrificing the part surface quality.

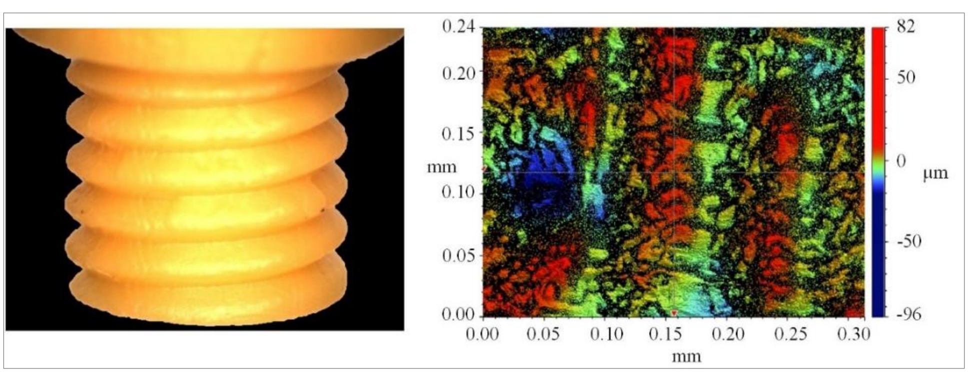

Figure 18. Part surface quality (different layer thickness)

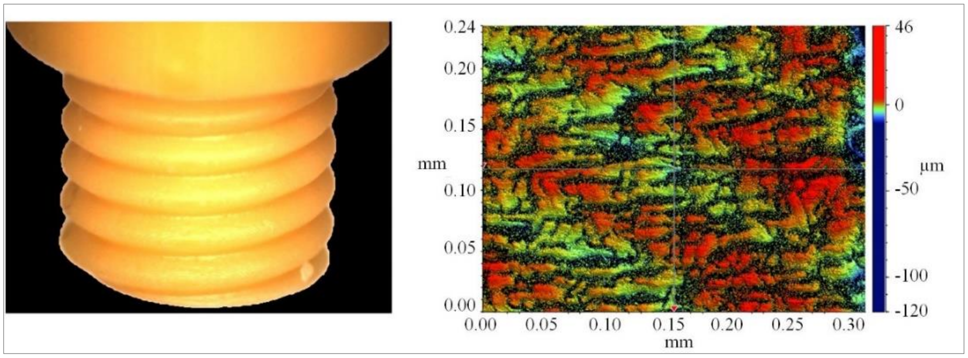

Figure 19. Part surface quality (different curing time)

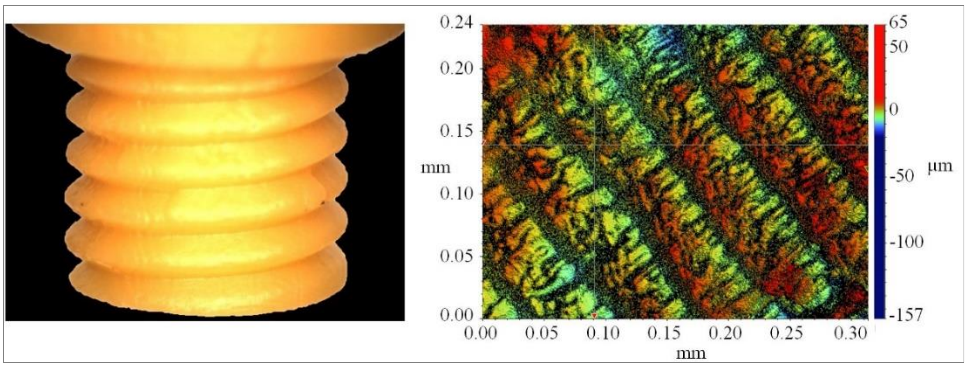

Figure 20. Part surface quality (optimized condition)

2.5 Section Conclusion

In this section, the mathematical model for the energy consumption of the SLA AM process is established. Experiments are conducted, and the results are analyzed to validate the proposed mathematical model. In addition, using the RSM, we obtained the optimal parameters that can lead to minimized energy consumption, compared to the default parameter configuration. Significant energy saving and CO_2/GHG emission reduction can be achieved while maintaining the product quality.

3. VOLATILE ORGANIC COMPOUND EMISSION MODELING, EVALUATION AND CONTROL IN STEREOLITHOGRAPHY ADDITIVE MANUFACTURING

(Previously published in (Yang and Li, 2018a) as “Yang, Y., and Li., L., 2018. Total Volatile Organic Compound Emission Evaluation and Control for Stereolithography Additive Manufacturing. *Journal of Cleaner Production* 170(1): 1268-1278”, and published in (Yang and Li, 2017) as “Yang, Y., and Li, L., 2017. Evaluation of Environmental Sustainability for Additive Manufacturing Batch Production. ASME 2017 12th International Manufacturing Science and Engineering Conference. P. V002T01A038. DOI: 10.1115/MSEC2017-2957.” The copyright statement can be found in Appendix.)

In this section, the process emission evaluation methodologies are presented to theoretically estimate the TVOC emission for indoor environments equipped with SLA machines. To achieve this goal, an analytical model is established to describe the TVOC emission from two sources: the raw material volatilization and AM production activities. The developed model is then validated through experiments. Using this model, the TVOC emission concentration for an indoor space can be estimated with or without a 3D printer in operation. Furthermore, current commercial emission control technology is tested and compared to two new methods proposed in this section.

Proper emission control strategies can provide promising opportunities to improve the environmental sustainability for AM and lower the associated health risks by significantly reducing the TVOC emission towards cleaner production. The results of the proposed emission evaluation methodology will help provide understandings on the emissions of AM processes, evaluate the emission level, and establish emission guidelines for AM processes. Accordingly, the rest of this section is organized as follows. The TVOC emission modeling is presented in Section

3.1. The experimental design is introduced in Section 3.2 and includes the experimental procedure and apparatus. The experimental results and discussion are provided in Section 3.3. Finally, this section is concluded in Section 3.4.

3.1 Total Volatile Organic Compound Emission Modeling

Generally, the TVOC emissions in indoor environments equipped with SLA machines come from the raw material liquid resin volatilization and AM production activities. The volatilization process is modeled based on the physical properties of the liquid resin and chemical reactions from the volatilization process. However, the AM-caused TVOC emissions cannot be easily modeled because they may be affected by different parameters such as printing time and printing surface temperature. In addition, the total mass of AM-caused TVOC might be at different levels with different production parameters including batch size (or printing surface area) and material type (or material viscosity). Therefore, the AM-caused TVOC emissions are modeled by combining theoretical estimation and experimental approaches.

The total TVOC emissions can be expressed as follows.

$$ER(t)_{total} = ER(t)_{AM} + ER(t)_{volatilization} \tag{10}$$

In this equation, $ER(t)_{total}$ refers to the total TVOC emission rate in an indoor space at time t; $ER(t)_{AM}$ denotes the AM-caused emission rate; and $ER(t)_{volatilization}$ represents the emission due to the volatilization process. In Equation (10), the AM-caused emission rate is calculated using Equation (11) which is adapted from (Afshar-Mohajer et al., 2015).

$$ER(t)_{AM} = (C(t)_{AM} - C_{reference}) \cdot V \cdot AER \tag{11}$$

In this equation, $C(t)_{AM}$ is the TVOC concentration at time t; $C_{reference}$ is the reference TVOC concentration measured when the AM machine is not in operation; V is the volume of the indoor environment, and AER is indoor air exchange rate.

Based on preliminary understanding on AM-caused emissions, the following two relationships shown in Equation (12)-(13) are proposed and are validated through experimentally.

$$C(t)_{AM} = f(T,t) \tag{12}$$

$$E_{AM} = \int_{t=T_s}^{t=T_e} ER(t)_{AM} = f(S_p, V_m) \tag{13}$$

T is printing surface temperature; E_{AM} stands for the total TVOC mass emitted from the AM process, which is the integration of $ER(t)_{AM}$ from Ts (subscript s stands for the AM production starting time) to Te (subscript e represents the AM production ending time). Furthermore, E_{AM} is a function of Sp and Vm, where Sp represents the printing surface area and Vm is the viscosity of the liquid resin. More comprehensive relationships between AM-caused emissions and multiple parameters are explored and proposed based on experimental results.

Additionally, the emission rate due to the volatilization process $ER(t)_{volatilization}$ can be calculated by using Equation (14).

$$ER(t)_{volatilization} = Q \times M \times S \tag{14}$$

In this equation, Q denotes the mass transfer rate (g-moles/cm^2-sec); M represents the molecular weight (g/g-mole); and S denotes the surface area (cm^2). The mass transfer rate across an interface Q can be written as follows.

$$Q = K\frac{\rho_v}{RT} \tag{15}$$

In Equation (15), K denotes the mass transfer coefficient (cm/sec); ρ_v represents the vapor pressure of the liquid (kPa); R denotes the universal gas constant ($8.314\times10^3 cm^3$-kPa/g-mole-K); and T stands for the absolute temperature (K). As proposed in (Mackay and Matsugu, 1973), the mass transfer coefficient K can be expressed as a function of wind speed and liquid pool size, which in our model is the liquid resin tank size.

$$K = 0.0220 \times {v_z}^{0.78} \times \Delta z^{-0.11} \times Sc^{-0.67} \tag{16}$$

v_z represents the wind speed (cm/sec); ΔZ stands for the length of the air-liquid interface in the direction of flow (cm); and Sc denotes the Schmidt number. The air viscosity μ, air density ρ, and diffusivity D can be approximated using the following equations as stated in (Arnold and Engel, 2001).

$$\mu = -9.426\times10^{-5} + 1.610\times10^{-5}\times\sqrt{T} \tag{17}$$

$$\rho = 0.352\frac{P}{T} \tag{18}$$

$$D = \frac{4.09\times10^{-5}\times T^{1.9}\times\sqrt{\frac{1}{28.97}+\frac{1}{M}}}{P\times M^{0.33}} \tag{19}$$

P denotes the ambient air pressure.

In summary, the AM-caused emission rate $ER(t)_{AM}$ is calculated by combining the theoretical relationships shown in Equations (11)-(13) and experimental approach, and the volatilization-caused emission rate $ER(t)_{volatilization}$ is calculated by Equations (14)-(19).

3.2 Experimentation

3.2.1 Experiment Procedure

To validate the proposed TVOC emission model and further explore the relationships described in Equation (12) and Equation (13), a set of experiments are designed and conducted in a 41m^2 indoor laboratory with a ceiling height of 3 meters, average room temperature of 25.2ºC and relative humidity of 44.6%. The laboratory is equipped with one SLA machine, and it has not held any AM production for more than two days to ensure accurate measurements. To measure the TVOC emissions, methyl methacrylate is selected as the target gas by treating all types of VOCs as one. According to the data sheet for the liquid resin e-shell 600 (DeltaMed, 2014), methyl methacrylate is the most volatile compound. In addition, the 3D printing material LS 600 M is a methyl methacrylate-based resin (Lucite, 2010). Therefore, methyl methacrylate is used as the target as for any TVOC emission measurement. The experiment procedure is designed as follows:

(1) Real-Time Total Volatile Organic Compound Measurement

To investigate the relationship described in Equation (12), three real-time measurement stages are performed. In the first stage, the reference TVOC concentration is measured when the AM machine is not in operation (10min). By doing so, the reference TVOC concentration can indicate whether the liquid resin emits VOCs when the machine is not in operation. Furthermore, the reference TVOC concentration can be used to calculate the actual AM-caused emissions by subtracting the reference concentration from the measured results obtained in the second stage. $C_{reference}$ in Equation (11) is calculated using the TVOC concentration measured in this stage. Within the reference measurement period, preparations for the production process are conducted, including importing the CAD file into the control software, setting up the software, etc.

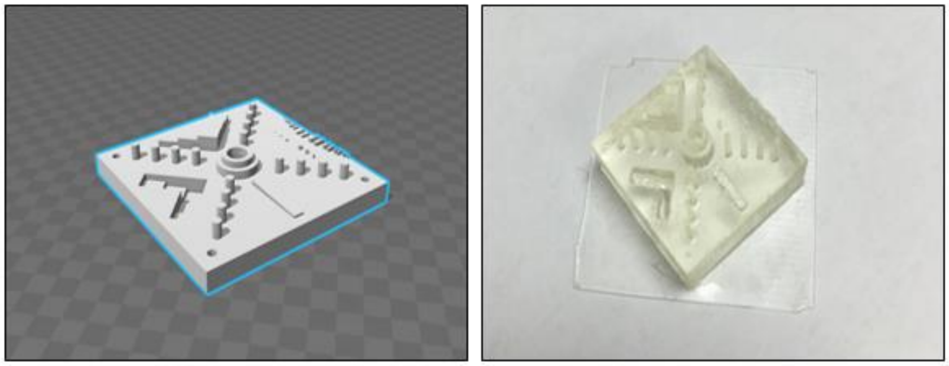

Figure 21. The standard test artifact, adapted from (Moylan et al., 2014)

The second stage deals with the AM production measurement (93min). In this stage the SLA machine is in continuous operation to fabricate an object, in this study a 3D test artifact adapted from the National Institute of Standards and Technology (NIST) (Moylan et al., 2014) is used and shown in Figure 21. By measuring the TVOC concentration in this stage, a clear profile of how the TVOC concentration varies over time throughout the printing stage can be obtained. Possible parameters such as printing surface temperature, which are suspected to be related to the TVOC emissions, can also be investigated. The third stage includes the post-processing measurement (10min). Within this stage, additional VOCs might be released from the over curing and ethanol cleaning procedure. Based on the emission trend and the time where the emission peaks occur, targeted emission control strategies can be proposed.

(2) Total Mass of AM-Caused Total Volatile Organic Compound

As illustrated in Equation (13), different types of liquid resins with different viscosities are expected to cause diverse emission levels. Therefore, e-shell 600 (EnvisionTec, 2014) and LS 600M (EnvisionTec, 2019) materials are both printed for comparison, with a viscosity of 339.8mPa.s and 140mPa.s, respectively. In addition, different printing surface areas are explored by changing the production batch size (i.e., the number of the test artifacts in one batch). The three different printing surface areas that are investigated are 25cm^2, 50cm^2, and 75cm^2.

3.2.2 Experiment Apparatus

The SLA machine used in this study is a Perfactory Micro EDU 3D printer, which is the smallest high resolution desktop 3D printer (XY resolution of 150 µm and dynamic Z resolution of 50-100 µm) (EnvisionTec, 2015). Multiple material types can be printed using this AM machine. The SLA production procedure illustration and the 3D printer are shown in Figure 8. Before the actual production process, the 3D geometry is sliced into layers with uniform layer thickness using the 3D printer control software to generate a series of building profiles. Then based on the building profiles, the 3D printer control system creates a certain exposure area on the building platform, where the layer image is reflected. Next the layer is cured by the Digital Micromirror Device (DMD) and UV light source. After one layer is finalized, the building platform moves up a distance equivalent to the layer thickness, and the layer image is automatically replaced by the next layer image. This building process repeats until the product is finished. After the production process is finished, the printed product is removed from the building platform and post-processed. The finished product is overly cured by the UV light to ensure the strength of the surface layer. Next, it is cleaned by an ultrasonic cleaner to remove the liquid resin attached on the surface of the product. Finally, the support structure is removed if necessary.

The TVOC measurement equipment is located approximately one meter away from the SLA printer. Due to the possible hazardous effects, the operator must wear mask and goggles. The hardware used for the TVOC concentration measurement is the MiniRAE 3000 by Honeywell, which is one of the most advanced handheld VOC monitors in the market. It is equipped with a 10.6 eV photoionization detector (PID) and can measure ranges of 0-15,000 ppm. Calibration is performed before any measurement.

3.2.3 Response Surface Methodology

To explore and estimate the relationships proposed in Equation (12) and Equation (13), RSM is used. Equation (12) defines the relationship between the response variable, $C(t)_{AM}$ (the TVOC concentration at time t), and two explanatory variables, T (the printing surface temperature) and t (time). Equation (13) describes the relationship between the response variable, E_{AM} (the total TVOC mass emitted from the AM process), and two explanatory variables, S_p (the printing surface area) and V_m (the viscosity of the liquid resin). By adopting the RSM in Minitab, a clear illustration of the relationship between the response variable and explanatory variables can be obtained from measurements, so that the relationships proposed in Equation (12) and Equation (13) can be more clearly defined.

3.2.4 Risk Assessment

The risk assessment for emissions in indoor environments helps evaluate the emission health risks that are imposed on humans. It also provides a scientific foundation for regulatory guidelines. In this research, two types of risks are considered: cancer related risks and non-cancer related risks. The cancer risks, more specifically the inhalation cancer risk, is calculated through the following equation.

$$CancerRisk = EC \cdot URF \tag{20}$$

EC is exposure concentration (g/m^3) and URF is unit risk factor (g/m^3). A cancer risk of less than one in a million is usually considered negligible. For the non-cancer hazard evaluation, the hazard quotient (HQ) is used. HQ is calculated by the following equation.

$$HQ = \frac{MC}{RfC} \tag{21}$$

In this equation, *MC* is the mean concentration ($\mu g/m^3$), and *RfC* is the inhalation reference concentration without adverse effects. Both Equation (11) and Equation (12) are adapted from (Sivak, 2006).

The most popular method of calculating the cancer and/or non-cancer risks from literature is to calculate them for each type of VOCs in the gas mixture, and then add them as the overall risks (de Gennaro et al., 2013). Due to the limited access to the composition of VOCs mixture, methyl methacrylate, which is the target gas of TVOC, is used to obtain the *URF* and *RfC*, and the TVOC meausred concentration is used to find *EC* and *MC*.

3.2.5 Emission Control Strategy

For most commercial 3D printers in the market, the current technology for reducing emissions is by adding a machine cover. For strategy comparison and emission control purposes, two new strategies are proposed in this research. The first method is the usage of Titanium Dioxide (TiO_2) photo catalytic oxidation, where TiO_2 is used as a catalyst to oxidize the organic compounds in the gas phase (Jo and Kim, 2009). The second method uses activated Carbon absorption (Sidheswaran et al., 2012). These two proposed strategies are incorporated into the SLA process and tested through experiments.

3.3 Results and Discussion

In this section, model calculation results are compared with experimental results to validate the mathematical model. Also, current commercial emission control technology and new proposed strategies are compared.

3.3.1 Total Volatile Organic Compound Emission Model Calculation

The TVOC emissions due to the liquid resin volatilization are calculated using Equations (14)-(19). The AM-caused TVOC emissions are modeled and estimated based on proposed relationships in Equation (12) and Equation (13) as well as experimental approaches. The parameter setup and the calculation are illustrated in Figure 22. The TVOC concentration caused by the volatilization process based on the model calculation is 106.504µg/m3.

Parameter	Value (source)
S (surface area)	75 cm^2 (material tank property)
M (molecular weight)	100.121 g/mol (common knowledge)
T (temperature)	298.65 K (experiment environment)
V_z (wind speed)	1.2 cm/s (estimated experiment environment)
Δz (length)	2 cm (estimated experiment environment)

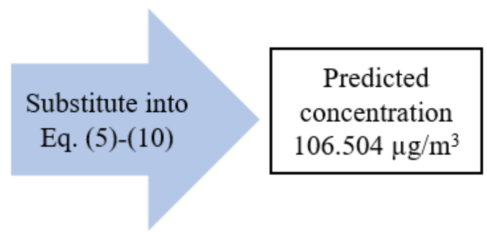

Figure 22. The VOC emission model calculation

3.3.2 Real-Time Total Volatile Organic Compound Measurement

The real-time measurement results are shown in Figure 23. The total measurement time is 6,780s (113min), where the first 600s are used for the reference concentration measurement, the AM production period is from 601s to 6,180s, and the post-processing stage is from 6,181s to 6,780s. The primary vertical axis (left) is the TVOC concentration (μg/m^3), and the secondary vertical axis (right) is the emission rate (μg/s), calculated using Equation (11). The peak TVOC concentration level is defined as the maximum concentration which is significantly larger than the neighbor results. According to the emission profile in Figure 23, three peaks can be clearly identified.

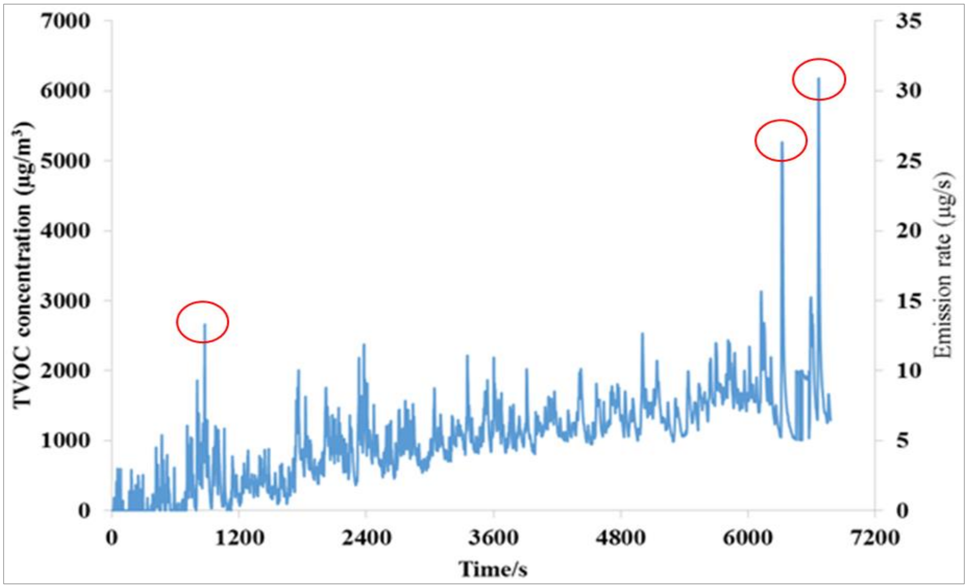

Figure 23. The real-time TVOC measurement (batch size=1, e-shell 600 resin)

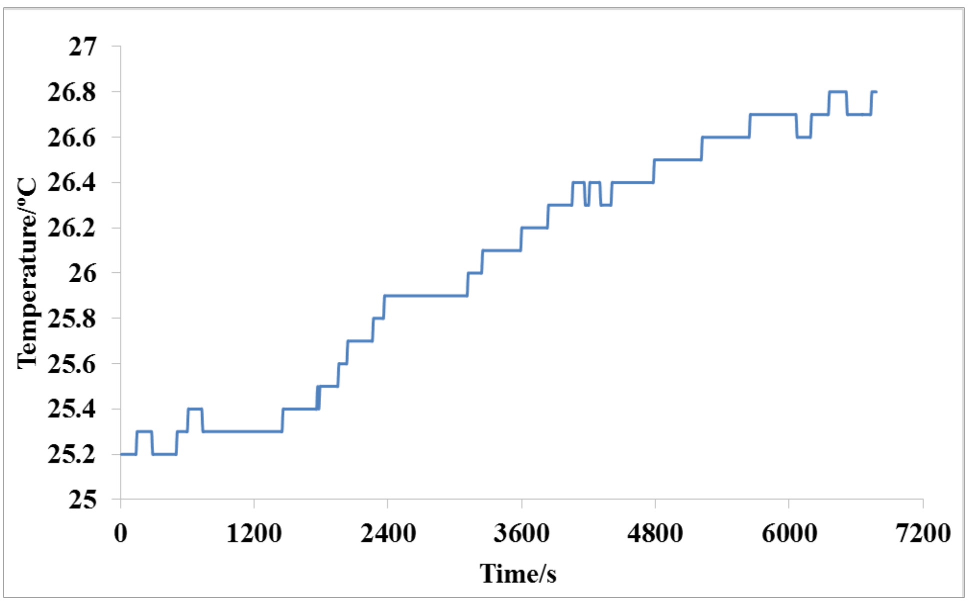

Figure 24. The real-time temperature profile (batch size=1, e-shell 600 resin)

The first peak is 2,629μg/m^3, which occurs after 877s (14.62min) from the measurement and 4.62min after the printing starts. The occurrence of this peak is due to the start of AM production activities. The second peak is 5,235μg/m^3, and it occurs at 6,323s (105.38min) and 2min after the printing ends. This is because after production is finished, the building platform rises and releases a huge amount of TVOC. The third peak (6,177μg/m^3) is around 6,668s (111.13min) and only 1.87min before the measurement ends. This is possibly because of the post-processing activities such as ethanol cleaning and over curing.

During the reference measurement stage (0s to 600s), the TVOC concentration fluctuates. During the AM production stage (601s to 6180s), the TVOC emissions rise to the first peak, then drop down and finally maintain an increasing trend while fluctuating. In the post-processing stage (6,181s to 6,780s), the TVOC concentration has two peaks and then drops down. The mean TVOC concentrations for the three stages are 122.70μg/m^3, 1,052.71μg/m^3, and 1,774.15μg/m^3, respectively; and the overall average is 1,034.25μg/m^3. Compared to the mean TVOC concentration from the first stage 122.70μg/m^3, the proposed model predicts the value as 106.504μg/m^3, which has less than 14% prediction error.

The temperature profile is also obtained using a temperature sensor installed under the liquid resin container, and it is used to better understand and analyze the increasing TVOC trend. From the temperature results shown in Figure 24, an increasing trend is identified. Therefore, the rise in TVOC emissions in the AM production period might be triggered by the increasing temperature, which might cause more liquid resin volatilization or other chemical reactions. To further understand the relationship between time, temperature, and TVOC concentration, the RSM is adopted. The regression model obtained is shown in Equation (22).

$$C(t)_{AM} = -5{,}133{,}831 - 0.0086t + 228426T - 2541T \cdot T + 0.000195t \cdot T \qquad (22)$$

In this equation, the unit for the TVOC concentration caused by AM production, $C(t)_{AM}$, is in μg/m^3; the time, t, is in second; and the temperature, T, is in ºC.

The response surface and the residual plots are shown in Figure 25 and Figure 26, respectively. The average TVOC levels from the reference stage is 122.70μg/m^3, which falls into the liquid resin volatilization range (i.e., 68.997 to 1,728.238μg/m^3) calculated by the proposed model. In addition, Equation (22) provides a specific relationship for Equation (12).

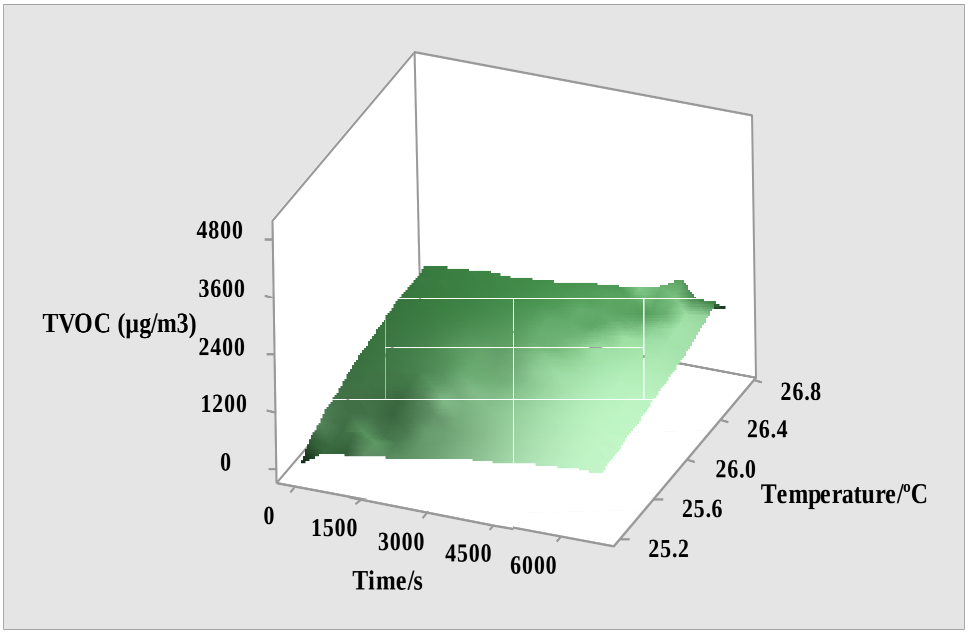

Figure 25. The response surface plot for $C(t)_{AM}$

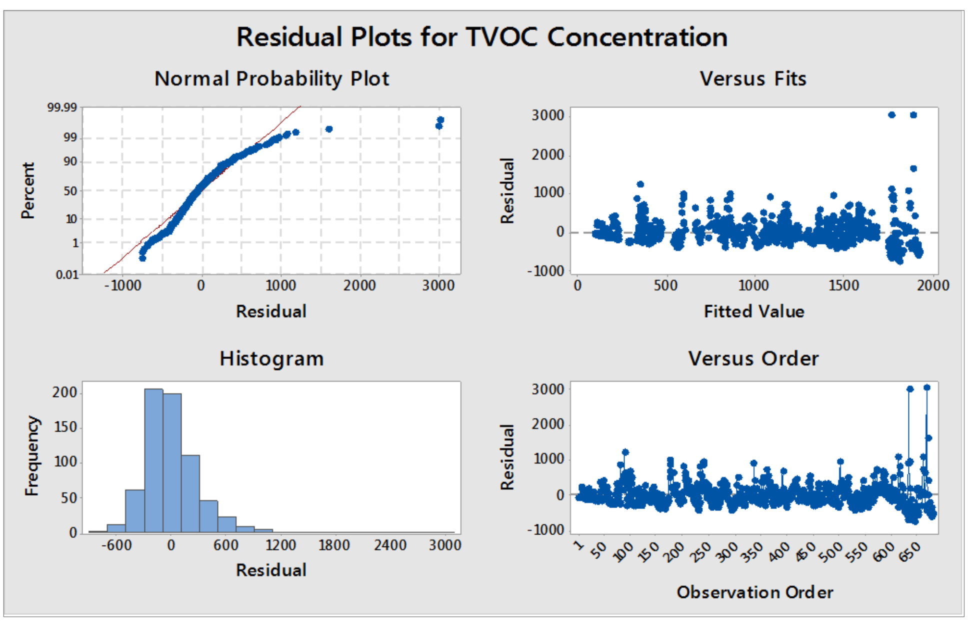

Figure 26. The residuals plots for $C(t)_{AM}$

The real-time measurement results and model calculation results are compared to those found in literature as shown in Table 5. The results of this study have a larger average TVOC concentration level and peak value obtained by Afshar-Mohajer et al. (2015). The difference is possibly due to the different AM processes and target gases used for the measurement. In addition, the experimental results from this dissertation have similar TVOC concentration levels (both average level and peak level) compared to the studies conducted by Helmis et al. (2007) and Daisey et al. (1994). In addition, some recommended or advised TVOC emission levels from different studies and institutions are also shown in Table 5 for comparison purposes. For example, 500μg/m^3 is proposed and recommended by ALS Environmental Institute as the maximum TVOC concentration for indoor environments. It should be noted that currently there lacks a more comprehensive TVOC emission level standard.

Table 5. The real-time TVOC measurement compared to current literature

	Environment	**Target VOC**	**Average (μg/m3)**	**Peak (μg/m3)**
Real-Time Measurement	Indoor lab with SLA process	Methyl Methacrylate	1,034.25	6,177
(Afshar-Mohajer et al., 2015)	Indoor lab with BJ process	Isobutylene	510	1,750
(Helmis et al., 2007)	Dentistry clinic	Isobutylene	1,300	2,000-5,500
(Daisey et al., 1994)	Office building	39 VOCs	510	7,000
(Environmental, 2009)	Indoor building	/	/	500
(Kim et al., 2011)	Sensitive facilities (Korea)	/	/	400
(KEI, 2004)	Indoor (Japan)	/	/	400
(Kim et al., 2011)	Indoor (Finland)	/	/	200-600
(Kim et al., 2011)	Indoor (Germany)	/	/	1000-3000

3.3.3 Total Mass of AM-Caused Total Volatile Organic Compound

To better understand how the printing surface area and material viscosity affect the AM-caused TVOC emissions, further experiments are conducted with different combinations of parameters and their results as shown in Table 6.

Table 6. The comparison results of AM-caused TVOC

Case No.	Printing Surface Area (cm^2)	Material Viscosity (mPa.s)	E_{AM} (μg)
1	25	339.8	26,994.02
2	50	339.8	31,124.00
3	75	339.8	33,126.39
4	25	140	15,104.24
5	50	140	27,075.50
6	75	140	49,341.45

According to the results from Cases 1, 2, and 3 (material type e-shell 600), the total AM-caused emissions increase as the printing surface area increases. When the printing surface area changes from 25cm^2 to 50cm^2, the total AM-caused emissions increase by 15.30%; however, there is only a 6.43% increase when the printing surface area changes from 50cm^2 to 75cm^2. It can be concluded that the printing surface area affects the total AM-caused emissions less significantly given a larger printing surface area for e-shell 600. From the results for Cases 4, 5, and 6 (material type LS600 M), the total AM-caused emissions increase by 79.26% when increasing the printing surface area from 25cm^2 to 50cm^2, and it increases by 82.23% when further increasing the printing surface area from 50cm^2 to 75cm^2. The difference in increasing percentages might be caused by the material type, such that different resins may release dissimilar amounts of emissions during AM production and respond to printing surface areas differently.

As shown from Figure 27 to Figure 32, although Cases 1 through 6 have different results regarding the total AM-caused emissions, their real-time TVOC concentration profiles are similar. The above comparison validates the relationship proposed in Equation (12). Both printing surface area and material viscosity affect the total AM-caused emissions. The relationship obtained based on the experimental results is shown in Equation (23) and has an R-squared of 97.94%.

$$E_{AM} = \int_{t=T_s}^{t=T_e} ER(t)_{AM} = -16553 + 752S_p + 140.2V_m + 3.27S_p \cdot S_p - 2.813S_p \cdot V_m \tag{23}$$

In this equation, the unit for total AM-caused TVOC emissions, E_{AM}, is in µg; printing surface area, S_p, is in cm^2; and material viscosity, V_m, is in mPa.s.

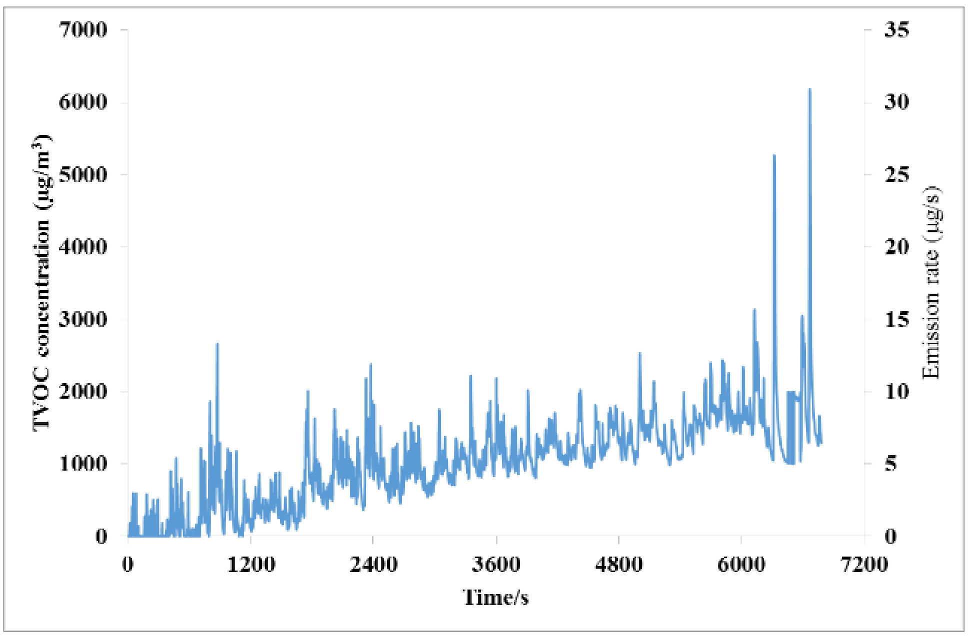

Figure 27. The real-time TVOC measurement for Case 1

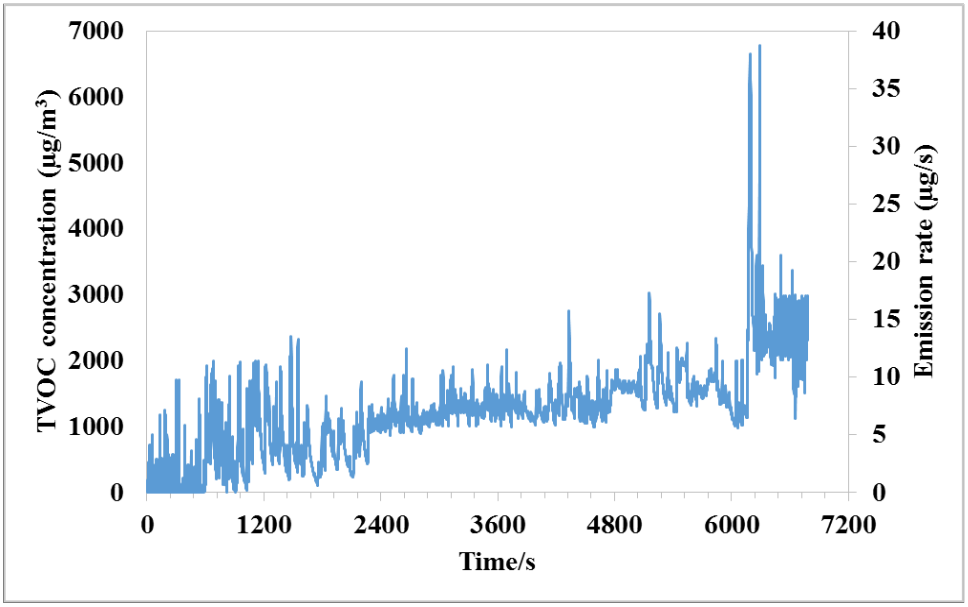

Figure 28. The real-time TVOC measurement for Case 2

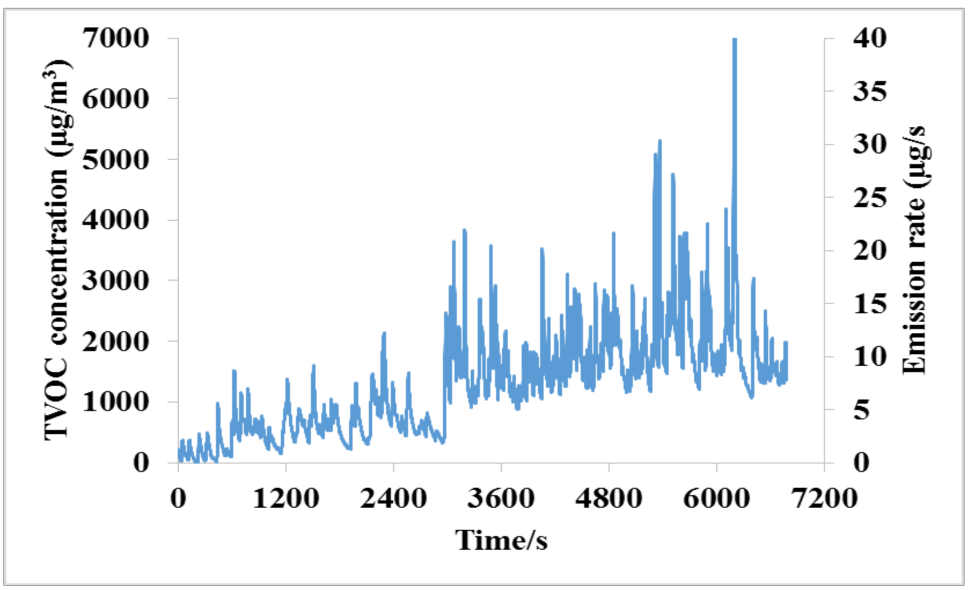

Figure 29. The real-time TVOC measurement for Case 3

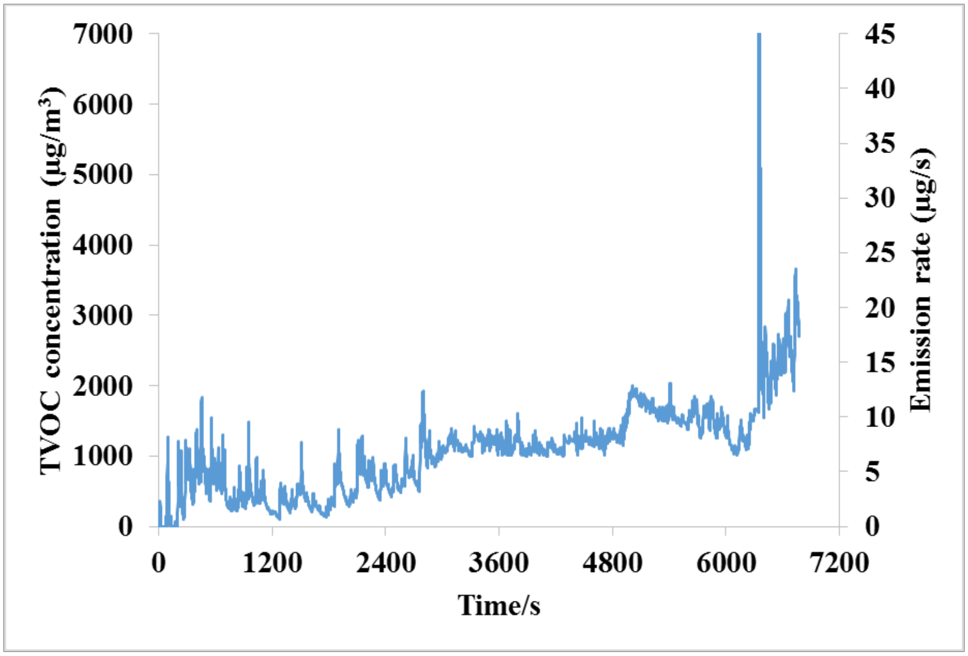

Figure 30. The real-time TVOC measurement for Case 4

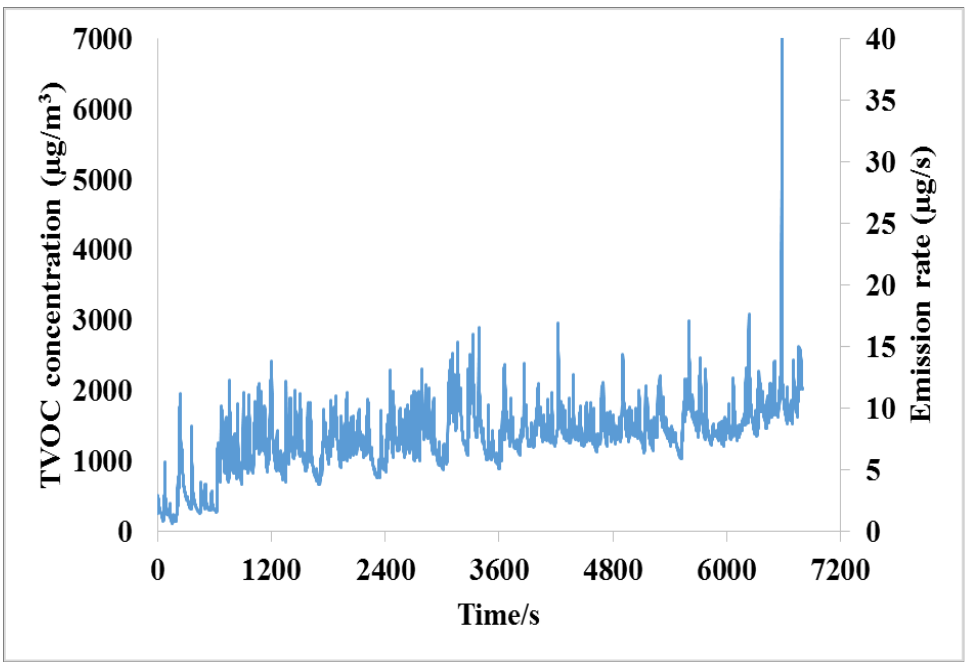

Figure 31. The real-time TVOC measurement for Case 5

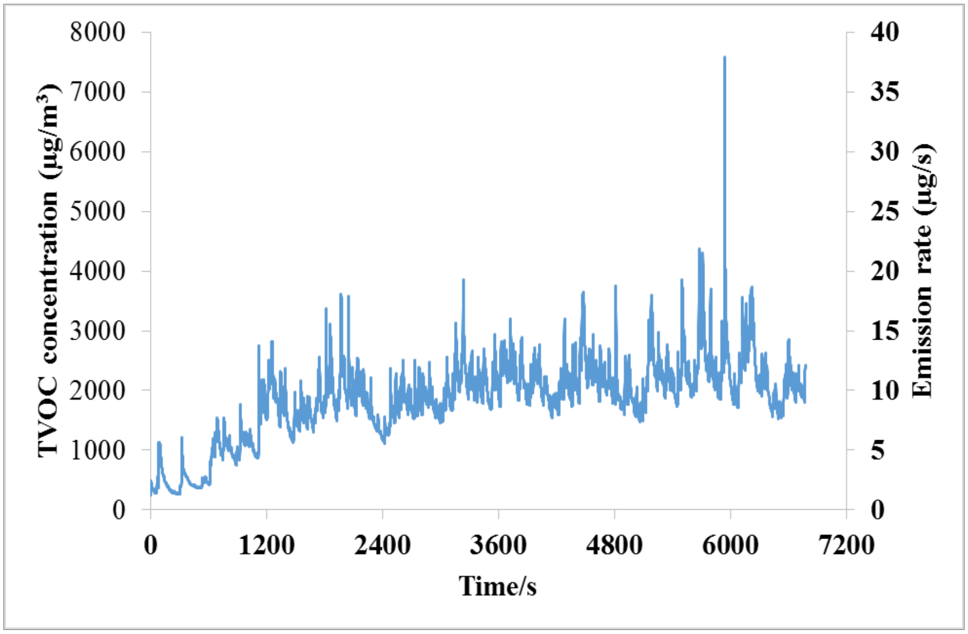

Figure 32. The real-time TVOC measurement for Case 6

The response surface and residual plots are shown in Figure 33 and Figure 34, respectively.

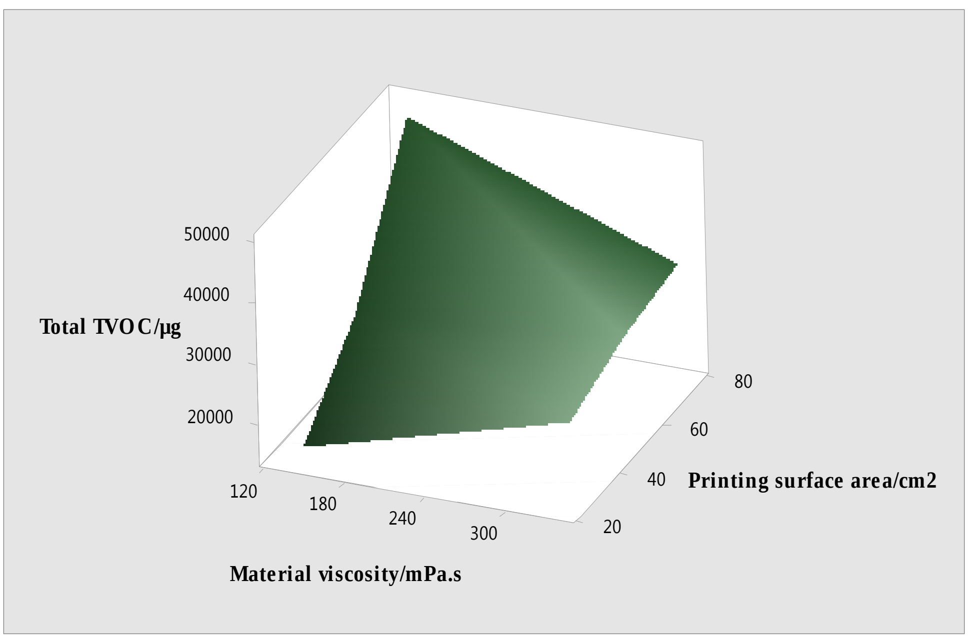

Figure 33. The response surface plot for E_{AM}

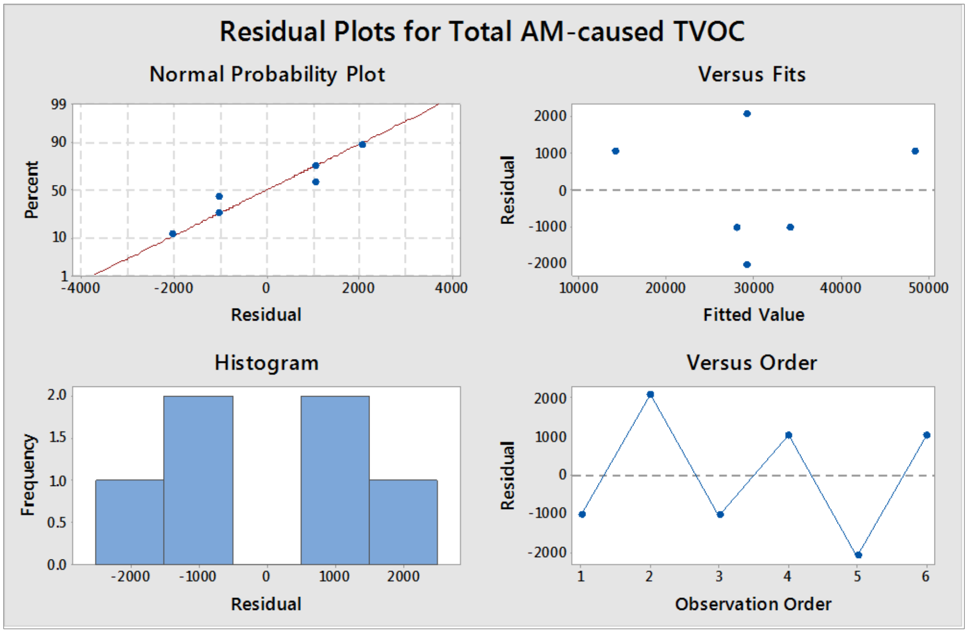

Figure 34. The residual plots for E_{AM}

3.3.4 Risk Assessment

According to the risk assessment methodology, two types of risks are calculated and evaluated: cancer risks and non-cancer risks. Methyl methacrylate, the target gas used for TVOC measurement, is not likely to be carcinogenic to humans because it has been evaluated in a few well-conducted studies and animal tests (United States Environmental Protection Agency, 2000). Therefore, the cancer risk for Methyl methacrylate is not considered in this research. On the other hand, according to the GSI chemical database by GSI Environmental Inc., *RfC* of methyl methacrylate is 0.7 mg/m^3, which is used for calculation.

Using the measured mean concentration of 1,034.25μg/m^3, *HQ* is calculated as 1.4775. Since *HQ* is greater than 1, it is possible that adverse health effects will occur. Based on the risk assessment, the SLA process emits hazardous gases and possibly causes health concerns and adverse effects on operators. Therefore, effective emission control approaches need to be proposed for the SLA process.

3.3.5 Emission Control Strategies

A comparison of the TVOC emissions for different strategies is shown in Table 7. The comparison between the original level and the commercial strategy shows a 91.64% decrease in average concentration from the reference stage, but no obvious reduction in overall average concentration and AM-caused emission. During AM production, TVOC still leaks through the machine cover. When the machine cover is lifted open for retrieving the finished product, a large amount of TVOC is subsequently released instantly leading to serious hazardous effects. By trying to entrap the TVOC inside the machine cover, TVOC is only temporarily reduced and when released suddenly at a much higher concentration can lead to even more serious health risks.

Table 7. The TVOC emission control strategies comparison

	Reference Average (μg/m^3)	**Production Average (μg/m^3)**	**Post-Processing Average (μg/m^3)**	**Overall Average (μg/m^3)**	**AM-Caused Emissions (μg)**
Original Level	122.70	1,052.71	1,774.15	1,034.25	26,994.02
Commercial Machine	10.26	1,100.92	2,148.61	1,096.86	31,659.06
Strategy 1	140.30	486.87	1,858.46	577.58	10,058.92
Strategy 2	0	292.52	661.65	299.29	8,491.09

The two proposed strategies have shown to significantly reduce the TVOC concentration in each stage, overall mean concentration, and AM-caused emissions. By implementing Strategy 1, the average concentrations from the reference value and the post-processing stages are not considerably reduced. However, the results in the three indexes (i.e., production average concentration, the overall average concentration, and AM-caused emissions) achieved 53.75%, 44.15%, and 62.74% reductions compared to the original level, respectively. The adoption of

Strategy 2 leads to reductions of the reference average concentration, the production average concentration, the post-processing average, the overall average, and AM-caused emissions by 100%, 72.21%, 62.71%, 71.06%, and 68.54%, respectively. The results show that the two proposed approaches can significantly reduce the TVOC emissions from the SLA process. The real-time TVOC concentration measurements for these three strategies are shown from Figure 35 to Figure 37.

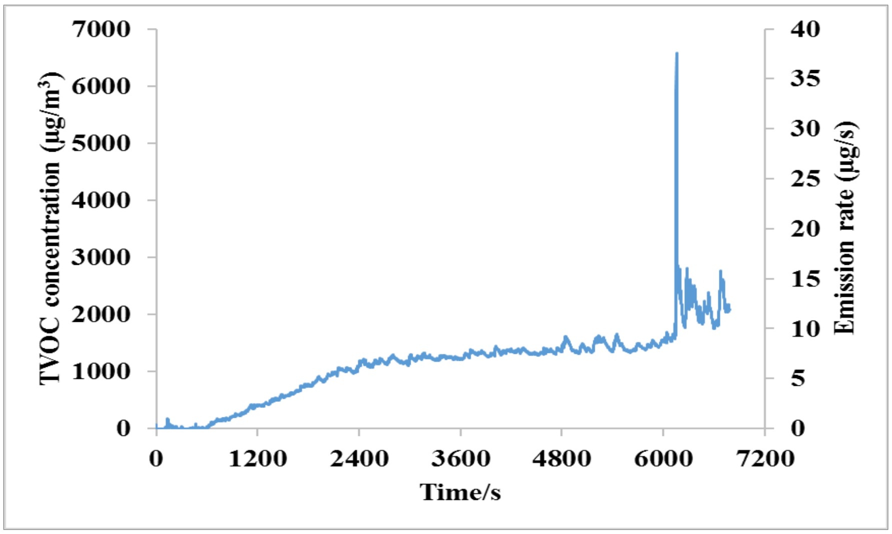

Figure 35. The real-time TVOC concentration when adopting commercial method

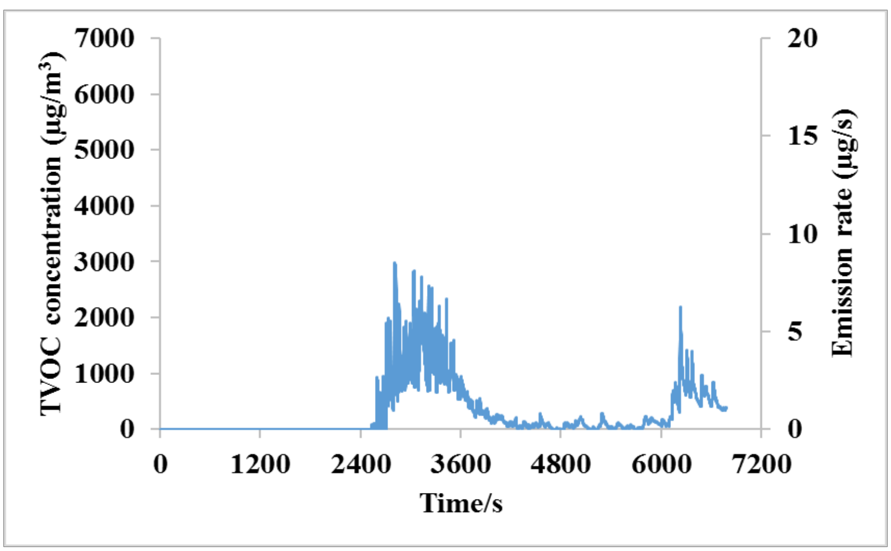

Figure 36. The real-time TVOC concentration when adopting proposed strategy 1

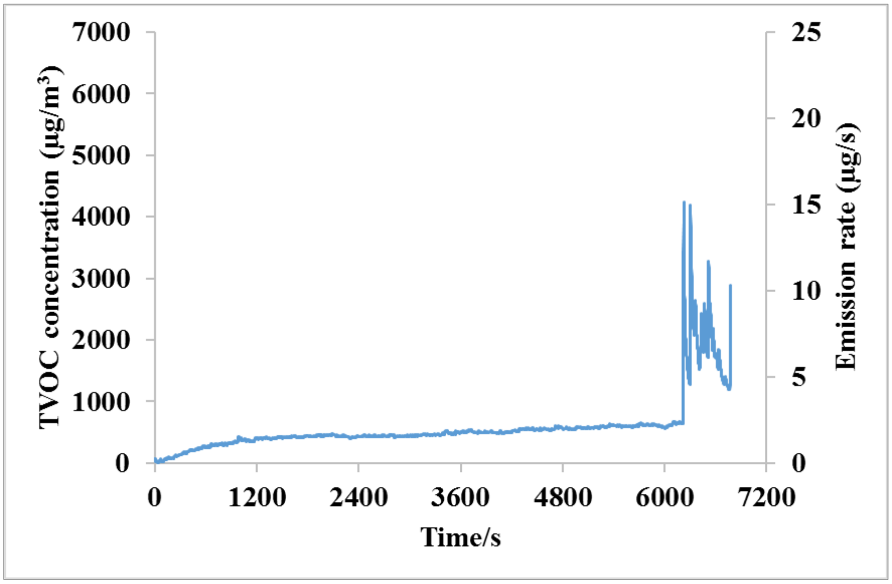

Figure 37. The real-time TVOC concentration when adopting proposed strategy 2

3.4 Section Conclusion

In this section, an analytical model is proposed to theoretically estimate the TVOC emission for indoor environments equipped with SLA machines, by considering emissions from both the raw material liquid resin volatilization and AM production activities. The emission model for the volatilization process is validated through experimental measurements. The preliminary relationships described in the proposed model concerning AM-caused emissions are further identified using the regression model obtained using RSM. Based on the experimental results, the TVOC emission levels are significantly higher than the reported value in literature and the recommended value reported by environmental agencies. Subsequently, two TVOC emission control strategies that use Titanium Dioxide photo catalytic oxidation and activated Carbon absorption, are suggested to promote cleaner AM processes. The two proposed emission control methods have been implemented and lead to 44.14% and 71.06% reductions in the average TVOC concentration and 62.74% and 68.54% in the TVOC caused by AM activities.

The analytic approach proposed in this section improves the understanding of the VOC emissions for AM processes by theoretically evaluating the emission level. Moreover, the emission control strategies tested in the experiments significantly improve the environmental sustainability of AM and reduce the health risks for operators. In addition, the emission control methods can be incorporated into the design of new AM processes towards environmental sustainability. The outcomes of this dissertation provide AM enterprises with practical guidelines for establishing emission standards, and further assist the development of sustainable AM.

3.5 Environmental Sustainability Evaluation for Additive Manufacturing Batch Production

Using the methodology proposed in the previous sections, environmental sustainability evaluation is performed for AM batch production by experimentally identifying the relationships between different batch production sizes and three key environmental performance metrics (i.e., energy consumption, emission, and material waste). To achieve this goal, experiments are designed to characterize the three chosen environmental aspects with different batch sizes, followed by experimental results and discussions. The outcomes of this part of the research will be used to aid the evaluation of AM batch production method from an environmental sustainability perspective, enhance the understanding of AM batch production performance from different environmental aspects, and facilitate the development and improvement of feasible AM batch production method.

3.5.1 Evaluation Methodology

To evaluate the environmental sustainability performance of the SLA process, three main factors, i.e., energy consumption, emission, and material waste, are considered. From the energy consumption perspective, the total energy consumed by the SLA process during the manufacturing period are calculated based on measured current and voltage. TVOC is considered as the target emission type, since it has been proven that a wide variety of VOCs are emitted during the thermal operation of such materials like ABS or PLA (Contos et al., 1995)(Rutkowski and Levin, 1986). Three different measurement stages are executed for TVOC emission: background measurement stage which refers to the period before the start of manufacturing, manufacturing measurement stage, and post-processing measurement stage when the finished part is retrieved for the removal of support material. The TVOC measurement equipment is placed 1 meter away from the SLA machine. After post-processing, the material waste is obtained by measuring the material usage (the weight difference of the material tank before and after manufacturing) and each final part's weight (after removing support material).

The experiment is designed with three different batch sizes (1, 2, and 3), where three aspects of environmental sustainability, i.e., energy consumption, TVOC emission, and material waste, are measured. The geometry of the part that is built in the experiment is derived from the standardized test artifact proposed by NIST (Moylan et al., 2014) with minor geometry size change and layer thickness of 0.025mm (manufacturing time 5580s).

3.5.2 Results and Discussions

Energy Consumption

The energy consumption results are shown in Table 8, where the total energy consumption refers to the total power usage by the SLA machine during the manufacturing period, and the specific energy consumption (SEC) represents the power usage per Kg of the printed part. When the batch size increases from 1 to 3, the total energy consumption remains constant, while the results for SEC drop dramatically.

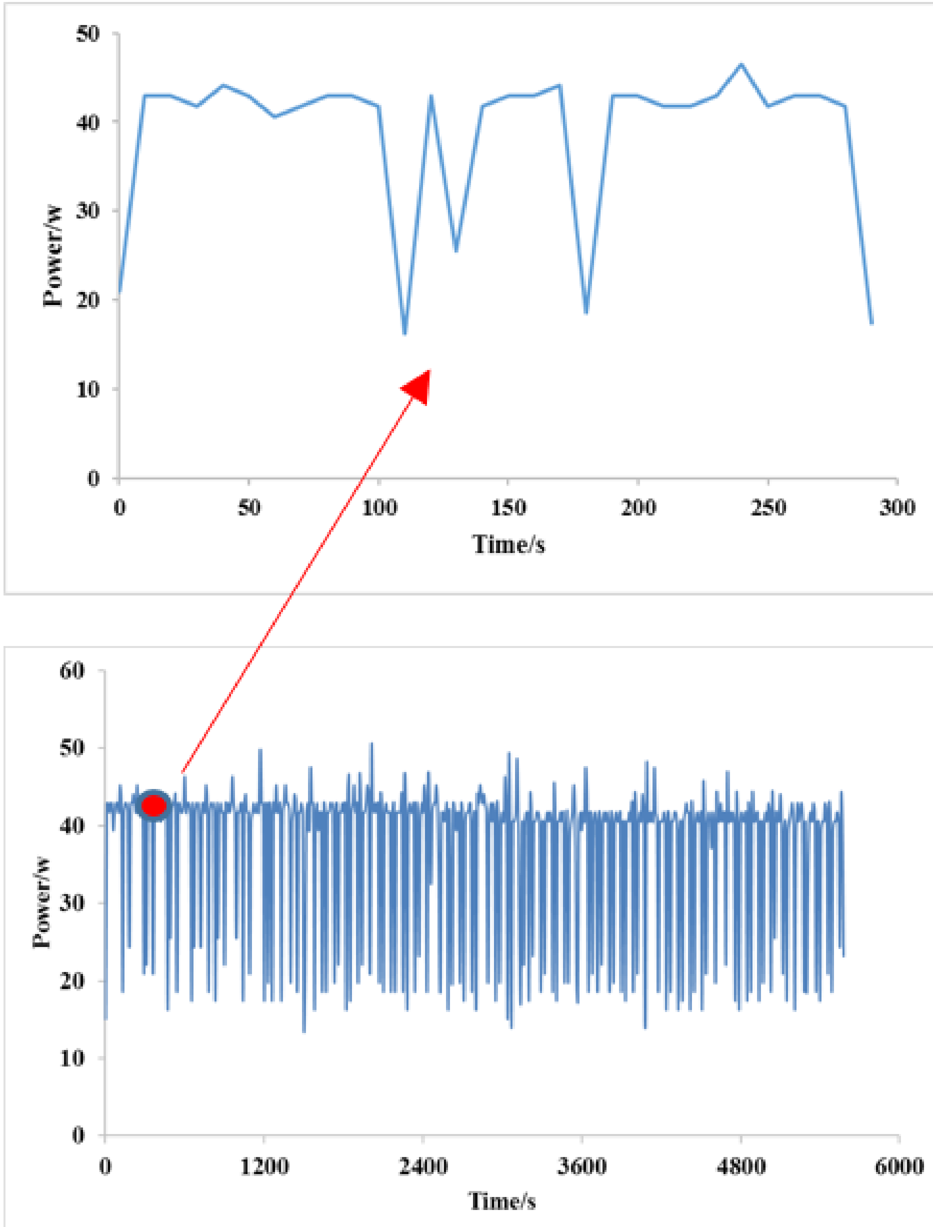

Figure 38. The power profile for batch size=1

Table 8. The energy consumption results for batch production

Batch Size	Energy Consumption (kWh)	Specific Energy Consumption (kWh/Kg)
1	0.0581	30.7407
2	0.0563	15.7703
3	0.0556	10.5303

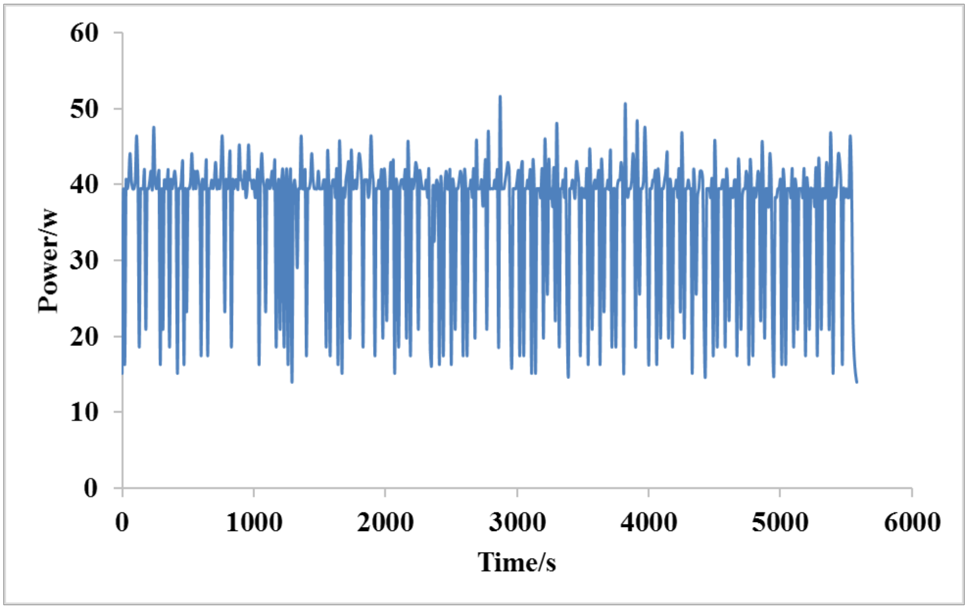

Figure 39. The power profile for batch size=2

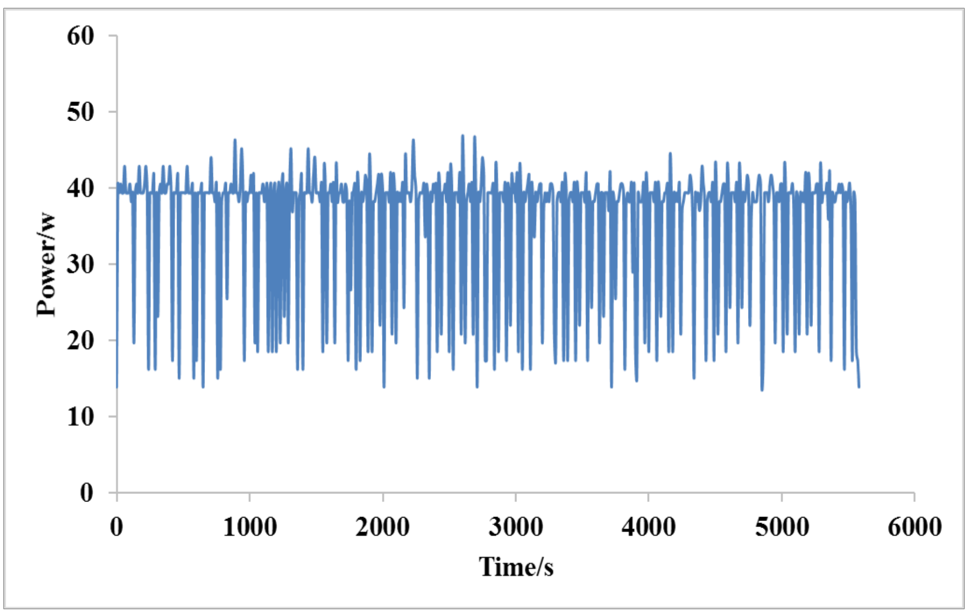

Figure 40. The power profile for batch size=3

For each batch production process, the power profiles are shown in Figure 38, Figure 39, and Figure 40, a typical 300-second period power profile is extracted and enlarged. When the building platform moves up, the projector projects the layer image, or when the UV light cures the liquid resin, the power consumption increases significantly.

Energy consumption or electricity usage leads to a great amount of carbon dioxide (CO_2) emission. According to U.S. Environmental Protection Agency (EPA), the electricity generation leads to the largest share (30%) of the total U.S. greenhouse gas emissions in 2014. As proposed by U.S. EPA (U.S. Environmental Protection Agency, 2015), 7.03×10^{-4} metric tons (1000 Kg) CO_2 is emitted from per kWh electricity generation. In this experiment, 0.0581 kWh electricity was consumed to fabricate a part using SLA process, correlated to 0.041 Kg CO_2 emission.

TVOC Emissions

The results of total TVOC emission and TVOC emission per Kg of parts built are shown in Table 9. It can be observed that when the batch size increases from 1 to 2, the total TVOC emitted increases by 79.26%; when the batch size continues increasing from 2 to 3, the total TVOC emitted increases by 82.23%. However, for the TVOC emission per Kg of final part, the result reduces from batch size 1 to 2, but then it increases dramatically from batch size 2 to 3. The relationship between batch size and TVOC emission per Kg part is not obvious. This favors the adoption of batch production method with further research in AM.

Table 9. The TVOC emission for batch production

Batch Size	Total TVOC Emission (μg)	TVOC Emission (μg) per kg Part Built
1	15,104.24	7991.66
2	27,075.50	7584.17
3	49,341.45	9362.70

The TVOC emission profiles are shown in Figure 41, Figure 42, and Figure 43. During the first 600s period, the TVOC emissions are measured as a reference level, which provides information on the TVOC concentration in the room without the SLA machine working. Around

600s, the manufacturing activities start and last 5580s. In the three profiles, the TVOC concentration peak is identified around 6180s. After the manufacturing activities end, the TVOC concentration level decreases.

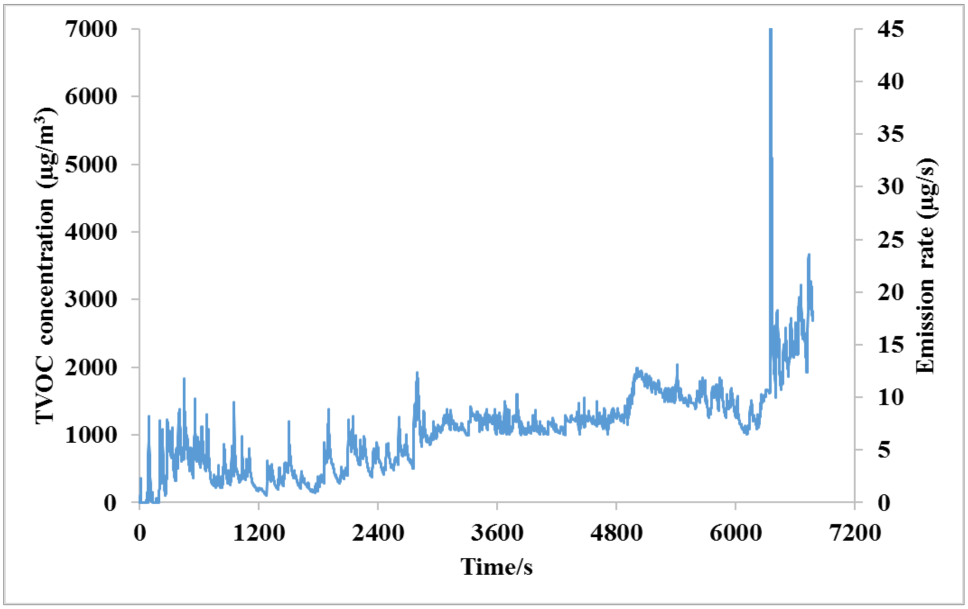

Figure 41. The real-time TVOC emission for batch size=1

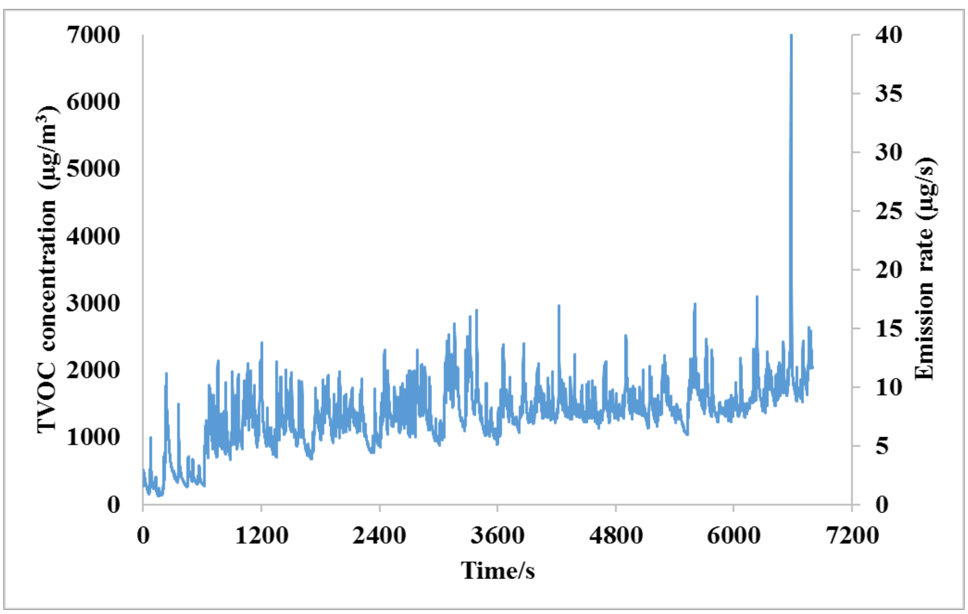

Figure 42. The real-time TVOC emission for batch size=2

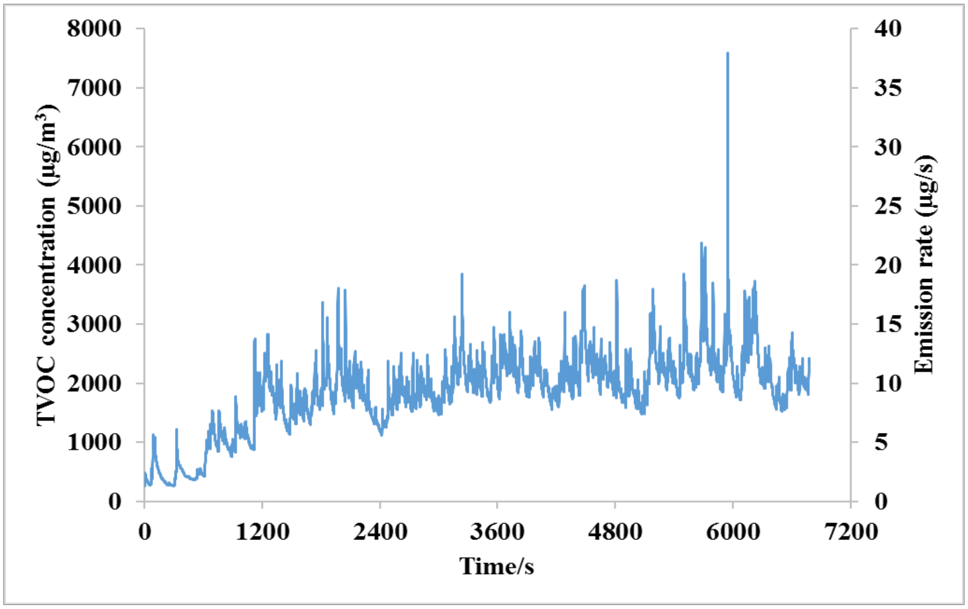

Figure 43. The real-time TVOC emission for batch size=3

The average TVOC concentration levels for the multiple measurement stages are shown in Table 10. For batch sizes from 1 to 3. Although these three manufacturing processes have different batch sizes, they have the similar TVOC concentration evolution profiles. During the background period, there is no AM activity, leading to the relatively low average TVOC concentration, which is possibly caused by liquid resin volatilization process. After the AM process starts, the average TVOC concentration increases to high level and even higher which further increases when the process ends, and post-processing starts.

Table 10. The average TVOC concentration for batch production

Batch size	Overall	Background	Manufacturing	Post-Processing
1	1068.451	476.085	859.796	3601.310
2	1335.023	435.572	1378.415	1874.142
3	1849.496	451.147	1968.835	2148.160

The average TVOC concentration levels from both the manufacturing period and post-processing period significantly exceed the maximum allowed TVOC concentration inside a building-500 μg/m^3 proposed by LEED-NC (Leadership in Energy and Environmental Design Green Building Rating System for New Construction) (Environmental, 2009). The excessive TVOC emission from AM processes could lead to serious environmental concerns and human health risks. Due to the potential negative consequences of TVOC emission from AM processes, effective emission control strategies need to be proposed and validated in future research efforts. Additionally, more comprehensive standards need to be established to regulate the AM process emissions.

Material Waste

The material waste for each of the three different batch productions is shown in Table 11. Although the material waste per part does not necessarily increase with batch size, the total material waste increases considerably with a larger batch size. It is also observed that the material waste per part is similar for different batch sizes. However, material waste per part for the SLA process is extremely high (about 70% for these three cases) and needs further process/equipment improvements.

Overall, based on our experimental results, AM batch production has great potential for being an environmentally sustainable manufacturing method. First, AM batch production leads to significant reduction on specific energy consumption, and further results in decreasing in CO_2 emissions caused by electricity generation. Second, TVOC emissions per Kg part do not necessarily increase, which benefits the AM batch production method. Third, the material waste per part does not noticeably increase with larger batch size, which is also one of the advantages for AM batch production method.

Table 11. The material waste for batch production

Batch Size	Total Material Usage (g)	Total Material Waste (g)	Final Part without Support (g)	Material Waste per Part
1	3.23	1.34	1.89	70.90%
2	5.89	2.32	1.74	69.25%
			1.83	60.92%
3	9.27	4.00	1.69	82.84%
			1.81	70.72%
			1.77	74.58%

3.5.3 Section Conclusion and Prototype Development

In this section, the environmental sustainability performance for the AM batch production method is evaluated by measuring and comparing energy consumption, TVOC emissions, and material waste while considering different batch size. Based on the experimental results, batch production using SLA process has great potential for energy saving, but still needs improvement concerning TVOC emission and material waste. The environmental sustainability evaluation performed in this dissertation greatly enhances our understanding of the performances of AM batch production method. Moreover, the outcomes of this part of the research also facilitate the AM batch production development by unveiling the relationships between batch size and environmental performance.

Using the research outcome from both energy consumption and emission study, a prototype based on SLA process (as shown in Figure 44) is developed, which consumes minimal energy consumption while ensuring the satisfactory surface quality, and reduces the TVOC emissions through physical absorption and chemical oxidation processes. It has been tested that this prototype is able to reduce both the average TVOC concentration and AM-caused emissions by more than 70%.

Figure 44. The environmentally sustainable SLA prototype

4. COST MODELING AND OPTIMIZATION IN STEREOLITHOGRAPHY ADDITIVE MANUFACTURING

(Previously published in (Yang and Li, 2018b) as "Yang, Y., and Li, L., 2018. Cost Modeling and Analysis for Mask Image Projection Stereolithography Additive Manufacturing: Simultaneous Production with Mixed Geometries. *International Journal of Production Economics* 206: 146-158", and published in (Li et al., 2018a) as "Li, L., Haghighi, A., and Yang, Y., 2018. Theoretical Modeling and Prediction of Surface Roughness for Hybrid Additive-Subtractive Manufacturing Processes. *IISE Transactions* 1-40".)

In addition to the environmental sustainability considered in the Section 2 and Section 3, the production cost in SLA process is modeled and optimized as shown in Section 4. More specifically, the cost model is illustrated in Section 4.1, followed with the optimization problem formulated in Section 4.2. Numerical case studies are conducted in Section 4.3, including the cost model performance analysis in Section 4.3.1 and cost optimization results in Section 4.3.2. The sensitivity analysis is performed to identify the most sensitive cost drivers in current market, as shown in Section 4.4. Finally, the section conclusion is discussed in Section 4.5.

4.1 The Mask Image Projection Stereolithography Process Cost Model

To formulate the costs generated from the MIP SLA process, it is necessary to investigate the MIP SLA process to identify different cost components from various stages of the process. The MIP SLA process is illustrated in Figure 45. The MIP SLA process has great potentials for high-precision (Sun et al., 2005) and fast 3D printing (Pan et al., 2012b) due to the use of high-resolution projection. The MIP SLA process has been used for diverse applications such as the fabrication of high electric capacitor (Yang et al., 2016), smooth surfaces (Pan et al., 2012a), etc.

The main manufacturing process can be summarized into three sub-processes. First, during the pre-processing stage, the machine operator performs process planning activities such as the control software set-up, the machine set-up, etc. Second, during the production stage, the first layer image is projected to the bottom of the building platform and solidified by the Ultraviolet (UV) light source. After the first layer is finished, the building platform vertically moves up for the distance of a layer thickness and continues with the next layer until the entire production is finished. Third, during the post-processing stage, the machine operator retrieves the parts, performs additional procedures to improve the surface quality if necessary, and cleans the AM machine for the next production batch.

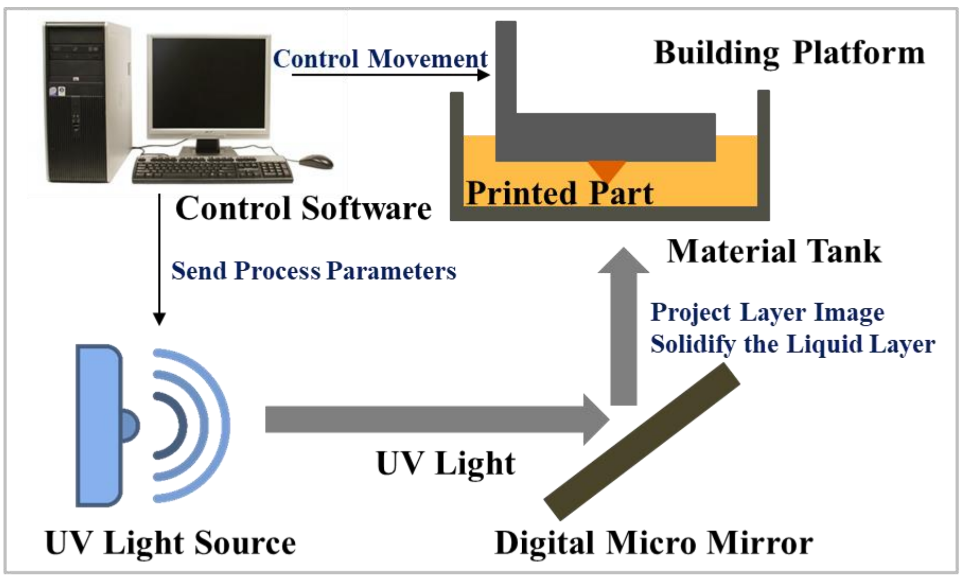

Figure 45. The Mask Image Projection Stereolithography process illustration

To enable the estimation of the unit cost per part for mixed production schemes, the mixed geometries in the batch need to be sorted so that they can be determined with different unit costs. A sorting algorithm is proposed in this section considering the various levels of part height, volume, and complexity.

Let i be the index of various levels of part height, and P_i be parts with height h_i. The set of parts with different heights, I_i, can be written as follows.

$$I_i = \{P_1, P_2, P_3, \cdots P_{N_h}\}, i \in [1, N_h] \tag{24}$$

N_h denotes the total number of various levels of height in the mixed batch. Let j be the index of different volumes of parts with a specific height h_i. $P_{i,j}$ refers to parts with height h_i and volume $V_{i,j}$. The set of parts with different volume and specific height i, $P_{i,j}$, can be written as follows.

$$I_{i,j} = \{P_{i,1}, P_{i,2}, P_{i,3}, \cdots P_{i,N_{v,i}}\}, j \in [1, N_{v,i}] \tag{25}$$

$N_{v,i}$ represents the total number of various levels of volume for height i.

Let k be the index of different complexity levels of parts with a specific height h_i and volume $V_{i,j}$. $P_{i,j,k}$ denotes a specific part in the mixed batch with height i, volume j, and complexity level k. $\delta_{i,j,k}$ represents the complexity level of parts with index i, j, and k, where the complexity level is defined as $\delta_{i,j,k} = S_{i,j,k}/V_{i,j}$. Note that the proposed ratio $\delta_{i,j,k}$ cannot be used solely for geometry evaluation, but in combination with other indices it can provide useful guidance for estimating the complexity level. The set of parts in the production batch with specific height h_i and specific volume $V_{i,j}$ can be written as follows.

$$I_{i,j,k} = \left\{P_{i,j,1}, P_{i,j,2}, P_{i,j,3}, \cdots P_{i,j,N_{c,i,j}}\right\}, k \in [1, N_{c,i,j}] \tag{26}$$

$N_{c,i,j}$ is the total number of different complexity levels for height i and volume j. It should be noted that above sets P_i, $P_{i,j}$, and $P_{i,j,k}$ are all sequenced in a monotonically increasing order.

Thus, the total number of parts in the production batch are calculated by $N_{tot} = \sum_{i=1}^{i=N_h} \sum_{j=1}^{j=N_{v,i}} N_{c,i,j}$. Successively, the total cost for mixed batch can be formulated as follows.

$$C_{tot}^{b} = \sum_{i=1}^{i=N_h} \sum_{j=1}^{j=N_{v,i}} \sum_{k=1}^{k=N_{c,i,j}} \left[C_{tot}(P_{i,j,k})\right] \tag{27}$$

$C_{tot}(P_{i,j,k})$ denotes the total cost for part $P_{i,j,k}$, which contains several different cost components.

The above sorting algorithm for the mixed parts can be summarized as follows.

Step 1. GET h_i, $V_{i,j}$ and $\delta_{i,j,k}$ from the mixed production batch
Step 2. FOR $i = 2: N_h$
    CHECK IF $h_i > h_{i-1}$, CONTINUE LOOP
    ELSE, exchange the order of P_i and P_{i-1}, and CONTINUE LOOP
    END LOOP
Step 3. REPEAT **Step 2** until no exchange is necessary
Step 4. FOR $i = 1: N_h$
      FOR $j = 2: N_{v,i}$
      CHECK IF $V_{i,j} > V_{i,j-1}$, CONTINUE LOOP
      ELSE, exchange the order of $P_{i,j}$ and $P_{i,j-1}$, and CONTINUE LOOP
      END LOOP
    END LOOP
Step 5. REPEAT **Step 4** until no exchange is necessary
Step 6. FOR $i = 1: N_h$
      FOR $j = 1: N_{v,i}$
        FOR $k = 2: N_{c,i,j}$
        CHECK IF $\delta_{i,j,k} > \delta_{i,j,k-1}$, CONTINUE LOOP
        ELSE, exchange the order of $P_{i,j,k}$ and $P_{i,j,k-1}$, and CONTINUE LOOP
        END LOOP
      END LOOP
    END LOOP
Step 7. REPEAT **Step 6** until no exchange is necessary
Step 8. END

Based on the production activities in various stages, multiple cost components can be identified, i.e., energy consumption cost, labor cost, material cost (both part material cost and support material cost), and other overheads. These cost components are highly related to AM production activities, as illustrated in Figure 46.

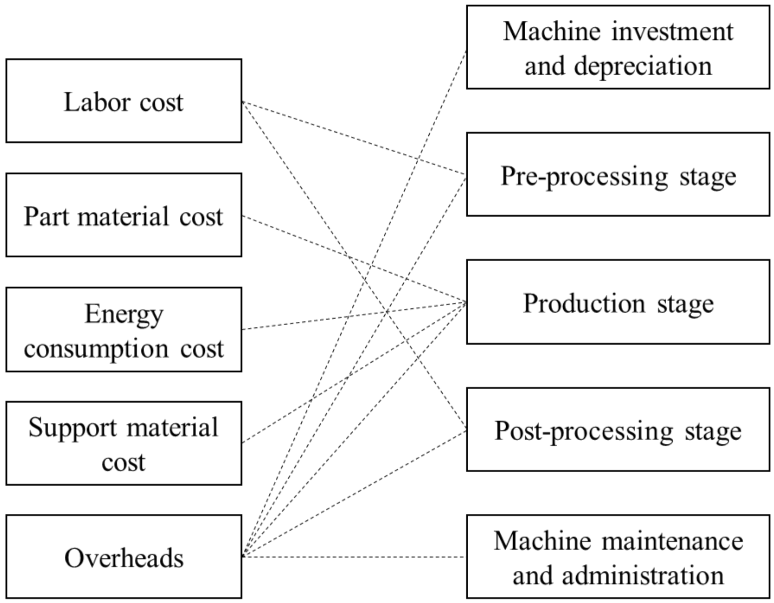

Figure 46. Illustrations of the cost components and the production activities

Energy Consumption Cost

The energy consumption cost of the MIP SLA process is highly time-dependent, and thus mainly determined by the maximum height of the geometries in the production batch with a specific layer thickness. Hence, the energy cost per part cannot be assumed to be uniform for various geometries. Generally, geometries with greater height should contribute more regarding the energy consumption cost.

To formulate the energy cost per part for a specific geometry $P_{i,j,k}$, a time-related ratio τ_1 is proposed to determine the energy cost per part for different geometries in a mixed production scheme and is shown in Equation (28).

$$\tau_1(P_{i,j,k}) = T_{layer} \times \left[\left(\frac{1}{N_{tot}}\right) \times \left(\frac{h_1}{d}\right) + \left(\frac{1}{N_{tot} - N_{v,1}}\right) \times \left(\frac{h_2 - h_1}{d}\right) + \cdots + \left(\frac{1}{N_{tot} - N_{v,1} - N_{v,2} - \cdots - N_{v,i-1}}\right) \times \left(\frac{h_i - h_{i-1}}{d}\right)\right] + T_{support} \times \left(\frac{N_{support}}{N_{tot}}\right) \tag{28}$$

In this equation, N_{tot} represents the total number of geometries in the production batch, $T_{support}$ denotes the production time for each support layer, and $N_{support}$ is the total number of required support layers.

In addition, T_{layer} represents the production time for each part layer. In the MIP SLA process, T_{layer} is assumed to be identical for all part layers, and it can be calculated by Equation (29). It should be noted that for some types of AM processes, e.g., the FDM process and the SLS process, T_{layer} can be different for each layer as it can be significantly affected by different building paths.

$$T_{layer} = T_{expo} + T_{lift} \tag{29}$$

In Equation (29), T_{expo} is the layer image exposure time and T_{lift} is the building platform life and sequence time. Therefore, the unit energy consumption cost for part $P_{i,j,k}$ in the mixed production scheme can be formulated as follows.

$$C_E(P_{i,j,k}) = C_E^* \times P_{machine} \times \tau_1(P_{i,j,k}) \tag{30}$$

where C_E^* denotes the unit electricity price (\$/kWh), and $P_{machine}$ denotes the rated power of the AM machine that can be obtained from the machine nameplate specifications.

Labor Cost

It is assumed that during the AM production period, there is no need for the machine operator's involvement. In other words, the machine operator only participates in the activities before and after the manufacturing process. More specifically, the operator sets up the AM machine and the control software during the preprocessing stage and performs post-processing activities when the production is finished (i.e., removing the support structure, cleaning the AM machine, over-curing the finished parts, and surface finishing).

Hence, the unit labor cost for part $P_{i,j,k}$ in the mixed production scheme can be formulated as the sum of the labor costs from the preprocessing and post-processing stages, which can be calculated by Equation (31) and Equation (32), respectively.

$$C_{L,pre}(P_{i,j,k}) = C_L^* \times T_{pre}(P_{i,j,k}) = C_L^* \times \left[\left(T_{setup,s}^b + T_{setup,m}^b\right)/N_{tot}\right] \tag{31}$$

C_L^* is the labor cost per unit time, which refers to the hourly rate ($/hour) of the AM machine operator. $T_{setup,s}^b$ and $T_{setup,m}^b$ represent the total software and the machine set-up costs of the production batch.

$$\begin{aligned} C_{L,post} &= C_L^* \times T_{post}(P_{i,j,k}) \\ &= C_L^* \times \left[T_{overcure}(P_{i,j,k}) + T_{surface}(P_{i,j,k}) + \frac{T_{remove}^b}{N_{tot}} + \frac{T_{clean}^b}{N_{tot}}\right] \end{aligned} \tag{32}$$

T_{remove}^b and T_{clean}^b are the support removal time and the machine cleaning time of the production batch. To estimate the over-curing cost and surface finishing cost to different geometries, the following relationships are proposed.

$$T_{overcure}(P_{i,j,k}) = \begin{cases} T_{overcure}^* & if\ V_{i,j,k} = V_{min} \\ T_{overcure}^* \times exp\left(\dfrac{V_{i,j,k}}{V_{min} \times \gamma_1}\right) & otherwise \end{cases} \tag{33}$$

$$T_{surface}(P_{i,j,k}) = \begin{cases} T_{surface}^* & if\ S_{i,j,k} = S_{min} \\ T_{surface}^* \times \left[exp\left(\dfrac{S_{i,j,k}}{S_{min} \times \gamma_2}\right) + exp\left(\dfrac{\delta_{i,j,k}}{\delta_{min} \times \gamma_3}\right)\right] & otherwise \end{cases} \tag{34}$$

where $T^*_{overcure}$ is the over-curing time for the part with minimum volume, and $T^*_{surface}$ is the surface finishing time for the part with minimum surface area. In addition, γ_1, γ_2, and γ_3 are constant values determined by the skills and experiences of the AM machine operator.

Material Costs

The material costs of a specific part $P_{i,j,k}$ mainly contain two sources, i.e., part material cost and support structure material cost, and can be formulated as follows.

$$\begin{aligned} C_M(P_{i,j,k}) &= C_{M,p}(P_{i,j,k}) + C_{M,s}(P_{i,j,k}) \\ &= (1+\varphi) \times C^*_M \times \rho_M \times \left[V_{i,j} + V^b_{support}/N_{tot}\right] \end{aligned} \tag{35}$$

φ denotes the material waste ratio, which represents the percentage of material wasted to unit material needed for production. When $\varphi = 0$, there is no material waste. In addition, C^*_M stands for the unit price of the material ($/kg), and ρ_M is the density of the material. Note that, in the MIP SLA process, the material types for the part and the support structure are the same. Moreover, material recycling is not considered in the MIP SLA process.

Overheads

The overheads of part $P_{i,j,k}$ include the machine depreciation cost, the maintenance cost, and the administration cost. Using the straight-line depreciation method (Hulten and Wykoff, 1980), the depreciation cost for a specific part $P_{i,j,k}$ can be formulated as follows.

$$C_{overheads}(P_{i,j,k}) = \frac{C_{invest}/N_{life} + C^b_{main} + C^b_{adm}}{TP} \times \tau_2(P_{i,j,k}) \tag{36}$$

where C_{invest} is the initial cost the AM machine and software, N_{life} denotes the estimated useful life of the AM machine and software, C^b_{main} is the maintenance cost per year of the production batch, and C^b_{adm} is the miscellaneous administration cost per year for the whole mixed production.

In addition, $\tau_2(P_{i,j,k})$ denotes a time-related ratio of the total time (i.e., preprocessing time, production time, and postprocessing time) of part $P_{i,j,k}$ and the total time of the production batch, as shown in the following equation.

$$\tau_2(P_{i,j,k}) = \frac{T_{pre}(P_{i,j,k}) + \tau_1 + T_{post}(P_{i,j,k})}{T_{pre}^b + T_{prod}^b + T_{post}^b} \tag{37}$$

T_{pre}^b, T_{prod}^b, and T_{post}^b are the total preprocessing time, production time, and postprocessing time for the production batch.

Therefore, the total cost for part $P_{i,j,k}$ can be formulated as follows.

$$C_{tot}(P_{i,j,k}) = C_E(P_{i,j,k}) + C_{L,pre}(P_{i,j,k}) + C_{L,post} + C_{overheads}(P_{i,j,k}) \tag{38}$$

4.2 Optimization Problem

The objective of the optimization problem is to minimize the total cost by obtaining the optimal set of decision variables (i.e., layer thickness d and stratification angle θ), considering multiple constraints regarding the part surface quality and production throughput. Hence, the objective function of the optimization problem can be formulated as follows.

$$\min_{d,\theta}\{TP \times C_{tot}^b\} \tag{39}$$

C_{tot}^b denotes the total cost per production batch, and TP is the production throughput, which is defined as the number of batches in this work. Note that, in this work, a certain production layout is adopted and remains the same for all production batches. The two decision variables are the layer thickness d, which is defined as the height of each successive layer, and the stratification angle θ of the surface of interest, which refers to the angle between the normal vector of the surface of interest and the build direction. Based on our preliminary analysis, the total cost C_{tot}^b consists of two types of cost components, i.e., fixed and variable cost components, determined by if the cost component is altered with different values of decision variables. Hence, the objective function (39) can be rewritten as follows.

$$\min_{d,\theta}\{TP \times C_{tot}^{b}(variable)\} \tag{40}$$

In the optimization problem, four constraints are considered, i.e., the desired surface roughness of the surface of interest, the required annual throughput, and the ranges of two decision variables. As one of the most critical measures for evaluating the printed part quality, surface roughness R_a of the surface of interest is usually limited within a specific range considering the design requirement and specifications.

Generally, R_a is defined as "the arithmetic average of the absolute values of the profile height deviations from the mean line, recorded within the evaluation length" (ASME, 2010). The desired range for R_a can be formulated as follows.

$$R_{a,min} \le R_a \le R_{a,max} \tag{41}$$

Both $R_{a,min}$ and $R_{a,max}$ are determined by the designer.

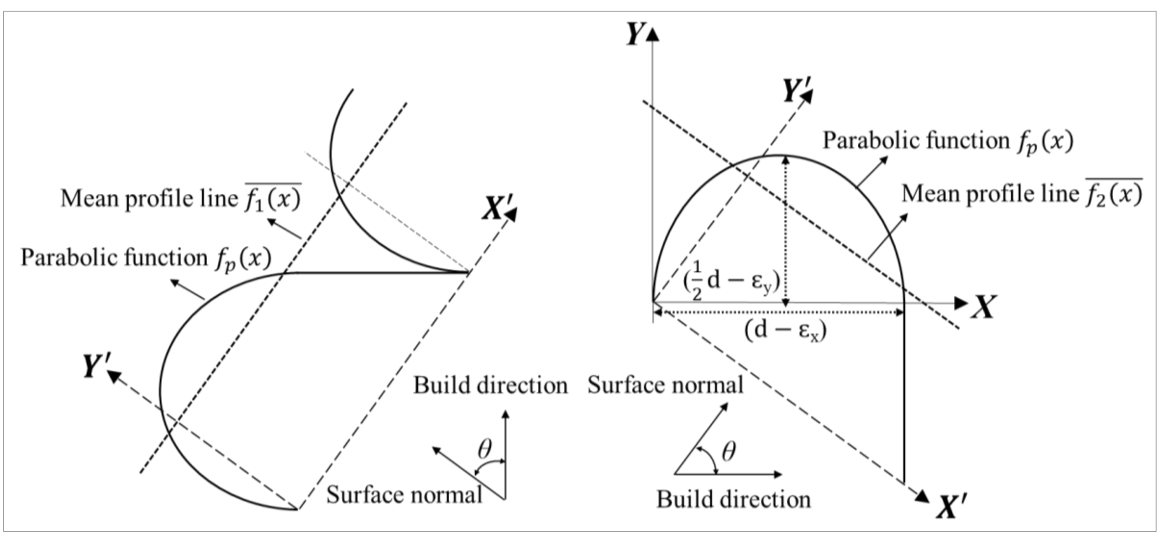

Figure 47. The surface profile of 3D printed surfaces, adapted from (Li et al., 2018b)

To represent the surface profile of additive manufactured surfaces, a combination of a parabolic curve and a straight line is used as proposed by Li et al. (2018) as shown in Figure 47.

Accordingly, the surface roughness value can be calculated by the following equation.

$$R_a = \frac{sin\theta}{(d-\varepsilon_x)}\int_0^{(d-\varepsilon_x)} \left| -2\left[\frac{d-2\varepsilon_y}{(d-\varepsilon_x)^2}\right]x^2 + 2\left[\frac{d-2\varepsilon_y}{(d-\varepsilon_x)}\right]x + (cot\theta)x - \frac{1}{3}\left(d-2\varepsilon_y\right) - \frac{1}{2}(d-\varepsilon_x)cot\theta \right| dx \tag{42}$$

In this equation, ε_x and ε_y are the error coefficients of the layer thickness deviation along the X and Y axis, respectively. It is assumed that both error coefficients follow normal distributions, where $\varepsilon_x \sim N\left(\mu_{\varepsilon_x}, \sigma_{\varepsilon_x}^2\right)$ and $\varepsilon_y \sim N\left(\mu_{\varepsilon_y}, \sigma_{\varepsilon_y}^2\right)$.

In addition to the surface quality, the production throughput is also a critical requirement and therefore considered in the optimization problem. To formulate the production throughput TP, the AM machine utilization rate σ is used and it represents the percentage of time that the AM machine is in operation per year (%).

$$\frac{(8760 \times \sigma)}{\left(T_{pre}^b + T_{prod}^b + T_{post}^b\right)} \leq TP \leq \frac{8760}{\left(T_{pre}^b + T_{prod}^b + T_{post}^b\right)} \tag{43}$$

Note that it is assumed that each year has 8760 hours.

Furthermore, the ranges regarding the decision variables are also considered and formulated as follows.

$$d_{min} \leq d \leq d_{max} \tag{44}$$

$$0° \leq \theta \leq 90° \tag{45}$$

where d_{max} and d_{min} are the maximum and minimum layer thickness values, which are usually limited by the AM machine capability.

4.3 Numerical Case Studies

To investigate the cost performance of the MIP SLA process using the developed cost model, numerical case studies are conducted in this section. More specifically, comparative case studies are performed in Section 4.3.1 by considering non-mixed and mixed production layouts, as well as different methods to quantify the unit cost in mixed production schemes. In addition, the optimization problem is solved in Section 4.3.2.

4.3.1 Cost Performance Analysis

4.3.1.1 Comparison of Non-Mixed and Mixed Production Layouts

To demonstrate the ability of established model in terms of estimating the AM cost for both non-mixed and mixed production layouts, comparative case studies are performed to investigate the cost-saving potential by adopting mixed production schemes. More specifically, three different manufacturing scenarios are considered. In Scenario I, a non-mixed production layout is adopted with 40% of the machine capacity, which, in this work, refers to the percentage area of the building platform used for printing. In Scenario II, 60% of the machine capacity is used for a non-mixed production layout. In Scenario III, a mixed production scheme is adopted with productivity of 57.04% (σ), which implies that the AM machine is in operation for 100 hours/week and 50 weeks/year. These three scenarios are designed to achieve the same yearly yield.

Table 12. The geometry information and production scenario layout

	Geometry 1	**Geometry 2**	**Geometry 3**
Description	Screw (M5*30)	Screw (M6*15)	Screw (M8*25)
Height (mm)	35	21	33
Volume (mm^3)	708.44	690.58	888.01
Surface area (mm^2)	1028.40	1919.10	1738.5

Three different geometries are considered in these scenarios as shown in Table 12. The quantities of Geometry 1, 2, and 3 considered in Scenario I are 38, 18, and 11; in Scenario II are 50, 27, and 17; and in Scenario III are 10, 28, and 4, respectively.

To perform the cost calculation using the proposed model, additional assumptions are applied as shown in Table 13. Note that the same assumptions are adopted in all three manufacturing scenarios. The target yield is calculated based on the productivity of Scenario III, and it includes 10,808 of Geometry 1, 30,262 of Geometry 2, and 4323 of Geometry 3. In addition, the values for the two decision variables are set as: d=0.1mm and θ=90°.

Table 13. The assumptions used in cost model calculation

Parameter	**Value**	**Source**
C_E^*	\$0.1038/kWh	The average electricity price in the U.S. in November 2017 (U.S. Energy Information Administration, 2017)
$P_{machine}$	0.33kW	Machine specification (EnvisionTEC, 2017)
C_L^*	\$7.25/hour	The federal minimum wage in the U.S. in 2017 (U.S. Department of Labor, 2017)
ρ_P	1100 kg/m^3	Material property (EnvisionTec, 2019)
C_M^*	\$600/kg	Quote from the material supplier
φ	0.05	Assumed by this work
C_{invest}	\$13,000	Quote from the 3D printer supplier
C_{main}^b, C_{adm}^b	10% of C_{invest}	Assumed by this work
N_{life}	8 years	Assumed by this work
σ	57.08%	Adapted from (Ruffo et al., 2006)

The cost model calculation results are illustrated in Figure 48. Different manufacturing scenarios are shown to have significantly different cost performance. The mixed production scheme, used in Scenario III, lead to around \$37,668 of the total yearly cost of all three geometries, which is 15.68% and 6.18% less than the non-mixed production layouts in Scenario I and II, respectively. In addition, it can be observed from the results that production schemes affect the cost performance differently according to different geometries. The yearly costs for Geometry 2 and 3 by using mixed production in Scenario III are less than those in Scenario I and II; while the yearly cost for Geometry 1 in Scenario III is slightly less than Scenario I but more than Scenario II. Furthermore, in the same manufacturing scenario, different geometries can have different cost performance as well. For example, in Scenario III, Geometry 1, 2, and 3 accounts for 22.56%, 59.09%, and 18.35% of the total yearly cost, respectively.

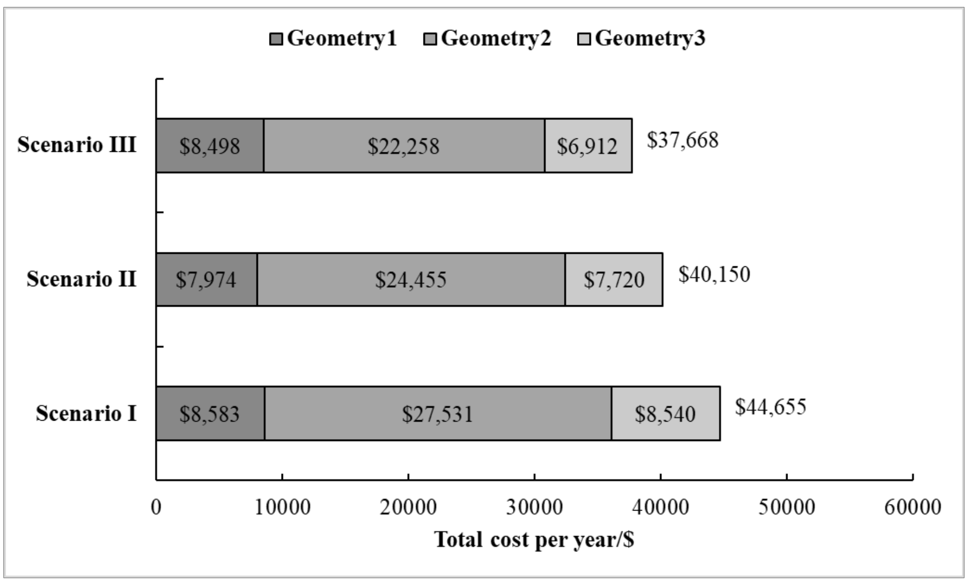

Figure 48. The cost comparison of different geometries in three scenarios

In addition, the detailed cost breakdown regarding different cost components for three manufacturing scenarios is illustrated in Figure 49. It can be observed that the production layout affects not only the cost per part but also the cost behaviors of different cost components. For example, the material cost that plays the most significant role in the total cost varies from accounting for 66.53% of the total cost in Scenario I and 69.79% in Scenario II, to 71.53% in Scenario III.

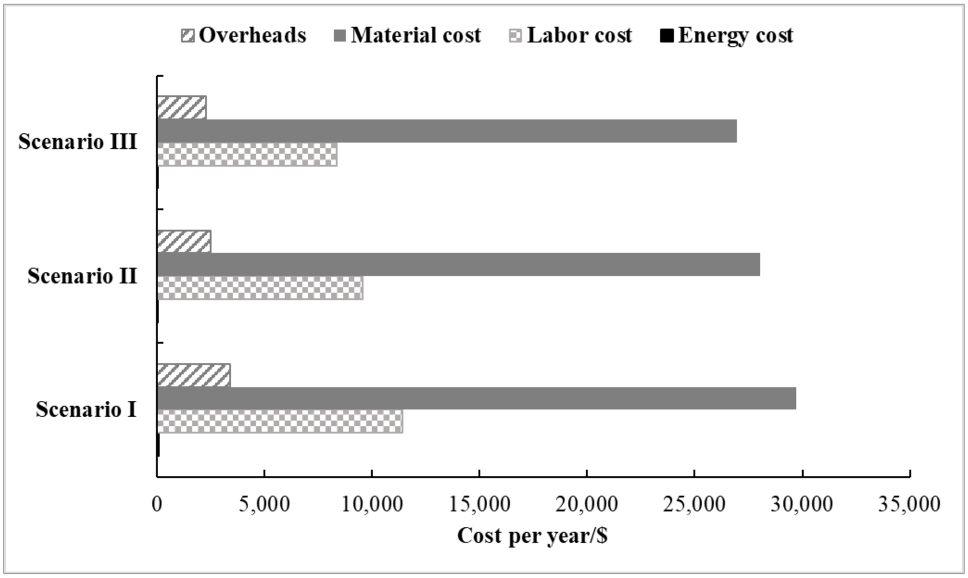

Figure 49. The cost comparison of different cost components in three scenarios

4.3.1.2 Comparison of Existing Methods of Estimating Unit Cost of Mixed Production Layout

As illustrated in the previous section, the mixed production method shows great cost-saving potential. To implement mixed production schemes, how to quantify the unit cost per part can be critical and complex as the parts in the mixed production batch have different geometries. In this section, four cost allocation methods are studied, namely, Method I, II, and III proposed by Ruffo and Hague (2007), and Method IV proposed by this work.

More precisely, by using Method I, the unit cost per part is calculated as a fraction of the total cost using the ratio of the part volume and the total volume of all the parts in the production batch. Method II relates the unit cost per part in mixed production with the total cost of printing the same parts using non-mixed production layout. By using Method III, the unit cost per part is estimated by considering the cost of high-volume non-mixed production. Note that the mixed production layout, Scenario III, in Section 4.3.1.1 is considered for adopting different cost allocation methods. In other words, each mixed production batch contains 35 of Geometry 1, 21 of Geometry 2, and 33 of Geometry 3.

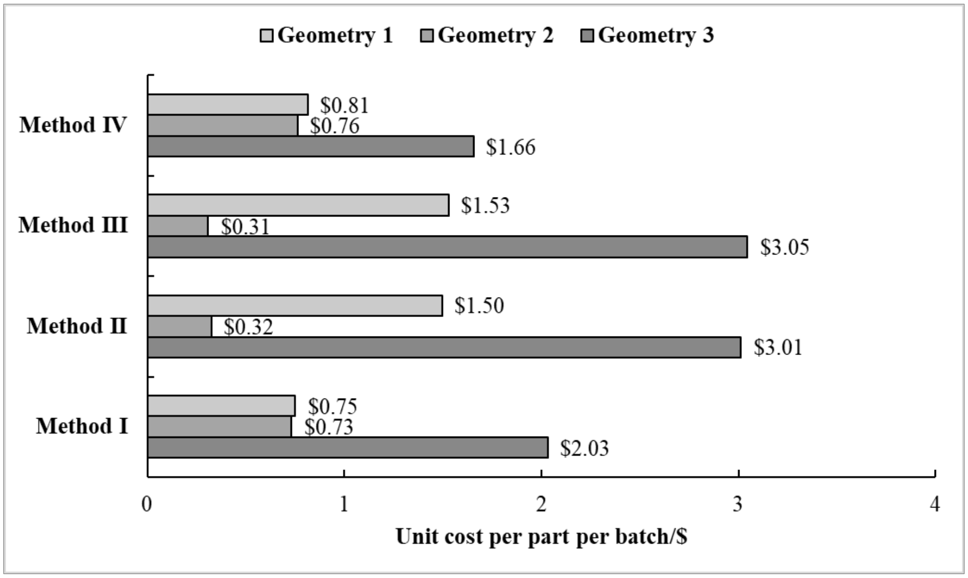

Figure 50. The unit cost comparison by using different methods

The total cost for the whole production batch is calculated as $36.09. The unit cost per part calculations using different cost allocation methods are illustrated in Figure 50. The same geometry can have different contributions to the total cost by using different cost allocation methods. For example, the unit cost for Geometry 1 can vary from $0.75 by using Method I to $1.53 by using Method III. In addition, different methods have different criterion and considerations, leading to diverse allocation results. It can be observed from the results that Geometry 1 and 2 have similar values of volume, and therefore they have similar level of the unit cost by using Method I. It can be also observed that since Method II and III both are related to the cost calculation results by using non-mixed production schemes, so they have similar behaviors. Furthermore, the proposed Method IV, comparing to other existing methods in the literature (Method I, II, and III), has reasonable but slightly different estimations for the unit cost. The main reasons for such differences are the joint consideration of the part height, volume, and complexity level, whereas Method I, II, and III fail to consider all necessary geometric characteristics.

4.3.2 Cost Optimization

According to the results in previous case studies, the proposed cost model can be used to estimate the total cost as well as the unit cost per part for both non-mixed and mixed production schemes. In this section, a more complex mixed production layout is considered for minimizing the total variable cost components (i.e., energy consumption cost, support material cost, and overheads) under the constraints of yearly throughput TP and surface roughness R_a. Two cases are considered, i.e., the Baseline Case in which the same set of decision variables are used as in Section 4, and the Optimized Case solved by using the exhaust search method where all possible feasible solutions are examined to ensure the global optimal solution.

The detailed mixed production layout is shown in Figure 51, and the geometry information is shown in Table 14. Note that the surface of interest in this production layout is the bearing surface of the nut plate (as illustrated in Figure 51), and the printing direction is along the Z axis. Note that the same assumptions are adopted as illustrated in Table 13.

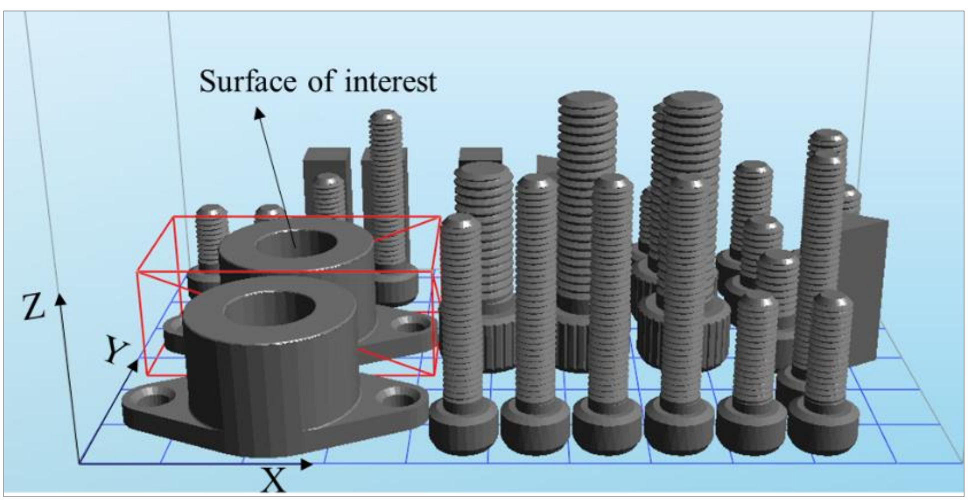

Figure 51. The mixed production layout

Table 14. The mixed production scheme for the cost minimization problem

	Description	Number per batch	Height (mm)	Volume (mm^3)	Surface area (mm^2)
Geometry 1	Screw M5*30	4	35	708.44	1028.40
Geometry 2	Screw M6*15	2	21	690.58	1028.40
Geometry 3	Screw M8*25	1	33	1919.10	1738.5
Geometry 4	Screw M5*25	2	30	629.10	896.07
Geometry 5	Prism	1	21	839.95	812.85
Geometry 6	Cube	2	21	911.99	640.42
Geometry 7	Prism with hole	2	21	911.95	716.84
Geometry 8	Cube with hole	1	21	911.99	688.42
Geometry 9	Screw M8*30	2	38	2131.8	1945.10
Geometry 10	Screw M5*10	4	15	395.24	499.22
Geometry 11	Screw M5*15	3	20	472.49	633.68
Geometry 12	Screw M6*10	3	16	575.25	734.94
Geometry 13	Screw M6*20	1	26	803.54	1044.80
Geometry 14	Screw M8*20	1	28	1709.30	1535.20
Geometry 15	Nut plate	2	15	4637.50	2621.30

Calculated from the proposed cost model, the detailed unit cost per part for fifteen geometries is obtained and shown in Figure 52, Figure 53, and Figure 54 with respect to different geometry information (i.e., height, volume, and complexity level). According to the figures, it can be observed that the relationships between cost and geometry characteristics are quite complex, and they can be varied considering different cost components. As an example, the overheads cost grows with increasing order of geometry height, but it does not necessarily change in the same pattern with increasing order of geometry volume and complexity level. Therefore, geometry characteristics need to be considered when quantifying the unit cost per geometry especially for simultaneously production with mixed geometries.

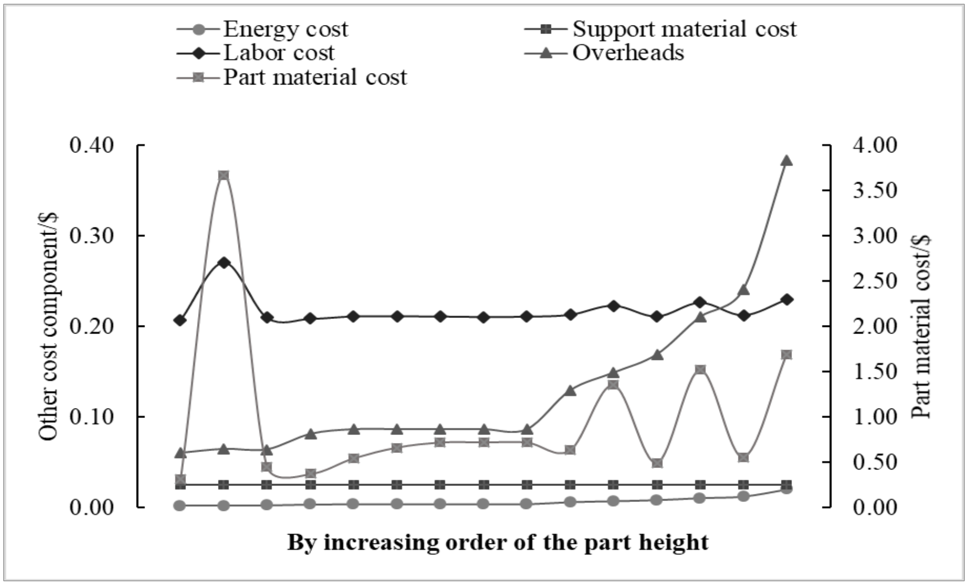

Figure 52. The unit cost per part by increasing height

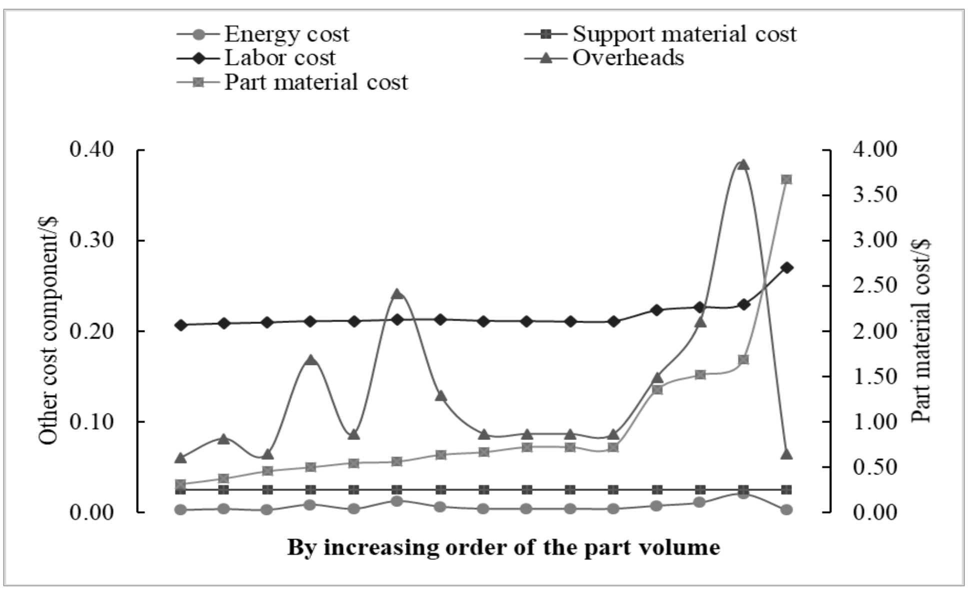

Figure 53. The unit cost per part by increasing volume

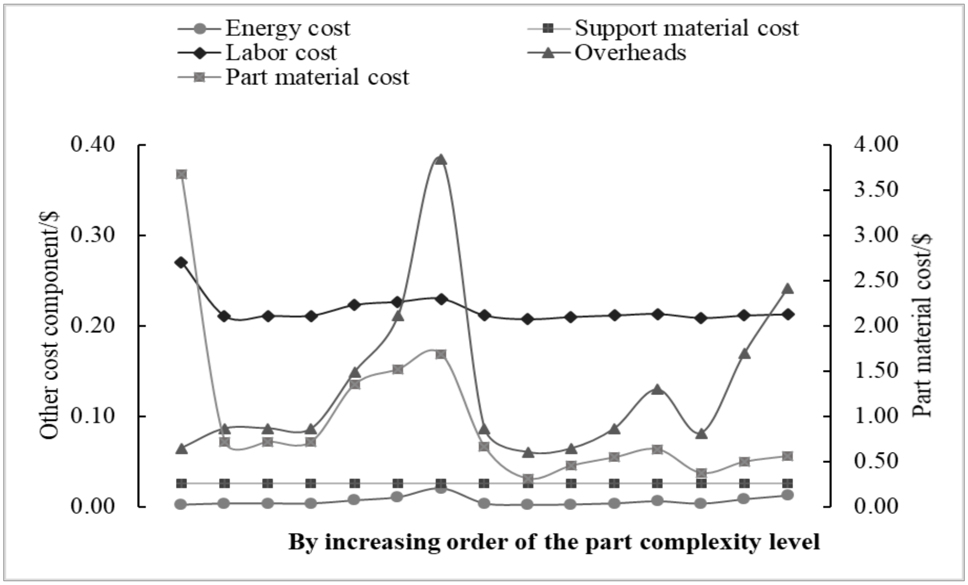

Figure 54. The unit cost per part by increasing complexity level

Four constraints are considered in the optimization problem as follows. (1) The layer thickness $d \in [0.025mm, 0.15mm]$, which is limited by the AM machine capability (EnvisionTEC, 2017); (2) The stratification angle of the surface of interest $\theta \in [0°, 90°]$, as the current production layout shown in Figure 51 is 90°; (3) The surface roughness of the surface of interest $R_a \in [0, 3.81\mu m]$, which is adapted from the specification for the nut plate used in Aerospace (Cherry Aerospace LLC, 2007); (4) The yearly throughput $\frac{(8760\times\sigma)}{\left(T^b_{pre}+T^b_{prod}+T^b_{post}\right)} \leq TP \leq \frac{8760}{\left(T^b_{pre}+T^b_{prod}+T^b_{post}\right)}$.

The comparison of the Baseline Case and the Optimized Case is shown in Table 15. By adopting the optimal values of decision variables ($d = 0.046mm, \theta = 69° - 90°$), the variable cost components in the Optimized Case is \$6443.64 per year, which is reduced by 25.47% comparing to the Baseline Case. This great cost savings indicates that the two decision variables (layer thickness and stratification angle) can significantly affect the variable cost components.

Table 15. The cost optimization results comparison

	Baseline Case	**Optimized Case**
Decision variables		
Layer thickness (mm)	0.1	0.046
Stratification angle (deg)	90°	69°-90°
Constraints		
Throughput (No. of batches/year)	1975	1975
Surface roughness (μm)	3.64	3.29-3.81
Yearly production time (hour/year)	5000	8671
Variable cost ($/year)	8645.96	6443.64

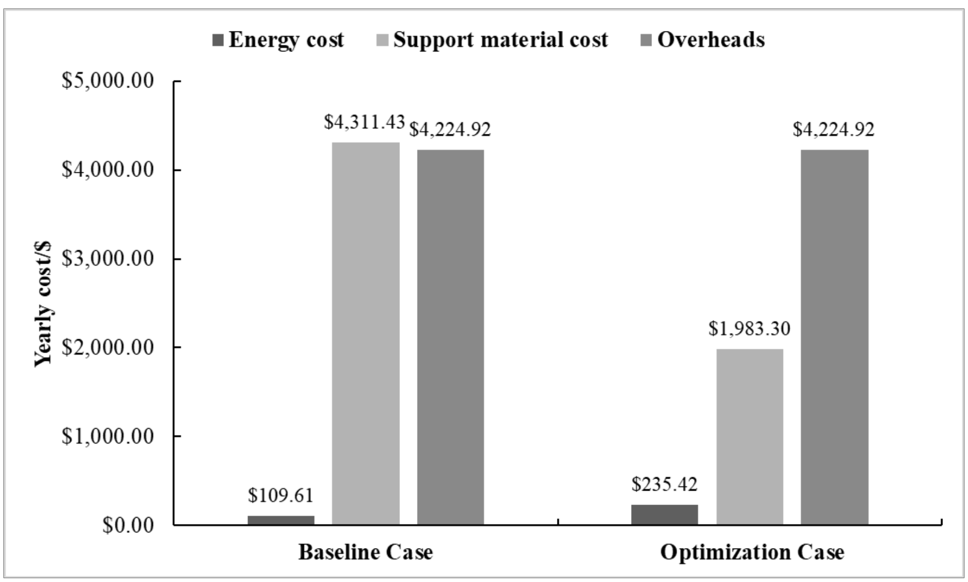

Figure 55. The variable cost breakdown of the Baseline Case and the Optimized Case

In addition, it can be observed that the characteristics of different cost components are altered in the Optimization Case. More specifically, by adjusting the decision variables, the energy consumption cost is increased from $109.61 per year to $235.42 per year by 114.78%, comparing to the Baseline Case. The support material cost has the opposite behaviors as in the Optimization Case it is reduced by around 54%, comparing to the Baseline Case. The overheads per year remain the same value for both cases, while the percentages in the total variable cost are changed from 48.87% in the Baseline Case to 65.57% in the Optimization Case. The cost breakdown for both cases is illustrated in Figure 55.

4.4 Sensitivity Analysis

In the AM cost model, several parameters and assumptions can lead to different cost performance. These parameters can be categorized into two groups: external parameters (e.g., material unit price, initial investment, and operator hourly rate) that have fluctuations due to market changes, and internal parameters (e.g., material waste ratio, and the total working time of the operator on each production batch) that depend on the characteristics of the AM production system and the skills of the AM operator. Both types of parameters are investigated to characterize their different influence on the optimized variable cost as well as the optimized total cost. Moreover, the results of the sensitivity analysis will help identify the key cost drivers for AM.

The same mixed production layout from Section 4.2 is used in the sensitivity analysis. The values of parameters shown in Table 13 serve as benchmarks for comparison. The values of the parameters are varied by $\pm$20%. The sensitivity analysis results are illustrated in Figure 56. It can be observed that, in terms of the optimized variable cost components (energy cost, support material cost, and overheads), the initial investment is the main cost driver. More specifically, 20% of the initial investment price drop can lead to 13.11% of the variable cost savings. This result indicates that in order to facilitate the enlargement of AM system applications, it is critical to reduce the prices of AM hardware and software.

In addition, the second most significant factor is the material unit cost, where a 20% of reduction in the material unit cost can lead to 6.16% reduction in the variable cost. Currently, the raw material unit prices of AM often exceed those of traditional manufacturing processes (Thomas and Gilbert, 2014). Hence, further reducing material unit costs of AM can be an effective and efficient means for reducing AM costs. Recently, numerous efforts have been dedicated to reducing the AM raw material cost by finding alternative materials (Pattinson and Hart, 2017) and reusing and recycling waste material (Baechler et al., 2013).

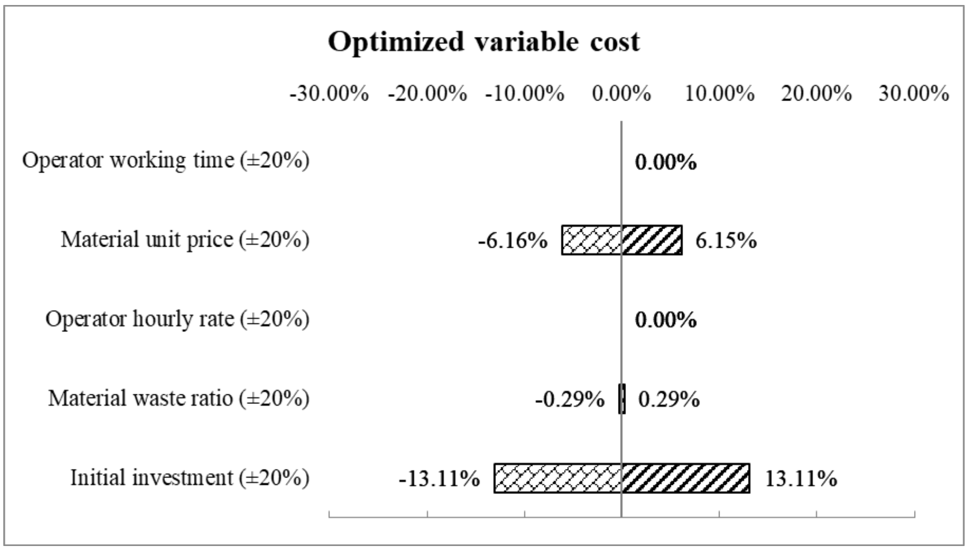

Figure 56. The effects of parameters on optimized variable cost

Furthermore, parameters like operator working time, operator hourly rate, and material waste ratio have minor impact on the optimized variable costs, but they can cause different influence on the total cost (both fixed and variable costs), as illustrated in Figure 57. For example, the operator hourly rate has no effect on the optimized variable costs, but it can affect the optimized total cost. In addition, the material unit cost can lead to the most significant fluctuations in terms of the total cost, which further emphasizes the importance of the raw material price in the future development of AM. In addition, operator working time and initial investment affect the total cost with different extents. Furthermore, $\pm$20% of material waste ratio and initial investment can cause 0.70% of the total cost change, which indicates that the AM cost is not obviously affected by the material waste ratio.

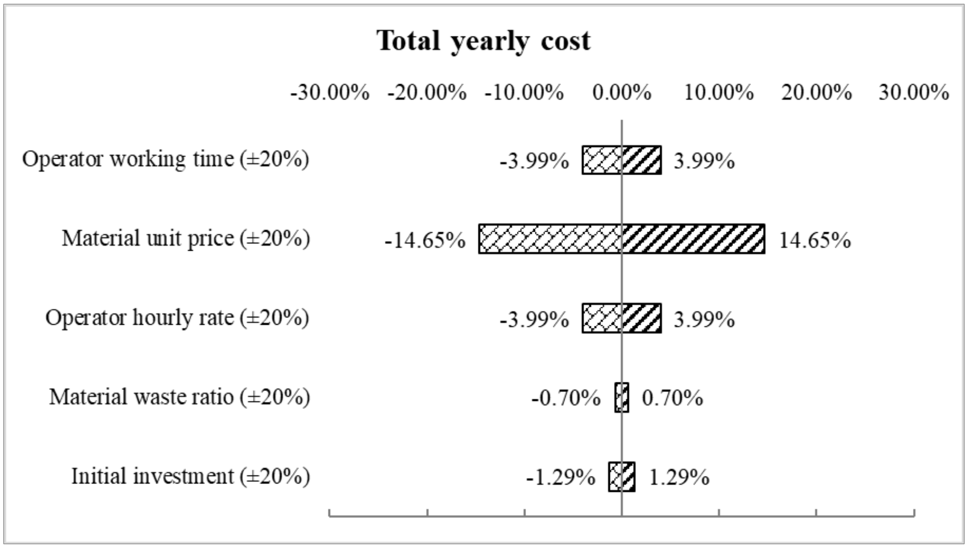

Figure 57. The effects of parameters on total cost

4.5 Section Conclusion

In this section, a comprehensive cost model is established to investigate the cost performance of simultaneous production with mixed geometries. To quantify the unit cost, a mixed geometry sorting algorithm is proposed to jointly consider and classify the mixed geometries according to the part height, volume, and complexity level. In addition, the proposed cost model is used in the cost optimization problem considering the constraints of the part surface roughness and the production throughput. The case study results show that the optimal set of the decision variables can lead to around 26% reduction in variable cost without sacrificing the yearly throughput and part surface quality. Furthermore, according to the sensitivity analysis results, the material unit price and the initial investment are identified as the key cost drivers considering their influence on the optimized variable cost. The results of this research can facilitate the AM production design, planning and setup, enhance the evaluation of AM cost performance, and help evaluate the AM market.

Future work of this section includes the extended considerations of other types of AM processes, e.g., the PolyJet process, the FDM process, etc. To formulate the unit cost in mixed production using these AM processes, the modeling approach for the production time needs to be slightly altered. In addition, more constraints can be considered in the cost optimization problem, e.g., the dimensional accuracy and the environmental sustainability performance of the AM process such as production emissions and energy consumption.

5. SUMMARY AND FUTURE WORK

Motivated by the increasing concerns on AM environmental sustainability and cost performance as well as the lack of thorough evaluation and comprehensive life cycle inventory database, this dissertation is conducted to advance the state-of-the-art of the environmental sustainability and cost analysis for SLA AM process. More specifically, the SLA process energy consumption model is established and used to study different process parameters and their influence on the overall energy consumption. In addition, the SLA process TVOC emission model is proposed and validated through experiments with less than 14% prediction error. Furthermore, two effective emission control strategies are proposed and implemented into the SLA process. The experimental results show that the average TVOC concentration is reduced by 44.15% and 71.06%, respectively. Based on the modeling and methodology obtained for energy consumption and TVOC emission, the AM batch production method is evaluated in terms of the environmental sustainability including energy consumption, TVOC emission, and material waste. Additionally, the production cost of SLA AM process is theoretically modelled and optimized while considering production throughput and achieved surfaced roughness.

The academic contributions of this dissertation are threefold. Firstly, this research is among the first a few research efforts that comprehensively evaluate the environmental and cost sustainability of SLA AM process. This research will open up opportunities for the AM and sustainable manufacturing community to work together towards significant enhancement in environmental sustainability and cost effectiveness of AM technologies. Secondly, the mathematical models established in this dissertation will fill the knowledge gap by providing theoretical estimation and prediction methodologies for evaluating the environmental and cost performance of AM processes. By formulating the relationships between AM process parameters and sustainability measures, the outcomes of this research will provide understandings and insights to facilitate the design and redesign stages. Last but not the least, the methodologies for reducing energy consumption, VOC emission and production cost that presented in this dissertation will significantly aid the long-term development of more efficient and sustainable AM operational practices. In all, this research will promote sustainable additive manufacturing and enhance the life cycle performance of AM.

As an extension of this dissertation, a comprehensive life cycle assessment for SLA process is being conducted. Additional future research extensions are shown as follows. The linkages between the 3D model's geometric characteristics and the environmental sustainability can be explored to provide more insights on reducing the environmental impact in the model design stage. Furthermore, comparative studies can be conducted between different AM technologies, raw material types, or model designs. In addition, more environmental measures can be included in the environmental sustainability evaluation, such as material flow, recycling of disposed AM materials or parts, etc.

REFERENCES

Aboutaleb, A.M., Bian, L., Elwany, A., Shamsaei, N., Thompson, S.M., Tapia, G., 2017. Accelerated process optimization for laser-based additive manufacturing by leveraging similar prior studies. IISE Trans. 49, 31–44. doi:10.1080/0740817X.2016.1189629

Afshar-Mohajer, N., Wu, C.Y., Ladun, T., Rajon, D.A., Huang, Y., 2015. Characterization of particulate matters and total VOC emissions from a binder jetting 3D printer. Build. Environ. 93, 293–301. doi:10.1016/j.buildenv.2015.07.013

Alexander, P., Allen, S., Dutta, D., 1998. Part orientation and build cost determination in layered manufacturing. Comput. Des. 30, 343–356. doi:10.1016/S0010-4485(97)00083-3

Arnold, F.C., Engel, A.J., 2001. Evaporation of pure liquids from open surfaces, in: Modeling of Environmental Chemical Exposure and Risk. pp. 61–71.

ASME, 2010. ASME B46.1 Surface Texture [WWW Document].

ASTM, 2012. Standard Terminology for Additive Manufacturing Technologies. F2792-12a i, 11–13. doi:10.1520/F2792-12A.2

Atzeni, E., Iuliano, L., Minetola, P., Salmi, A., 2010. Redesign and cost estimation of rapid manufactured plastic parts. Rapid Prototyp. J. 16, 308–317. doi:10.1108/13552541011065704

Atzeni, E., Salmi, A., 2012. Economics of additive manufacturing for end-usable metal parts. Int. J. Adv. Manuf. Technol. 62, 1147–1155. doi:10.1007/s00170-011-3878-1

Azimi, P., Zhao, D., Pouzet, C., Crain, N.E., Stephens, B., 2016. Emissions of Ultrafine Particles and Volatile Organic Compounds from Commercially Available Desktop Three-Dimensional Printers with Multiple Filaments. Environ. Sci. Technol. 50, 1260–1268. doi:10.1021/acs.est.5b04983

Baechler, C., DeVuono, M., Pearce, J.M., 2013. Distributed recycling of waste polymer into RepRap feedstock. Rapid Prototyp. J. 19, 118–125. doi:10.1108/13552541311302978

Bajpai, M., Shukla, V., Kumar, A., 2002. Film performance and UV curing of epoxy acrylate resins. Prog. Org. Coatings 44, 271–278. doi:10.1016/S0300-9440(02)00059-0

Baumers, M., Beltrametti, L., Gasparre, A., Hague, R., 2017. Informing additive manufacturing technology adoption: total cost and the impact of capacity utilisation. Int. J. Prod. Res. 1–14. doi:10.1080/00207543.2017.1334978

Baumers, M., Dickens, P., Tuck, C., Hague, R., 2016a. The cost of additive manufacturing: Machine productivity, economies of scale and technology-push. Technol. Forecast. Soc. Change 102, 193–201. doi:10.1016/j.techfore.2015.02.015

Baumers, M., Tuck, C., Bourell, D.L., Sreenivasan, R., Hague, R., 2011. Sustainability of additive manufacturing: measuring the energy consumption of the laser sintering process. Proc. Inst. Mech. Eng. Part B J. Eng. Manuf. 225, 2228–2239. doi:10.1177/0954405411406044

Baumers, M., Tuck, C., Wildman, R., Ashcroft, I., Hague, R., 2016b. Shape Complexity and Process Energy Consumption in Electron Beam Melting: A Case of Something for Nothing in Additive Manufacturing? J. Ind. Ecol. doi:10.1111/jiec.12397

Baumers, M., Tuck, C., Wildman, R., Ashcroft, I., Hague, R., 2011. Energy inputs to additive manufacturing: Does capacity utilization matter? Solid Free. Fabr. Symp. 30–40. doi:10.1017/CBO9781107415324.004

Bours, J., Adzima, B., Gladwin, S., Cabral, J., Mau, S., 2017. Addressing hazardous implications of additive manufacturing: Complementing life cycle assessment with a framework for evaluating direct human health and environmental impacts. J. Ind. Ecol. 21, S25–S36.

Brady, G.A., Chu, T.M., Halloran, J.W., 1996. Curing Behavior of Ceramic Resin for Stereolithography. Solid Free. Fabr. Symp. 403–410.

Burkhart, M., Aurich, J.C., 2015. Framework to predict the environmental impact of additive manufacturing in the life cycle of a commercial vehicle. Procedia CIRP 29, 408–413. doi:doi:10.1016/j.procir.2015.02.194

Buswell, R.A., Soar, R.C., Gibb, A.G.F., Thorpe, A., 2007. Freeform Construction: Mega-scale Rapid Manufacturing for construction. Autom. Constr. 16, 224–231. doi:10.1016/j.autcon.2006.05.002

Campbell, I., Bourell, D., Gibson, I., 2012. Additive manufacturing: rapid prototyping comes of age. Rapid Prototyp. J. 18, 255–258. doi:10.1108/13552541211231563

Cardelino, C.A., Chameides, W.L., 1995. An observation-based model for analyzing ozone precursor relationships in the urban atmosphere. J. Air Waste Manag. Assoc. 45, 161–180. doi:10.1080/10473289.1995.10467356

Cerdas, F., Juraschek, M., Thiede, S., Herrmann, C., 2017. Life cycle assessment of 3D printed products in a distributed manufacturing system. J. Ind. Ecol. 21, S80–S93.

Chang, G., Tu, Y., 2012. Closed-loop control in ultrafast laser milling process using laser triggered plasma. Int. J. Mach. Tools Manuf. 60, 35–39. doi:10.1016/j.ijmachtools.2012.04.002

Cherry Aerospace LLC, 2007. Procurement Specification for CNP19 Cherry Rivetless Nut Plate [WWW Document].

Columbus, L., 2015. 2015 Roundup of 3D Printing Market Forecasts and Estimates [WWW Document]. Forbes. URL https://www.forbes.com/sites/louiscolumbus/2015/03/31/2015-roundup-of-3d-printing-market-forecasts-and-estimates/#66e8b03d1b30 (accessed 2.6.19).

Contos, D.A., Holdren, M.W., Smith, D.L., Brooke, R.C., Rhodes, V.L., Rainey, M.L., 1995. SAMPLING AND ANALYSIS OF VOLATILE ORGANIC-COMPOUNDS EVOLVED DURING THERMAL-PROCESSING OF ACRYLONITRILE-BUTADIENE-STYRENE COMPOSITE RESINS. J. Air Waste Manage. Assoc. 45, 686–694.

Dai, D., Gu, D., 2015. Tailoring surface quality through mass and momentum transfer modeling using a volume of fluid method in selective laser melting of TiC/AlSi10Mg powder. Int. J. Mach. Tools Manuf. 88, 95–107. doi:http://dx.doi.org/10.1016/j.ijmachtools.2014.09.010

Daisey, J.M., Hodgson, A.T., Fisk, W.J., Mendell, M.J., Ten Brinke, J., 1994. Volatile organic compounds in twelve California office buildings: Classes, concentrations and sources, in: Atmospheric Environment. pp. 3557–3562. doi:10.1016/1352-2310(94)00200-5

De Benedetto, L., Klemeš, J., 2009. The Environmental Performance Strategy Map: an integrated LCA approach to support the strategic decision-making process. J. Clean. Prod. 17, 900–906. doi:10.1016/j.jclepro.2009.02.012

de Gennaro, G., Farella, G., Marzocca, A., Mazzone, A., Tutino, M., 2013. Indoor and outdoor monitoring of volatile organic compounds in school buildings: Indicators based on health risk assessment to single out critical issues. Int. J. Environ. Res. Public Health 10, 6273–6291. doi:10.3390/ijerph10126273

DeltaMed, 2014. e-shell 600 clear safety data sheet [WWW Document].

Ding, Y., Dwivedi, R., Kovacevic, R., 2017. Process planning for 8-axis robotized laser-based direct metal deposition system: A case on building revolved part. Robot. Comput. Integr. Manuf. 44, 67–76. doi:10.1016/j.rcim.2016.08.008

Drizo, A., Pegna, J., 2006. Environmental impacts of rapid prototyping: an overview of research to date. Rapid Prototyp. J. 12, 64–71. doi:10.1108/13552540610652393

Emelogu, A., Marufuzzaman, M., Thompson, S.M., Shamsaei, N., Bian, L., 2016. Additive manufacturing of biomedical implants: A feasibility assessment via supply-chain cost analysis. Addit. Manuf. 11, 97–113. doi:10.1016/j.addma.2016.04.006

Environmental, A., 2009. Total Volatile Organic Compound (TVOC) Measurement for LEED/Green Building Evaluation [WWW Document]. URL http://www.caslab.com/News/tvoc-leed.html (accessed 1.1.16).

EnvisionTec, 2019. LS600 [WWW Document]. URL https://envisiontec.com/3d-printing-materials/micro-materials/ls600/

EnvisionTec, 2015. Micro Plus Advantages [WWW Document].

EnvisionTec, 2014. E-Shell 600 [WWW Document].

EnvisionTEC, 2017. Vida [WWW Document].

EnvisionTEC, 2015. Perfactory Micro EDU [WWW Document]. URL envisiontec.com/envisiontec/wp-content/uploads/MK-MCS-MicroEDU-V01-FN-EN.pdf (accessed 1.11.15).

EPA, 2010. Annual non-basedload CO2 output emission rate, year 2010 data [WWW Document]. URL http://www.epa.gov/cleanenergy/energy-resources/refs.html (accessed 1.4.16).

EPA (U.S. Environmental Protection Agency), 2015. eGRID [WWW Document]. U.S. Environ.

Prot. Agency, Washington, DC. URL https://www.epa.gov/energy/egrid (accessed 1.1.16).

Eschl, J., Blumenstock, T., Eyerer, P., 1999. Comparison of the Curing Process of Epoxy and Acrylate Resins for Stereolithography by Means of Experimental Investigations and FEM-Simulation, in: Solid Freeform Fabrication Symposium. p. 453.

Faludi, J., Bayley, C., Bhogal, S., Iribarne, M., 2015. Comparing environmental impacts of additive manufacturing vs traditional machining via life-cycle assessment. Rapid Prototyp. J. 21, 14–33. doi:10.1108/RPJ-07-2013-0067

Fera, M., Fruggiero, F., Costabile, G., Lambiase, A., Pham, D.T., 2017. A new mixed production cost allocation model for additive manufacturing (MiProCAMAM). Int. J. Adv. Manuf. Technol. doi:10.1007/s00170-017-0492-x

Ford, S., Despeisse, M., 2015. Additive manufacturing and sustainability: An exploratory study of the advantages and challenges. J. Clean. Prod. doi:10.1016/j.jclepro.2016.04.150

Galante, R., Figueiredo-Pina, C.G., Serro, A.P., 2019. Additive manufacturing of ceramics for dental applications: A review. Dent. Mater. doi:10.1016/j.dental.2019.02.026

Giannatsis, J., Dedoussis, V., 2009. Additive fabrication technologies applied to medicine and health care: A review. Int. J. Adv. Manuf. Technol. 40, 116–127. doi:10.1007/s00170-007-1308-1

Goodman, M., Naiman, J.S., Goodman, D., Lakind, J.S., 2012. Cancer clusters in the USA: What do the last twenty years of state and federal investigations tell us? Crit. Revews Toxicol. 42, 474–490. doi:10.3109/10408444.2012.675315

GREENGUARD Certification, 2013. GREENGUARD Certification Program for Chemical and Particle Emissions for Electronic Equipment [WWW Document]. UL Environ.

Guo, H., 2012. Volatile organic compounds (VOCs) emitted from petroleum and their influence on photochemical smog formation in the atmosphere. J. Pet. Environ. Biotechnol. 3, 2380–2391. doi:10.4172/2157-7463.1000e104

Guo, N., Leu, M.C., 2013. Additive manufacturing: Technology, applications and research needs. Front. Mech. Eng. doi:10.1007/s11465-013-0248-8

Helmis, C.G., Tzoutzas, J., Flocas, H.A., Halios, C.H., Stathopoulou, O.I., Assimakopoulos, V.D., Panis, V., Apostolatou, M., Sgouros, G., Adam, E., 2007. Indoor air quality in a dentistry clinic. Sci. Total Environ. 377, 349–365. doi:10.1016/j.scitotenv.2007.01.100

Hopkinson, N., Dickens, P., 2003. Analysis of rapid manufacturing—using layer manufacturing processes for production. Proc. Inst. Mech. Eng. Part C J. Mech. Eng. Sci. 217, 31–39. doi:10.1243/095440603762554596

Huang, R., Riddle, M., Graziano, D., Warren, J., Das, S., Nimbalkar, S., Cresko, J., Masanet, E., 2015. Energy and emissions saving potential of additive manufacturing: the case of lightweight aircraft components. J. Clean. Prod. 1–12. doi:10.1016/j.jclepro.2015.04.109

Huang, R., Ulu, E., Kara, L.B., Whitefoot, K.S., 2017. Cost Minimization in Metal Additive Manufacturing Using Concurrent Structure and Process Optimization, in: Proceedings of the ASME 2017 International Design Engineering Technical Conference & Computers and Information in Engineering Conference IDETC2017.

Huang, S.H., Liu, P., Mokasdar, A., Hou, L., 2013. Additive manufacturing and its societal impact: A literature review. Int. J. Adv. Manuf. Technol. doi:10.1007/s00170-012-4558-5

Hulten, C.R., Wykoff, F.C., 1980. The measurement of economic depreciation, in: Hulten, C.R. (Ed.), Depreciation Inflation & The Taxation of Income from Capital. Urban Institute, pp. 81–125.

International Organization for Standardization, 2006. ISO 14044: 2006 Environmental management-Life cycle assessment-Requirements and guidelines [WWW Document].

Jeng, J.Y., Lin, M.C., 2001. Mold fabrication and modification using hybrid processes of selective laser cladding and milling. J. Mater. Process. Technol. 110, 98–103. doi:10.1016/S0924-0136(00)00850-5

Jo, W., Kim, J., 2009. Application of visible-light photocatalysis with nitrogen-doped or unmodified titanium dioxide for control of indoor-level volatile organic compounds. J. Hazard. Mater. 164, 360–366. doi:10.1016/j.jhazmat.2008.08.033

Kafara, M., S??chting, M., Kemnitzer, J., Westermann, H.H., Steinhilper, R., 2017. Comparative Life Cycle Assessment of Conventional and Additive Manufacturing in Mold Core Making for CFRP Production. Procedia Manuf. 8, 223–230. doi:10.1016/j.promfg.2017.02.028

KEI (Korea Environment Institute), 2004. Research on Improvement Measures for Indoor Air Quality Management. Seoul 33–82.

Kellens, K., Renaldi, R., Dewulf, W., Kruth, J., Duflou, J.R., 2014. Environmental impact modeling of selective laser sintering processes. Rapid Prototyp. J. 20, 459–470. doi:10.1108/RPJ-02-2013-0018

Kim, H.-H., Lim, Y.-W., Shin, D.-C., Sohn, J.R., Yang, J.-Y., 2011. Risk Assessment of Volatile Organic Compounds (VOCs) and Formaldehyde in Korean Public Facilities: Derivation of Health Protection Criteria Levels. Asian J. Atmos. Environ. 5, 121–133. doi:10.5572/ajae.2011.5.2.121

Kim, Y., Yoon, C., Ham, S., Park, J., Kim, S., Kwon, O., Tsai, P.J., 2015. Emissions of Nanoparticles and Gaseous Material from 3D Printer Operation. Environ. Sci. Technol. 49, 12044–12053. doi:10.1021/acs.est.5b02805

Kreiger, M., Pearce, J.M., 2013a. Environmental Impacts of Distributed Manufacturing from 3-D Printing of Polymer Components and Products. MRS Online Proc. Libr. 1492, 85–90. doi:10.1557/opl.2013.319

Kreiger, M., Pearce, J.M., 2013b. Environmental life cycle analysis of distributed three-dimensional printing and conventional manufacturing of polymer products. ACS Sustain. Chem. Eng. 1, 1511–1519. doi:10.1021/sc400093k

Kuo, C.-C., Liu, L.-C., Teng, W.-F., Chang, H.-Y., Chien, F.-M., Liao, S.-J., Kuo, W.-F., Chen, C.-M., 2016. Preparation of starch/acrylonitrile-butadiene-styrene copolymers (ABS) biomass alloys and their feasible evaluation for 3D printing applications. Compos. Part B Eng. 86, 36–39. doi:doi.org/10.1016/j.compositesb.2015.10.005

Lavery, N.P., Brown, S.G.R., Sienz, J., Cherry, J., 2014. A review of Computational Modelling of Additive Layer Manufacturing – multi-scale and multi-physics. Sustain. Des. Manuf. 1, 651–673. doi:10.13140/RG.2.1.3103.0884

Li, L., Haghighi, A., Yang, Y., 2018a. Theoretical modelling and prediction of surface roughness for hybrid additive–subtractive manufacturing processes. IISE Trans.

doi:10.1080/24725854.2018.1458268

Li, L., Haghighi, A., Yang, Y., 2018b. Theretical Modeling and Prediction of Surface Roughness for Hybrid Additive-Subtractive Manufacturing Processes. IISE Trans. In Press. doi:doi.org/10.1080/24725854.2018.1458268

Lindemann, C., Jahnke, U., Moi, M., Koch, R., 2013. Impact and Influence Factors of Additive Manufacturing on Product Lifecycle Costs. Proc. 24th Solid Free. Fabr. Symp. 998–1009.

Lindemann, C., Jahnke, U., Moi, M., Koch, R., 2012. Analyzing product lifecycle costs for a better understanding of cost drivers in additive manufacturing. Int. Solid Free. Fabr. Symp. 23, 177–188. doi:10.1007/s13398-014-0173-7.2

Lipton, J.I., Cutler, M., Nigl, F., Cohen, D., Lipson, H., 2015. Additive Manufacturing for the Food Industry - A review. Trends Food Sci. Technol. 43, 114–123. doi:10.1016/j.tifs.2015.02.004

Lopes, A.J., Lee, I.H., MacDonald, E., Quintana, R., Wicker, R., 2014. Laser curing of silver-based conductive inks for in situ 3D structural electronics fabrication in stereolithography. J. Mater. Process. Technol. 214, 1935–1945. doi:http://dx.doi.org/10.1016/j.jmatprotec.2014.04.009

Lucite, 2010. Lucite International Safety Data Sheet [WWW Document].

Luo, Y., Ji, Z., Leu, M.C., Caudill, R., 1999. Environmental Performance Analysis of Solid Freeform Fabrication Processes. Proc. 1999 IEEE Int. Symp. Electron. Environ. 1–6. doi:10.1109/ISEE.1999.765837

Lyndsey, G., 2014. The dark side of 3D printing: 10 things to watch [WWW Document]. TechRepublic.

Lynn-Charney, C., Rosen, D.W., 2000. Usage of accuracy models in stereolithography process planning. Rapid Prototyp. J. 6, 77–87. doi:10.1108/13552540010323600

Lyons, B., 2012. Additive Manufacturing in Aerospace: Examples and Research Outlook. Bridg. 42, 13–19. doi:10.1016/S0026-0657(14)70250-4

Mackay, D., Matsugu, R.S., 1973. Evaporation rates of liquid hydrocarbon spills on land and water.

Can. J. Chem. Eng. 51, 434–439. doi:10.1002/cjce.5450510407

Manyika, J., Chui, M., Bughin, J., Dobbs, R., Bisson, P., Marrs, 2013. Disruptive technologies: Advances that will transform life, business, and the global economy. McKinsey Glob. Insitute 163.

Marchesi, T.R., Lahuerta, R.D., Silva, E.C.N., Tsuzuki, M.S.G., Martins, T.C., Barari, A., Wood, I., 2015. Topologically optimized diesel engine support manufactured with additive manufacturing, in: IFAC-PapersOnLine. pp. 2333–2338. doi:10.1016/j.ifacol.2015.06.436

Martukanitz, R., Michaleris, P., Palmer, T., DebRoy, T., Liu, Z.-K., Otis, R., Heo, T.W., Chen, L.-Q., 2014. Toward an integrated computational system for describing the additive manufacturing process for metallic materials. Addit. Manuf. 1–4, 52–63. doi:http://dx.doi.org/10.1016/j.addma.2014.09.002

Meteyer, S., Xu, X., Perry, N., Zhao, Y.F., 2014. Energy and material flow analysis of binder-jetting additive manufacturing processes, in: Procedia CIRP. pp. 19–25. doi:10.1016/j.procir.2014.06.030

Mognol, P., Lepicart, D., Perry, N., 2006. Rapid prototyping: energy and environment in the spotlight. Rapid Prototyp. J. 12, 26–34. doi:10.1108/13552540610637246

Montgomery, D.C., 2012. Design and Analysis of Experiments, Design. doi:10.1198/tech.2006.s372

Moylan, S., Slotwinski, J., Cooke, A., Jurrens, K., Donmez, M.A., 2014. An additive manufacturing test artifact. J. Res. Natl. Inst. Stand. Technol. 119, 429–459. doi:10.6028/jres.119.017

National Energy Technology Laboratory, 2019. NATCARB/ATLAS [WWW Document]. U.S. Dep. Energy. URL https://www.netl.doe.gov/coal/carbon-storage/strategic-program-support/natcarb-atlas (accessed 2.6.19).

Newman, J., 2012. Standardizing Additive Manufacturing Process Terminology [WWW Document]. Digit. Eng. URL https://www.digitalengineering247.com/article/the-art-of-simplicity-standardized-process-terminology/ (accessed 2.6.19).

Newman, S.T., Zhu, Z., Dhokia, V., Shokrani, A., 2015. Process planning for additive and subtractive manufacturing technologies. CIRP Ann. - Manuf. Technol. 64, 467–470. doi:10.1016/j.cirp.2015.04.109

Nikzad, M., Masood, S.H., Sbarski, I., 2011. Thermo-mechanical properties of a highly filled polymeric composites for Fused Deposition Modeling. Mater. Des. 32, 3448–3456. doi:10.1016/j.matdes.2011.01.056

Pan, Y., Zhao, X., Zhou, C., Chen, Y., 2012a. Smooth surface fabrication in mask projection based stereolithography, in: Journal of Manufacturing Processes. pp. 460–470. doi:10.1016/j.jmapro.2012.09.003

Pan, Y., Zhou, C., Chen, Y., 2012b. A Fast Mask Projection Stereolithography Process for Fabricating Digital Models in Minutes. J. Manuf. Sci. Eng. 134, 051011–051011. doi:10.1115/1.4007465

Pattinson, S.W., Hart, A.J., 2017. Additive Manufacturing of Cellulosic Materials with Robust Mechanics and Antimicrobial Functionality. Adv. Mater. Technol. 2. doi:10.1002/admt.201600084

Peels, J., 2017. 3D Printing in the Military [WWW Document]. 3DPRINT.COM.

Peng, S., Li, T., Wang, X., Dong, M., Liu, Z., Shi, J., Zhang, H., 2017. Toward a Sustainable Impeller Production: Environmental Impact Comparison of Different Impeller Manufacturing Methods. J. Ind. Ecol. doi:10.1111/jiec.12628

Piili, H., Happonen, A., Väistö, T., Venkataramanan, V., Partanen, J., Salminen, A., 2015. Cost Estimation of Laser Additive Manufacturing of Stainless Steel, in: Physics Procedia. pp. 388–396. doi:10.1016/j.phpro.2015.11.053

Ponche, R., Kerbrat, O., Mognol, P., Hascoet, J.-Y., 2014. A novel methodology of design for Additive Manufacturing applied to Additive Laser Manufacturing process. Robot. Comput. Integr. Manuf. 30, 389–398. doi:http://dx.doi.org/10.1016/j.rcim.2013.12.001

Prasanna Kumar, C.S., Sabberwal, S.P., Mukharji, A.K., 1995. Power factor measurement and correction techniques. Electr. Power Syst. Res. 32, 141–143. doi:10.1016/0378-7796(94)00906-K

Reeves, P., 2009. Additive manufacturing - A supply chain wide response to economic uncertainty and environmental sustainability, in: Industrial Tools and Material Processing Technologies.

Rickenbacher, L., Spierings, A., Wegener, K., 2013. An integrated cost-model for selective laser melting (SLM). Rapid Prototyp. J. 19, 208–214. doi:10.1108/13552541311312201

Ruan, J., Eiamsa-ard, K., Liou, F.W., 2005. Automatic Process Planning and Toolpath Generation of a Multiaxis Hybrid Manufacturing System. J. Manuf. Process. 7, 57–68. doi:10.1016/S1526-6125(05)70082-7

Ruffo, M., Hague, R., 2007. Cost estimation for rapid manufacturing ' simultaneous production of mixed components using laser sintering. Proc. Inst. Mech. Eng. Part B J. Eng. Manuf. 221, 1585–1591. doi:10.1243/09544054JEM894

Ruffo, M., Tuck, C., Hague, R., 2006. Cost estimation for rapid manufacturing - laser sintering production for low to medium volumes. Proc. Inst. Mech. Eng. Part B J. Eng. Manuf. 220, 1417–1427. doi:10.1243/09544054JEM517

Rutkowski, J. V., Levin, B.C., 1986. Acrylonitrile???butadiene???styrene copolymers (ABS): Pyrolysis and combustion products and their toxicity???a review of the literature. Fire Mater. 10, 93–105. doi:10.1002/fam.810100303

Sax, S.N., Bennett, D.H., Chillrud, S.N., Ross, J., Kinney, P.L., Spengler, J.D., 2006. A cancer risk assessment of inner-city teenagers living in New York City and Los Angeles. Environ. Health Perspect. 114, 1558–1566. doi:10.1289/ehp.8507

Serrano, S., Barreneche, C., Cabeza, L.F., 2016. Use of by-products as additives in adobe bricks: Mechanical properties characterisation. Constr. Build. Mater. 108, 105–111. doi:10.1016/j.conbuildmat.2016.01.044

Short, D.B., Sirinterlikci, A., Badger, P., Artieri, B., 2015. Environmental , Health , and Safety Issues in Rapid Prototyping. Rapid Prototyp. J. 21, 105–110. doi:10.1108/RPJ-11-2012-0111

Sidheswaran, M.A., Destaillats, H., Sullivan, D.P., Cohn, S., Fisk, W.J., 2012. Energy efficient indoor VOC air cleaning with activated carbon fiber (ACF) filters. Build. Environ. 47, 357–367. doi:10.1016/j.buildenv.2011.07.002

Sivak, M., 2006. Guidance for the Calculation of Cancer and Non-cancer Risk from Inhalation Exposure: an Update [WWW Document]. EPA Risk Assessor. Annu. Conf.

Son, Y.K., 1991. A cost estimation model for advanced manufacturing systems. Int. J. Prod. Res. 29, 441–452. doi:10.1080/00207549108930081

Sreenivasan, R., Bourell, D.L., 2009. Sustainability study in selective laser sintering – An energy perspective. Solid Free. Fabr. Symp. 257–265.

Sreenivasan, R., Goel, a., Bourell, D.L., 2010. Sustainability issues in laser-based additive manufacturing. Phys. Procedia 5, 81–90. doi:10.1016/j.phpro.2010.08.124

Srinivas, M., Babu, B.S., 2017. A Critical Review on Recent Research Methodologies in Additive Manufacturing, in: Materials Today: Proceedings. pp. 9049–9059. doi:10.1016/j.matpr.2017.07.258

Sun, C., Fang, N., Wu, D.M., Zhang, X., 2005. Projection micro-stereolithography using digital micro-mirror dynamic mask. Sensors Actuators, A Phys. 121, 113–120. doi:10.1016/j.sna.2004.12.011

Telenko, C., Conner Seepersad, C., 2012. A comparison of the energy efficiency of selective laser sintering and injection molding of nylon parts. Rapid Prototyp. J. 18, 472–481. doi:10.1108/13552541211272018

Thomas, D., Gilbert, S., 2014. Costs and Cost Effectiveness of Additive Manufacturing - A Literature Review and Discussion. NIST Spec. Publ. 1176, 1–77. doi:10.6028/NIST.SP.1176

Tymrak, B.M., Kreiger, M., Pearce, J.M., 2014. Mechanical properties of components fabricated with open-source 3-D printers under realistic environmental conditions. Mater. Des. 58, 242–246. doi:10.1016/j.matdes.2014.02.038

U.S. Department of Commerce, 2017. Manufacturing and Trade Inventories and Sales, July 2017.

U.S. Department of Labor, 2017. Minimum Wage Laws in the States [WWW Document].

U.S. Energy Information Administration, 2017. Electric Power Monthly [WWW Document].

U.S. Energy Information Administration, 2010. Manufacturing energy consumption survey (MECS) [WWW Document].

U.S. Environmental Protection Agency, 2016a. Sources of Greenhouse Gas Emissions [WWW Document].

U.S. Environmental Protection Agency, 2016b. Glossary of Sustainable Manufacturing Terms [WWW Document].

U.S. Postal Service, 2014. If it prints, it ships: 3D printing and the postal service.

United States Environmental Protection Agency, 2000. Methyl Methacrylate [WWW Document].

Walachowicz, F., Bernsdorf, I., Papenfuss, U., Zeller, C., Graichen, A., Navrosky, V., Rajvanshi, N., Kiener, C., 2017. Comparative Energy, Resource and Recycling Lifecycle Analysis of the Industrial Repair Process of Gas Turbine Burners Using Conventional Machining and Additive Manufacturing. J. Ind. Ecol. doi:10.1111/jiec.12637

Wang, F., 2012. Mechanical property study on rapid additive layer manufacture Hastelloy?? X alloy by selective laser melting technology. Int. J. Adv. Manuf. Technol. 58, 545–551. doi:10.1007/s00170-011-3423-2

Weller, C., Kleer, R., Piller, F.T., 2015. Economic implications of 3D printing: Market structure models in light of additive manufacturing revisited. Int. J. Prod. Econ. 164, 43–56. doi:10.1016/j.ijpe.2015.02.020

Weng, Z., Wang, J., Senthil, T., Wu, L., 2016. Mechanical and thermal properties of ABS/montmorillonite nanocomposites for fused deposition modeling 3D printing. Mater. Des. 102, 276–283.

Wittbrodt, B.T., Glover, a. G., Laureto, J., Anzalone, G.C., Oppliger, D., Irwin, J.L., Pearce, J.M., 2013. Life-cycle economic analysis of distributed manufacturing with open-source 3-D printers. Mechatronics 23, 713–726. doi:10.1016/j.mechatronics.2013.06.002

Wohlers Associates, 2015. Wohlers Report 2015.

Wohlers Associates, 2012. Wohlers Report.

Xie, R., Li, D., 2012. Research on the curing performance of UV-LED light based stereolithography. Opt. Laser Technol. 44, 1163–1171. doi:10.1016/j.optlastec.2011.09.019

Xu, X., Meteyer, S., Perry, N., Zhao, Y.F., 2015. Energy consumption model of Binder-jetting additive manufacturing processes. Int. J. Prod. Res. 53, 7005–7015. doi:10.1080/00207543.2014.937013

Yang, S., Talekar, T., Sulthan, M.A., Zhao, Y.F., 2017. A Generic Sustainability Assessment Model towards Consolidated Parts Fabricated by Additive Manufacturing Process. Procedia Manuf. 10, 831–844. doi:10.1016/j.promfg.2017.07.086

Yang, Y., Chen, Z., Song, X., Zhu, B., Hsiai, T., Wu, P.I., Xiong, R., Shi, J., Chen, Y., Zhou, Q., Shung, K.K., 2016. Three dimensional printing of high dielectric capacitor using projection based stereolithography method. Nano Energy 22, 414–421. doi:10.1016/j.nanoen.2016.02.045

Yang, Y., Li, L., 2018a. Total volatile organic compound emission evaluation and control for stereolithography additive manufacturing process. J. Clean. Prod. 170, 1268–1278. doi:10.1016/j.jclepro.2017.09.193

Yang, Y., Li, L., 2018b. Cost Modeling and Analysis for Mask Image Projection Stereolithography Additive Manufacturing: Simultaneous Production with Mixed Geometries. Int. J. Prod. Econ. doi:https://doi.org/10.1016/j.ijpe.2018.09.023

Yang, Y., Li, L., 2017. Evaluation of Environmental Sustainability for Additive Manufacturing Batch Production, in: ASME 2017 12th International Manufacturing Science and Engineering Conference Collocated with the JSME/ASME 2017 6th International Conference on Materials and Processing. American Society of Mechanical Engineers, p. V002T01A038-V002T01A038.

Yang, Y., Li, L., Pan, Y., Sun, Z., 2017. Energy Consumption Modeling of Stereolithography-Based Additive Manufacturing Toward Environmental Sustainability. J. Ind. Ecol. doi:10.1111/jiec.12589

Yang, Y., Li, L., Zhao, J., 2019. Mechanical Property Modeling of Photosensitive Liquid Resin in Stereolithography Additive Manufacturing: Bridging Degree of Cure with Tensile Strength and Hardness. Mater. Des. 162, 418–428.

Zanardini, M., Bacchetti, A., Pour, M.A., Zanoni, S., 2015. Benefits and costs of additive manufacturing applications: An evaluation guideline. Proc. Summer Sch. Fr. Turco 43–48.

Zhang, Q., Zhang, G., 2007. Study on TVOCs concentration distribution and evaluation of inhaled air quality under a re-circulated ventilation system. Build. Environ. 42, 1110–1118. doi:10.1016/j.buildenv.2005.11.012

Zhou, W., Li, D., Chen, Z., 2011. The influence of ingredients of silica suspensions and laser exposure on UV curing behavior of aqueous ceramic suspensions in stereolithography. Int. J. Adv. Manuf. Technol. 52, 575–582. doi:10.1007/s00170-010-2746-8

Ziemian, C., Sharma, M., Ziemian, S., 2012. Anisotropic mechanical properties of ABS parts fabricated by fused deposition modelling. Mech. Eng. 159–180. doi:10.5772/34233

CURRICULUM VITAE

Yiran (Emma) Yang

842 West Taylor Street, Chicago, IL 60607

EDUCATION

Ph.D. in Industrial Engineering and Operations Research, University of Illinois at Chicago (UIC), Chicago, IL, USA.

08/2015-Present, ***expected graduation: 05/2019*** **GPA: 4.0/4.0**

M.S. in Mechanical Engineering, Purdue University Northwest (PNW), Hammond, IN, USA.

08/2013-05/2015 **GPA: 3.8/4.0**

B.S. in Automotive Engineering, Beijing Institute of Technology (BIT), Beijing, China.

08/2009-05/2013 **GPA: 3.5/4.0**

GRADUATE COURSEWORK

Operation Research, Time Series Analysis and Forecast, Data Mining and Machine Health, Advanced 3D Printing and Additive Manufacturing, Distributed Decision Making, Energy Storage, Finite Element Analysis, Quality Control, Introduction to Wind Energy, Combustion, Numerical Heat and Mass Transfer, Mechanical Vibration, Computational Fluid Dynamics Applications, Design and Analysis Heat Ventilation Air Conditioning, System Engineering, and Design of Heat Exchangers.

RESEARCH EXPERIENCE

Sustainable Manufacturing Systems Research Laboratory, UIC

Research Assistant *08/2015-Present*

NSF Collaborative Research: Environmental Sustainability of Additive Manufacturing Processes: Bridging Geometry and Life Cycle Inventory

- Establish analytical models for quantifying the energy consumption of stereolithography additive manufacturing process aiming to enhance the overall energy efficiency
- Characterize the volatile organic compound emission from stereolithography additive manufacturing process and propose effective emission control strategies towards green and sustainable additive manufacturing
- Design and develop an energy-saving and low-emission stereolithography prototype (in the process of patent application)

U.S. Department of Energy

Research Assistant *08/2015-Present*

Industrial Assessment Center for Energy Efficiency, Smart Manufacturing and Cyber Security of Illinois and Northwestern Indiana Small and Medium Sized Manufacturing Companies and Water Facilities

- Perform comprehensive energy assessment based on existing utility usages and potential recommendations towards energy efficiency
- Conduct in-depth utility analyses including electricity, natural gas, water and sewer
- Propose recommendations and provide associated energy and cost saving calculations

Center for Innovation through Visualization and Simulation, PNW

Research Assistant *08/2013-05/2015*

Finite Element Structural Analysis of a Vertical Edger in a Hot Rolling Mill: A Methodology for Vertical Edger Life Prediction

- Develop a finite element analysis (FEA) model for simulating the vertical edger to identify the areas with higher degree of deformation and stress
- Perform a fatigue analysis to predict the remaining life of each component of the vertical edger based on the material properties and loading cycles
- Employ a virtual reality visualization of the analysis results aiming to enable the field operators to analyze the results in an intuitive way

JOURNAL PUBLICATIONS

Journal Papers Published

[J6] **Yang, Y.**, Li, L., Pan, Y., Sun, Z., 2017. Energy Consumption Modeling of Stereolithography-Based Additive Manufacturing Toward Environmental Sustainability. *Journal of Industrial Ecology* 21(S1) S168-S178. (**IF=4.356**)

[J5] **Yang, Y.**, and Li, L., 2018. Total Volatile Organic Compound Emission Evaluation and Control for Stereolithography Additive Manufacturing. *Journal of Cleaner Production* 170(1) 1268-1278. (**IF=5.651**)

[J4] **Yang, Y.**, and Li, L., 2018. Cost Modeling and Analysis for Mask Image Projection Stereolithogrpahy Additive Manufacturing: Simultaneous Production with Mixed Geometries. *International Journal of Production Economics* 206: 146-158. (**IF=4.407)**

[J3] **Yang, Y.**, Li, L., and Zhao, J., 2019. Mechanical Property Modeling of Photosensitive Liquid Resin in Stereolithography Additive Manufacturing: Bridging Degree of Cure with Tensile Strength and Hardness. *Materials & Design* 162: 418-428 (**IF=4.525)**.

[J2] Li, L., Haghighi, A., and **Yang, Y.**, 2018. A Novel 6-Axis Hybrid Additive-Subtractive Manufacturing Process: Design and Case Studies. *Journal of Manufacturing Processes* 33: 150-160. (**IF=2.809)**

[J1] Li, L., Haghighi, A., and **Yang, Y.**, 2018. Theoretical Modeling and Prediction of Surface Roughness for Hybrid Additive-Subtractive Manufacturing Processes. *IISE Transactions* 1-40. (**IF=1.759**)

Journal Papers Under Review

Zhao, J., **Yang, Y**., and Li, L, 2018. A Comprehensive Evaluation of Three Popular Post Solidification Approaches Used in Stereolithography Additive Manufacturing. *Journal of Manufacturing Processes* (**IF=2.809)**. Under Review.

Yang, Y., He, M., and Li, L., 2018. Power Consumption Estimation for Mask Image Projection Stereolithography Additive Manufacturing Using Machine Learning Based Appraoch. *Journal of Cleaner Production* (**IF=5.651**). Under Review.

Simon, T., **Yang, Y**., Lee, WJ., Zhao, J., Li, L., and Zhao, F., 2019. Reusable Unit Life Cycle Inventory for Manufacturing: Stereolithography. Journal of Production Engineering. Revision.

CONFERENCE PUBLICATIONS

Conference Papers Published

[C5] **Yang, Y.**, He, M., and Li, L., 2019. A New Machine Learning Based Geometry Feature Extraction Approach for Energy Consumption Estimation in Mask Image Projection Stereolithography. *The 26th CIRP Conference in Life Cycle Engineering*. West Lafayette, IN.

[C4] **Yang, Y.**, Haghighi, A., and Li, L., 2018. Energy Consumption Study for 6-Axis Additive-Subtractive Manufacturing Process. *Proceedings of the 2018 Industrial and Systems Engineering Conference*. 1019-1024.

[C3] **Yang, Y.**, Li, L., 2017. Evaluation of Environmental Sustainability for Additive Manufacturing Batch Production. *ASME 2017 12th International Manufacturing Science and Engineering Conference*. p. V002T01A038. doi:10.1115/MSEC2017-2957.

[C2] Haghighi, A., **Yang, Y.**, Li, L., 2017. Dimensional Performance of As-Built Assemblies in Polyjet Additive Manufacturing Process. *ASME 2017 12th International Manufacturing Science and Engineering Conference*. p. V002T01A039. doi:10.1115/MSEC2017-2983.

[C1] **Yang, Y.**, He, M., and Mojtahed, M., 2014. Analysis of a Diesel Engine Exhaust Manifold. *ASME 2014 International Mechanical Engineering Congress and Exposition*. p. V009T12A093. doi:10.1115/IMECE2014-37606.

Conference Posters

[P2] Zhao, J., **Yang, Y**., Han, M., and Li, L. 2019. Sustainability Evaluation of Post-Curing Appraoches in Stereolithography Additive Manufacturing. *The 26th CIRP Conference in Life Cycle Engineering.* West Lafayette, IN.

[P1] Simon, T., **Yang, Y**., Lee, WJ., Zhao, J., Li, L., and Zhao, F., 2019. Sustainability Analysis of Stereolithography Using Unit Manufacturing Process Models. *The 26th CIRP Conference in Life Cycle Engineering.* West Lafayette, IN.

TEACHING EXPERIENCE

IE365 Work Productivity, *fall 2018*

IE442 Design Analysis of Experiment, *fall 2016, fall 2017, and spring 2018*

IE446 Quality Control and Reliability, *spring 2016, and spring 2017*

IE201 Financial Engineering, *fall 2015*

INDUSTRIAL EXPERIENCE

U.S. Department of Energy

Industrial Assessment Center 05/2017-Present

- Participate in energy assessments for facilities in different industries such as plastic injection molding, acoustic automotive parts, steel, lead oxides, etc.
- Evaluate the facilitate plant layout and propose recommendations aiming enhance the energy efficiency
- Write assessment report as the primary investigating student and give presentations to assessed facilities
- Search for alternative strategies to save energy cost and enhance energy efficiency

GE Transportation

Locomotive Paint Shop Production Scheduling 05/2015-05/2016

- Attend the plant visit and telecon meetings with the upper management
- Contribute to the development of simulation models based on locomotive line and paint shop, to assess the feasibility and potential of effective energy management
- Participate in the development of a scheduling algorithm to obtain the optimal paint shop production scheduling that can minimize the production make-span

SERVICE

- Member of Mechanical and Industrial Engineering Graduate Student Association, UIC, 08/2017-Present.
- Mentor in English Training in Engineering (ETIE) Program, PNW, 08/2013-05/2015.
- Tutor in Education Opportunities Program, PNW, 08/2014-05/2015.
- Volunteer in Red Cross Society of China, BIT, 09/2013-05/2014.

HONORS AND AWARDS

- First Place Award in 2018 Reusable Abstractions of Manufacturing Processes (RAMP) Challenge, hosted by NIST
- 2015 Purdue University Northwest Outstanding Student Organization Student Leader Award.
- 2012 Purdue University Northwest Dean’s List.
- Chinese National Scholarship 2009-2011.

APPENDIX: COPYRIGHT STATEMENT

Elsevier Copyright (Journal of Cleaner Production and International Journal of Production Economics)

See link: https://www.elsevier.com/about/policies/copyright/permissions.

"Authors can use their articles, in full or in part, for a wide range of scholarly, non-commercial purposes as outlined below:

- Use by an author in the author's classroom teaching (including distribution of copies, paper or electronic)
- Distribution of copies (including through email) to known research colleagues for their personal use (but not for Commercial Use)
- Inclusion in a thesis or dissertation (provided that this is not to be published commercially)
- Use in a subsequent compilation of the author's works
- Extending the Article to book-length form
- Preparation of other derivative works (but not for Commercial Use)
- Otherwise using or re-using portions or excerpts in other works

These rights apply for Elsevier authors who publish their article either a subscription article or an open access article. In all cases we require that all Elsevier authors always include a full acknowledgement and, if appropriate, a link to the final published version hosted on Science Direct."

Wiley Online Library (Journal of Industrial Ecology)

See link: https://onlinelibrary.wiley.com/page/journal/15309290/homepage/permissions.html.

"Authors-If you wish to reuse your own article (or an amended version of it) in a new publication of which you are the author, editor or co-editor, prior permission is not required (with the usual acknowledgements).

Taylor & Francis Online (IISE Transactions)

See link: https://www.tandfonline.com/terms-and-conditions.

"All articles published by Taylor & Francis / Routledge under the Creative Commons Attribution License http://creativecommons.org/licenses/by/3.0/ on an open-access basis are licensed by the respective authors of such articles for use and distribution by you subject to citation of the original source in accordance with the terms of the license under which the work was published (please check the license statement for the relevant article(s). No permission is required from the authors or publishers. Appropriate attribution can be provided by citing the original article, for example, "The Version of Scholarly Record of this Article is published in (JOURNAL TITLE) (year of publication), available online at: http://www.tandfonline.com/ (Article DOI)." For any reuse or redistribution of an article, users must also make clear the license terms under which the article was published and retain all copyright notices and disclaimers.

If an article is published under a Creative Commons Attribution License, you may access, download, copy, display, and redistribute Taylor & Francis and Routledge Open articles and Taylor & Francis and Routledge Open Select articles as well as adapt, translate, text- and datamine content contained in Taylor & Francis and Routledge Open articles and Taylor & Francis and Routledge Open Select articles, subject to the following conditions:

- you will not compromise the author's moral right to the integrity of their work and you will make proper attribution of the work but not in any way that suggests that you or your use of the work are in any way endorsed by the author or Taylor & Francis.
- this permission does not cover any third-party copyrighted work which may appear in the work requested. Where content in Taylor & Francis and Routledge Open articles and Taylor & Francis and Routledge Open Select articles is identified as belonging to a third party, you will be responsible for obtaining all necessary permissions and consents to any reuse from any such third party."